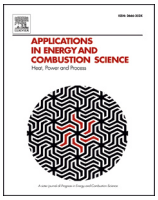
Applications in Energy and Combustion Science 27 (2026) 100550



Contents lists available at ScienceDirect

Applications in Energy and Combustion Science

journal homepage: www.sciencedirect.com/journal/applications-in-energy-and-combustion-science





Ammonia for power – fundamental combustion through computational fluid dynamics: Review

Shi H [a,1], Vigueras-Zuniga MO [b,1], Chong CT [c], Wang P [d], Yu C [e], Vargas-Ruiz H [f], Gicquel L [f], Jangi M [g], Shahsavari M [h], Chiong MC [i], Valera-Medina A [j,*]

[a] CARES, Cambridge University, Singapore
[b] School of Engineering, Universidad Veracruzana, Veracruz, Mexico
[c] China-UK Low Carbon College, Shanghai Jiao Tong University, Shanghai, China
[d] Institute for Energy Research, Jiangsu University, Jiangsu, China
[e] Institute of Technical Thermodynamics, Karlsruhe Institute of Technology, Karlsruhe, Germany
[f] CERFACS, Toulouse, France
[g] Department of Mechanical Engineering, University of Birmingham, UK
[h] Department of Engineering Science, University of Oxford, England, UK
[i] Department of Mechanical Engineering, Faculty of Engineering, UCSI University, Kuala Lumpur, Malaysia
[j] Centre of Excellence on Ammonia Technologies, Cardiff University, Cardiff, Wales, UK

ARTICLE INFO

Keywords:
Ammonia energy
Computational fluid dynamics CFD
Future NZ fuels
Combustion

ABSTRACT

Ammonia has gained considerable interest from the combustion community as an alternative fuel. The chemical promises to remove carbon entirely from heating, power and propulsion processes without incurring in extensive infrastructure developments, an important parameter for isolated regions located far from electrical or natural gas grids. As such, the work on ammonia combustion expands from fundamental analyses to giga-Watt practical applications in power generation. However, experimental research usually lacks further information about radical interactions, blends reactivity, emissions abatement, flame stability, and scalability parameters. Therefore, numerical modelling via Computational Fluid Dynamics (CFD) not only offers detailed insights into these combustion challenges using ammonia but also ensures that by applying novel methodologies ammonia resolution is accurate, relevant and affordable for a topic with such a large impactful potential. Therefore, this review addresses a large literature survey from researchers and technologist across the globe currently assessing ammonia as an energy vector. The review approaches the current situation of ammonia continuing with a brief description of the importance of CFD to analyse ammonia flames. After this section the review addresses relevant CFD research on topics that progress from the most fundamental combustion parameters to innovative applications such as liquid injection, plasmas and porous media systems. Finally, major challenges and future developments are presented, with conclusions that address the versatility of studies and most interesting areas of further research relevant to the use of CFD modelling in the resolution of fundamental parameters in ammonia combustion systems. The novelty of the review lays on the discussion of the latest research, via computational fluid dynamics, intended to delve new technologies such as small burners, liquid atomization, plasma systems and porous media to deploy ammonia energy concepts to new fields that include medium heating, small transport, domestic applications and even aerospace systems.

* Corresponding author.
E-mail address: valeramedinaa1@cardiff.ac.uk (V.-M. A).
[1] These authors contributed equally to this work.

https://doi.org/10.1016/j.jaecs.2026.100550

Available online 6 August 2026
2666-352X/© 2026 The Authors. Published by Elsevier Ltd. This is an open access article under the CC BY license (http://creativecommons.org/licenses/by/4.0/).

1. Introduction

1.1. Towards the 2030 net-zero agenda

The energy demand is expected to surge in the coming years, underscoring the need for sustainable energy sources. However, the spurt in emissions is leading to climate change, with the potential to cause irreversible harm to the environment as global temperatures are estimated to rise continuously. The Intergovernmental Panel on Climate Change (IPCC) has predicted that the global temperature rise could exceed 1.5ºC and could become irreversible at 2.0ºC [1]. This would have a profound impact on living standards and global economic performance. Hence, novel energy generation techniques like wind, solar, and marine energy are being explored. However, these renewable sources face challenges related to intermittency and high deployment costs, which need to be overcome through viable energy storage solutions.

Important bodies, such as the Hydrogen Council, currently evaluate the hydrogen case, which as the name implies, assesses the full hydrogen chain, overseeing not only past tendencies, but also predicting future scenarios for the production, storage, distribution and utilization of such a molecule. In recent analyses, the Council released a document with details of "about-to-emerge" hydrogen corridors (i.e. large scale distribution routes) that will partially power the world [2]. It has been estimated that ~180 Mton per year are required to stay on track with current climate change targets (below 1.9 °C), with an introduction of hydrogen in a multitude of sectors. However, the lack of infrastructure, final investment decisions bound to uncertain scenarios, and macroeconomic challenges, have made the progress on the topic slower than anticipated [2]. On those lines, it is expected that government support (and carbon taxing) combined with deeper hydrogen introduction in the domestic, commercial and industrial markets will enable the creation of >30 active hydrogen corridors by 2035, all of which will enable a cost reduction in hydrogen whilst also ensuring energy security, supply diversification, and an inclusive transition, ideally for every social and economic background, across nations towards the implementation of net zero concepts.

As such, out of the total hydrogen estimates of 180Mtons [3], it is anticipated that 40Mtons will be transported by ships or pipelines over long distances, Fig. 1. This scenario leads to the use of various derivatives that include synthetic kerosene, methanol, liquid organic hydrogen carriers (such as toluene), and ammonia.

Similarly, chemical storage via hydrogen presents an opportunity for the recovery of renewable resources with zero carbon content and high gravimetric energy density. However, hydrogen has inherent limitations, such as extremely high liquefaction pressure, high permeability, and low controllability due to high reactivity, which pose issues for storage, distribution, and infrastructure deployment [4]. The costs of long-term hydrogen storage can be economically unviable for many applications, as the molecule needs to be cooled to cryogenic conditions below 20 K (−253ºC). Hence, other molecules as those above mentioned, offer a unique method of delivery with the potential of using existing knowledge and infrastructure.

Ammonia, one of these solutions, being the second most commercialized chemical in the world and with a trading history of >150 years, will continue growing its share amongst hydrogen-deploying corridors. Simultaneously, it will also see a continuous growth in market share for its utilization as an energy vector.

Currently, the use of ammonia for energy has been mainly focused on its use for cracking purposes. Ammonia, with three hydrogen atoms, has more hydrogen than hydrogen itself, and without embedded carbon and unique properties, the chemical becomes a great candidate for green hydrogen transportation and storage, which are achieved at relatively low pressures (~8 bar at 15 °C) or high temperatures (−33 °C compared to −253 °C of hydrogen under atmospheric pressure). These characteristics enable ammonia to be moved globally relatively easily, with infrastructure that has served the fertilizing industry for decades. Hence, ammonia can be decomposed to obtain its hydrogen atoms, thus serving as hydrogen enabler. However, the decomposition or "cracking" process requires energy, which can account up to 13% of the total energy content of the ammonia molecule [5]. Therefore, some applications will find the use of direct ammonia simpler and more economic, thus positioning ammonia as a cost-effective fuelling net-zero vector.

Ammonia has tremendous potential as a carbon-free fuel through flexible infrastructure that can serve not only for fertilizing purposes but also for fuel delivery, making it a promising and cost-effective solution for power generation [6]. Furthermore, the mature infrastructure and the possibility of producing ammonia through renewable energy sources have spurred exploration of its transition as the next sustainable fuel solution [4]. However, ammonia still has several limitations that need to be overcome before it can be widely used in combustion devices, such as poor ignition quality, low burning velocity, low energy density, narrow flammability limits, and high nitrogen oxide (NO_x) emissions. More research is needed to overcome these limitations and promote ammonia as a sustainable fuel solution. To overcome these issues, some of the most interesting and impactful research currently takes place via

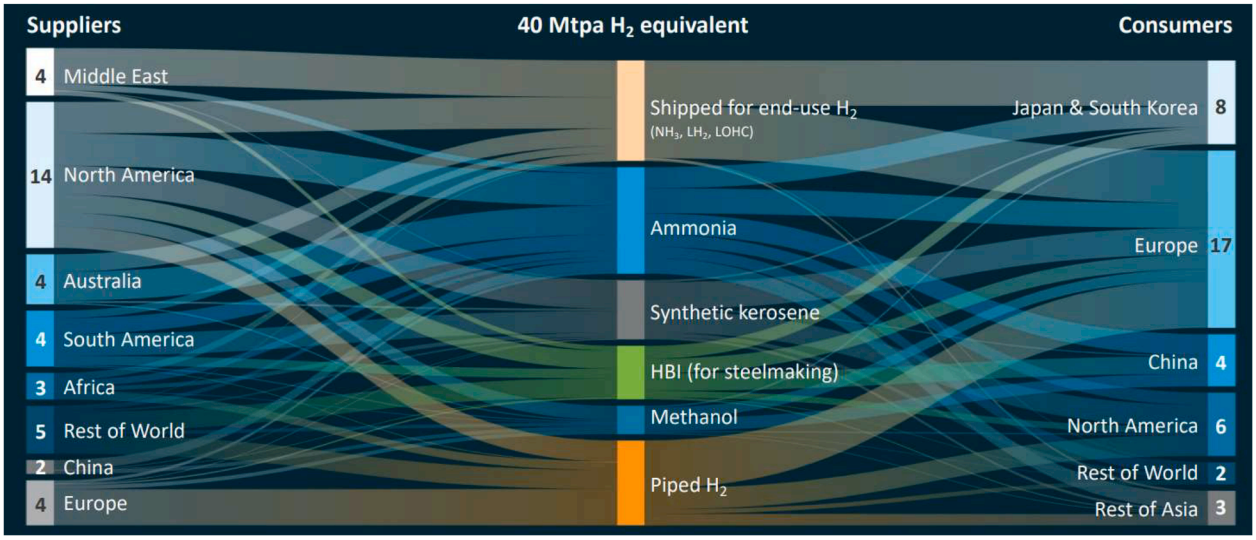


Fig. 1. Global clean hydrogen and derivatives long-distance trade flows, 2035 (Reprint from Ref. [3] with permission).

innovative modelling approaches, approaches that, due to their great variety, require a coherent literature review for those working on the subject or those interested in joining this research area.

Therefore, this review aims to cover the issues mentioned above by exploring the combustion fundamentals of ammonia as a fuel and emphasising the properties that influence its combustion performance and mixtures. Particularly, the manuscript will delve into crucial parameters currently evaluated via advanced modelling techniques through computational fluid dynamics that can provide valuable insights for improving our understanding of ammonia as a fuel.

1.2. The critical role of CFD modelling in ammonia combustion

In an era where computational capabilities expand exponentially, it is evident that CFD modelling would play an important role in the development of novel systems through the fundamental understanding of complex combustion processes. As computational capabilities increase and models become more flexible and economically viable, the use of CFD in areas such as ammonia energy will keep increasing, hence giving pace to a revolution of high-efficient components capable of using ammonia with high flame stability accompanied with ultra-low emissions. From the analyses of fundamental parameters via DNS to the development of large power stations operating at Gigawatts, CFD modelling will preclude some of the most interesting advancements that the community will see in the foreseeable future. Cost reductions, automated improvements, safe parameter evaluation, and customized implementations are just some of the great advantages that are now reachable thanks to CFD modelling of ammonia combustion systems.

Throughout these developments, CFD will keep playing a crucial role in understanding the complex physics of ammonia combustion, ranging from the underlying kinetics studied in 0D reactors to the turbulent flame behaviour captured by LES and DNS. RANS with tabulated chemistry will keep providing a pragmatic route for design-space search, whilst LES using finite-rate chemistry will keep expanding to gain insight into transient stability and emission mechanisms towards the abatement of instabilities and polluting emissions profiles.

It is also emphasized that ongoing algorithmic and hardware progresses are necessary to further facilitate high-fidelity methodologies for daily engineering designs. This includes leveraging emerging platforms like open-sources that will expand global contributions on the subject. By tackling current challenges (some of them described in the following sections), the CFD community can fully unlock its potential to accelerate the development of efficient, stable, and clean ammonia combustion systems for a sustainable energy future.

Particularly to this review, the novelty presented in this work relates to new ideas concerning concepts such as plasma system, liquid injection and porous media, all innovative concepts that are under scrutiny by the combustion community at the time of writing this manuscript. Without leaving behind concepts such as kernel propagation, laminar flames and turbulent burners, the review complements the work performed by others [6–10], where a combination of experimental and numerical findings are presented. Here, the review focuses mainly on numerical approaches to characterise and understand the intricate phenomena behind ammonia combustion. It is also emphasized that this review does not approach reaction mechanism analyses, as these have been reviewed elsewhere [11–15].

The scope of this review is therefore focused on CFD-based studies of ammonia combustion rather than on all aspects of ammonia fuel utilisation. The manuscript first discusses fundamental configurations, including ignition kernels, laminar flames, and turbulent research burners, because these studies provide the physical and chemical basis for model assessment. It then considers liquid ammonia injection, porous media combustion, and plasma-assisted combustion as emerging CFD-intensive topics where additional modelling challenges arise from multiphase flow, solid–gas heat transfer, radiation, or non-equilibrium chemistry. In this way, the review keeps the fundamental combustion discussion while highlighting novel modelling directions that are becoming increasingly relevant for ammonia power applications.

2. Fundamental combustion systems

2.1. Kernels

The fundamental study of ammonia combustion is heavily reliant on the chemical kinetic models employed for the resolution of ammonia's complex chemistry. However, it is also critical to emphasize the crucial role of the proper resolution of kernels, turbulence, curvature, instabilities and other fundamental parameters that occur along the flame. The adequate resolution leads to the improvement of methods that not only deliver better simulations but can also provide necessary amendments in the reaction mechanisms used with less highly computationally intensive methods, hence delivering strategies, equations and methods to make more efficient the modelling of complex ammonia combustion systems.

In order to acknowledge recent analyses, Kernel studies around small, immediately ignited volumes are addressed to identify some combustion tendencies of ammonia blends. Mukundakumar and Bastiaans [16], using 3D DNS analyses, showed the impact of hydrogen addition in premixed turbulent ammonia-hydrogen kernels, Fig. 2. By substituting 75, 50 and 25% ammonia at 0.8, 1.0 and 1.2 equivalence ratios, their results showed how the addition of hydrogen increases small-scale wrinkles, a phenomenon linked to the differential diffusion effects of hydrogen. As the hydrogen addition was reduced, these wrinkles diminished, as expected. However, an interesting effect was observed in which at constant hydrogen values but different equivalence ratios, with rich conditions denoting smoother profiles, an effect caused by the reduction of points on the surface where the flame speed is higher than the rest of the flame (in other words, less instabilities were observed). The study, also addressing flame curvature effects on the mixture's chemistry, found that getting closer to stoichiometric conditions would increase reactivity, with a critical effect caused by H radicals. As expected and observed experimentally in other studies [17], hydrogen reaches a point where reactivity changes and the molecule take over the reaction due to hydrogen's higher diffusivity and reactivity. Gaucherand et al. [10] evaluated dispersion relations for NH_3/H_2/air flames investigating a variety of blends with hydrogen ratios ranging from 0.4 to 1.0 under atmospheric conditions and equivalence ratios of $\phi = 0.4$, 0.5, and 1.0, as well as at elevated pressure of $p =$ 10 bar for $\phi = 0.5$. Their results show a monotonic reduction in instabilities with the reduction of hydrogen, a phenomenon caused by the increase in ammonia concentration that leads to a reduced peak growth rate, likely due to lower reactivity leading to a higher Zel'dovich number. However, their work also elucidates the impact of hydrogen preferential diffusion under lean conditions (phenomenon that will be described in more detailed later in this text). Some of these analyses were correlated to experiments performed by groups like Tohoku [18] and Orleans [19], where flame correlations and parameters such as the Markstein length -parameter that correlates burnt gas features and laminar flame thickness, quantifying a premixed flame's sensitivity to curvature and stretch, hence its propensity to be influenced by instabilities-, burning velocity and Lewis number were assessed. Although some results were not fully in agreement between models and experiments (as a consequence of the use of reduced mechanisms and removal of effects such as Soret, described in the following sections), most of the results fall within the observations of experimentalist groups, expanding the understanding behind the fundamental correlations under a variety of pressures, equivalence ratios and blends. For example, it was observed that by changes in hydrogen concentration, the Markstein number would increase, an indication of better resistance to intrinsic instabilities [18], whilst Zitouni et al. [19] found that the non-monotonic behaviour of the Markstein number is amplified when the equivalence ratio decreases. The group, using various Lewis

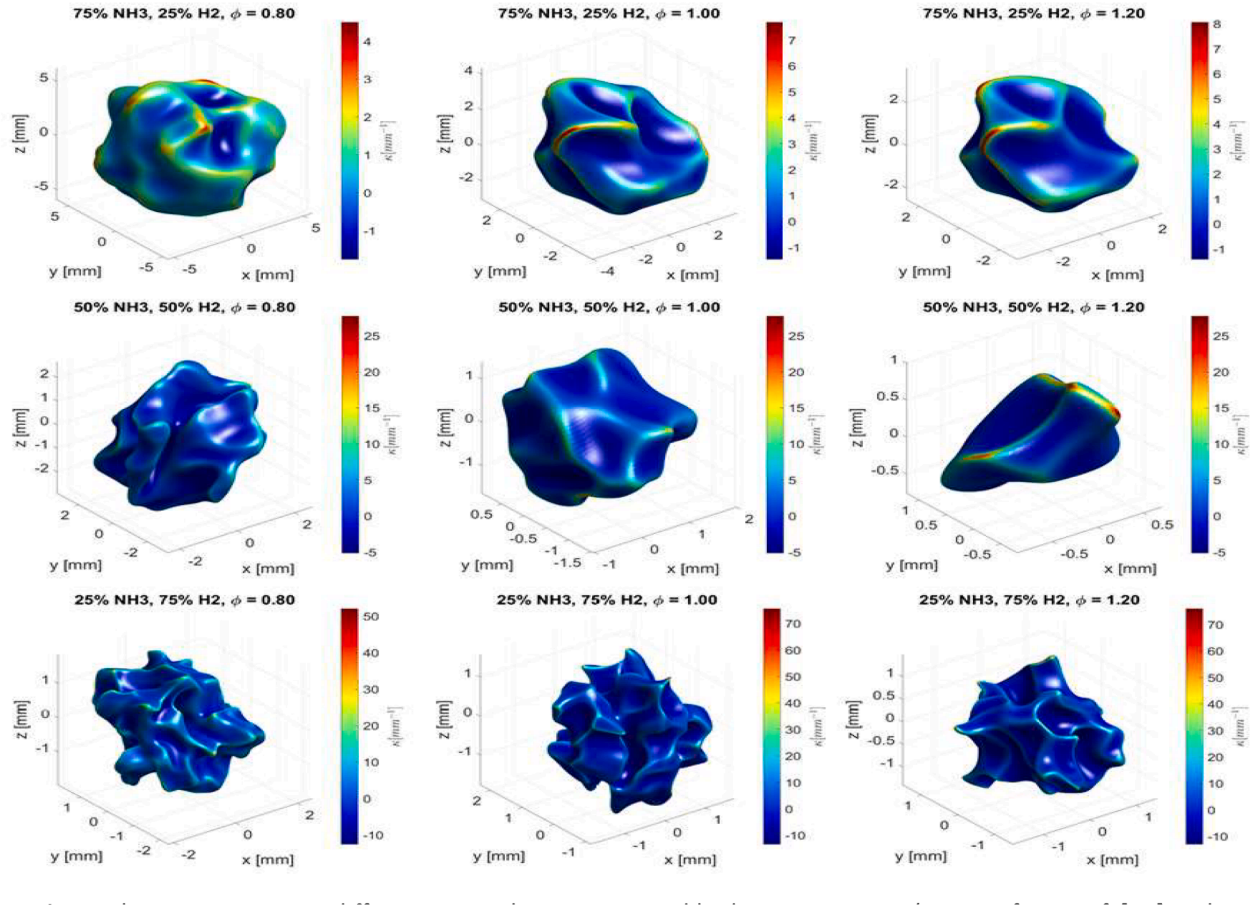


Fig. 2. Flame structures at different equivalence ratios and hydrogen contents (Reprint from Ref. [16] with permission).

correlations, demonstrated that a diffusional-based Lewis number would capture the non-linear stretch behaviour as function of H_2 addition under lean conditions, whilst a heat release-based Lewis number resulted in better agreement under richer conditions, thus reporting the impact of thermodiffusional instabilities with respect to equivalence ratio.

For more practical analyses, engine-relevant conditions have also been assessed to determine the impact of turbulent, pressurised atmospheres on the expansion and flame features of kernels in engine units. Yang et al. [20] tested a variety of cases (9) using up to 15% ammonia at initial pressures of 0.54 MPa and 445 K. Equivalence ratios at 0.9, 1.0 and 1.1 with turbulent fluctuations of 1 m/s were studied using 2D DNS analyses (all in line with experimental studies conducted elsewhere [21]). The results denote the impact caused by fuel content, with flame fronts less wrinkled with higher equivalence ratios (an analysis conducted using probability density functions). Similarly, higher heat release rates (HHR) occur in concave regions of the flame front, with convex zones showing the lower HHR, an effect that increases with hydrogen addition. As a consequence, the higher NO formation also increases within these concave zones. The work also addressed the importance of NH_2 as a HHR marker. Finally, and as expected, hydrogen addition not only showed higher laminar burning velocities, but also thinner flame thicknesses.

Du et al. [22] expanded the work by imposing gravitational constraints (1 g) that initially rose and stretched the flame, ultimately forming an inwardly curling vortex structure. By comparing the results with zero-gravitational and no radiation cases, the group found that the relationship between a density-weighted displacement speed (S^*_d) and the unstretched laminar speed had a direct impact on the propagation of the flame, with those cases under lean conditions (0.7 and 0.8 equivalence ratio) showing discrepancies between the lower and upper regions of the flame, hence leading to larger flame distortions. This emphasized the impact of gravity at leaner conditions. As expected, radiation pronounced this effect, but as a consequence of the reduced propagation speed caused by lower flame temperatures. Overall, gravity accelerates global flame propagation.

An et [23] investigated liquid ammonia flames at different conditions (temperature, droplet diameter, equivalence ratios, and ammonia content) to determine state change impacts on propagation, curvature and heat release. By using 2D LES analyses through OpenFOAM, the team found that the ignition from liquid propagates slower than in the gaseous form, a process caused by the heat losses of the evaporation process. Similarly, the change in initial temperature has also impacted on kernels, making more difficult to burn the chemical at lower temperature values (as expected), with most cases quenching the flame after ignition (at temperatures of 300 K vs 500 K). This process denotes the competing effect between heat production and phase change heat absorption during ignition. Also, diameter, equivalence ratios and ammonia fraction play important roles in the ignition process through heat losses phenomena.

Taken together, ignition-kernel studies show that the predictive accuracy of ammonia-kernel simulations is controlled by the competition between chemical reactivity, transport-driven flame deformation, and heat-loss processes. Hydrogen enrichment increases the availability of H radicals and accelerates early heat release, but it also strengthens differential diffusion effects, making local flame speed sensitive to curvature, Lewis number, and equivalence ratio. Under lean or highly stretched conditions, these transport effects can generate spatially non-uniform burning rates and promote local extinction or enhanced NO formation in curved regions of the flame front. In liquid-ammonia

kernels, this competition becomes more complex because evaporation cooling and phase change delay ignition and modify the local mixture composition. Therefore, kernel simulations are not only useful for reproducing ignition delay or flame radius, but also for identifying which transport and chemical parameters must be retained when reduced mechanisms or lower-cost CFD models are applied to larger configurations.

2.2. Laminar flames

Laminar flames correspond to the simplest combustion regime, where viscous forces dominate over inertial forces and the flow remains orderly. In this regime, heat and mass transfer occur through molecular diffusion, and the reactive zone remains spatially well defined, enabling direct examination of chemical pathways, transport effects, and pollutant formation mechanisms [24–26]. Because of their simplicity and deterministic behavior, laminar flames are routinely used to validate reaction mechanisms and quantify baseline flame properties for ammonia-based fuels. For emerging carbon-free energy carriers such as ammonia, these studies establish reference burning velocities, extinction behavior, nitrogen chemistry pathways, and fuel–oxidizer interaction characteristics prior to scaling toward turbulent or practical devices.

Laminar ammonia flames can be modeled numerically under one-dimensional or multidimensional configurations. One-dimensional flames are suited for mechanism development and parametric studies of chemical pathways, whereas two-dimensional configurations introduce geometric confinement, flame curvature, and wall effects. The combination of both approaches provides the basis for constructing predictive models for ammonia combustion.

2.2.1. One-Dimensional numerical studies

One-dimensional laminar flame simulations constitute the primary tool for assessing chemical kinetic models and extracting canonical flame properties. Depending on configuration, these flames may be freely propagating or counterflow-stretched, enabling determination of key quantities such as the laminar burning velocity (LBV), flame thickness, and Markstein length. These parameters are essential inputs for turbulent flame models and establish reference behavior for fuel blends [24]. Stretch effects are typically investigated through counterflow flames or spherically expanding flames, with the Markstein length characterizing the flame response to curvature and strain.

In premixed one-dimensional flames, fuel and oxidizer are fully mixed prior to entering the reaction zone. Freely propagating flames allow direct computation of LBV and internal flame structure, while counterflow flames quantify extinction strain rates. In non-premixed one-dimensional configurations, fuel and oxidizer diffuse toward one another prior to reaction, enabling assessment of transport-driven ignition and evaporation phenomena [27].

Early studies quantified the laminar burning behavior of ammonia and ammonia-containing mixtures. Hayakawa et al. [28] measured unstretched burning velocities and Markstein lengths for NH_3/air flames up to 0.5 MPa using spherically propagating flames, showing that ammonia has a significantly lower LBV than hydrocarbons and that its reactivity decreases with pressure. They compared their measurements with several detailed reaction mechanisms, including Miller et al. [29], Lindstedt et al. [30], Konnov [31], and Tian et al. [32], demonstrating substantial discrepancies in nitrogen chemistry predictions.

Subsequent mechanism development targeted improved prediction accuracy. Nakamura et al. [33] developed a model optimized for weak ammonia flames in micro-reactors. Da Rocha et al. [34] evaluated ten mechanisms for NH_3/H_2/air flames and reported significant sensitivity of ignition delay and LBV to hydrogen addition. Okafor et al. [35] extended GRI-Mech 3.0 [36] to incorporate ammonia pathways, improving reproduction of burning velocity and NO formation, and later proposed a reduced model validated at pressures up to 0.5 MPa. Stagni et al. [37] introduced a comprehensive kinetic mechanism based on high-fidelity reactor experiments, covering a wide range of temperatures relevant to industrial ammonia systems. More recent comparative studies reinforced the variability of current models: Zhu et al. [38] analyzed reaction pathways for NH_3/H_2 mixtures under engine-relevant conditions; Girhe et al. [39] assessed 16 mechanisms using quantitative similarity scores; Alnasif et al. [40] and a follow-up study [14] evaluated $>$30 models for laminar flame speeds and N_2O formation, respectively.

One-dimensional simulations have also been applied alongside experiments to interpret flame structure and pollutant formation. Han et al. [41] examined NH_3/air and blended flames using the heat flux method to obtain LBV and used numerical simulations to analyze radical distributions inside the flame. Similar hybrids of experimental and numerical studies continue to refine nitrogen sub-mechanisms, confirm dominant NOx pathways, and identify the impact of hydrogen enrichment.

Within the scope of laminar combustion, it is also important to distinguish detailed kinetic studies from the CFD-oriented use of reduced chemistry. The present review does not aim to provide a detailed discussion of elementary ammonia reaction mechanism development; however, laminar flame simulations remain essential because they provide reference quantities for mechanism selection in CFD. Parameters such as laminar burning velocity, flame thickness, Markstein length, extinction strain rate, ignition tendency, and $NO/N_2O/NH_3$ formation trends are commonly used to assess whether a reduced mechanism is suitable for multidimensional simulations.

Recent developments in mechanism reduction illustrate the practical realization of this modelling strategy. Nakamura et al. [42] generated a simplified ammonia reaction model with 14 species and 45 reactions using a genetic-algorithm approach and integrated it into CFD simulations of a 1 MW boiler test facility. More recently, other examples appear in the literature, such as the LTNGNH$_3$ mechanism [43] or the work from Pan et al. [44] where models were developed as intermediate-size mechanisms for $NH_3/CH_4/H_2$ combustion, comprising 52 species and 275 reactions and targeting CFD applications involving ammonia blends. These and other studies show how reduced mechanisms [45], stochastic/reactor-based approaches [46], tabulated chemistry [47], and virtual-chemistry strategies are valuable for CFD when they preserve the key laminar flame and emission characteristics relevant to the operating range considered.

2.2.2. Two-Dimensional numerical studies

While experimental studies have substantially characterized laminar ammonia flame behavior and one-dimensional simulations have enabled comprehensive mechanism development, the number of two-dimensional and three-dimensional numerical investigations remains comparatively limited. These multidimensional simulations are essential for capturing effects such as flame curvature, differential diffusion, flow recirculation, and wall interactions that cannot be represented in one-dimensional frameworks.

Two-dimensional laminar flame simulations extend one-dimensional models by resolving flame curvature, confinement, wall interaction, and localized heat-loss effects. These configurations typically solve the reacting Navier–Stokes equations under low-Mach or fully compressible formulations with finite-rate chemistry, allowing explicit treatment of differential diffusion and nitrogen pathways beyond the scope of 1D analyses. The resulting data quantify stabilization mechanisms, strain-induced extinction, and spatially resolved NO formation, phenomena inherently absent from one-dimensional flames.

Early 2D studies on ammonia flames focused on confined micro-combustors, using laminar finite-rate chemistry and detailed nitrogen mechanisms to investigate heat loss and NO formation under channel flows. Cai et al. [48] demonstrated that perforated plates inside micro-combustors promote localized recirculation, extend residence time, and modify NO generation pathways despite laminar flow conditions (Re $<$ 500). Fuel-related NO source terms dominated the overall NO production, whereas contributions from thermal-NO pathways were

negligible for pure ammonia, consistent with earlier conclusions from one-dimensional studies. Their simulations showed that recirculation pockets promote hot-spot formation and enhance flame stabilization, while NO production occurs predominantly along the reaction zone, modulated by local curvature rather than global equivalence ratio, Fig. 3.

Efforts then shifted toward resolving intrinsically multidimensional features (curvature, flame wrinkling, and differential diffusion) using compressible direct numerical simulation (DNS). Netzer et al. [49] investigated atmospheric-pressure premixed NH_3/H_2/air flames, in which flame wrinkling was induced by imposing a very weak turbulent velocity field. The imposed turbulence primarily served to generate flame-front curvature while maintaining an essentially laminar flame structure. All relevant diffusive and reactive scales were resolved using a grid spacing of 20 μm. Their results showed that hydrogen enrichment reduces local extinction sensitivity and alters NO formation location. Furthermore, it induces marked spatial separation between NO and OH peaks with peak NO displaced toward regions of stronger positive curvature and enhanced strain. This leads to non-uniform NO formation along the flame front, even under nominally laminar inlet conditions, Fig. 4. These DNS computations remain among the most resolved ammonia-blend flame simulations available.

Studies of burner-stabilized flames confirmed the strong influence of boundary conditions and wall temperature on flame structure. Da Rocha et al. [50] and Chen et al. [51] used axisymmetric domains with mixture-averaged transport to show that flame lift-off and NO emissions depend on co-flow velocity, wall heat losses, and burner material. More specifically, at elevated pressures, Rocha et al. [50] combined numerical simulations and laser diagnostics to study NH_3–CH_4–air flames and demonstrated pressure-dependent shifts in NO production pathways and enhanced NH formation zones. Their results confirmed that the dominant NO formation under pressure emerges as a dual-peak emissions profile, which is due to the convective transport of NO from the upstream region near the burner, an effect more prominent in premixed flames, a trend visible in the DNS–PLIF comparison, Fig. 5. Furthermore, NO under pressure is also suppressed as a consequence of three-body radical recombinations that impact on the radical formation in the inner premixed flames.

Subsequent studies introduced additional external forcing terms to alter flame structure. Gao et al. [52] used a finite-rate laminar model with the detailed Okafor's mechanism [35] and imposed a temperature-dependent magnetic body force on the momentum equation. Their simulations revealed upstream flame displacement and modification of the OH field under a magnetic gradient, establishing a feedback mechanism between oxygen susceptibility and diffusion rates, Fig. 6. In parallel, plasma-assisted ammonia flames were modelled using additional transport equations for vibrational energy and non-equilibrium effects, modifying radical pools and shifting stabilization positions, consistent with earlier plasma-assisted methane studies [53].

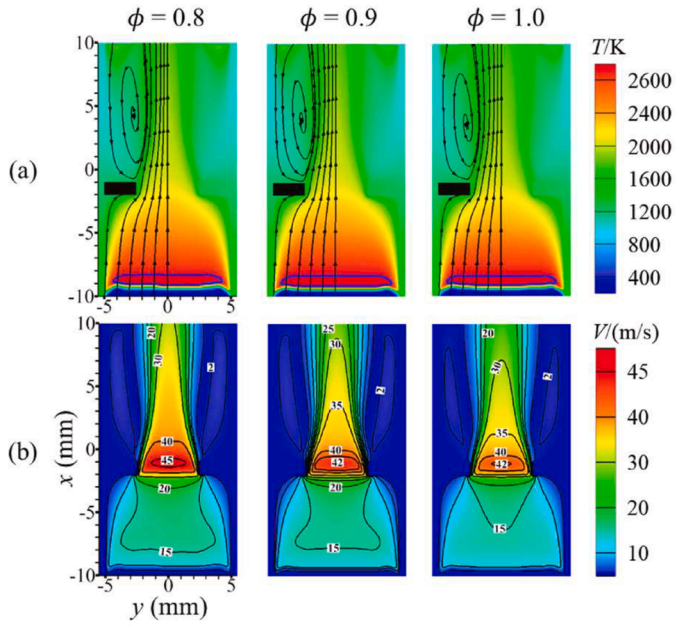


Fig. 3. Contours of temperature, streamlines, and OH mass fraction for varying equivalence ratios (Reproduce from Ref. [48] with permission).

Wall-quenching investigations have shown that heat losses modulate flame thickness and radical concentrations. Thomas et al. [54] employed full multicomponent diffusion and compared various kinetic models, finding that mixture-averaged diffusion overpredicts NO relative to multicomponent transport. Their simulations accurately reproduced measured NO distributions across hydrogen blending ratios, confirming the critical role of differential diffusion, Fig. 7.

Wang et al. [55,56] analyzed hybrid CH_4–NH_3 flames and demonstrated noticeable gradients in temperature and species profiles near cold walls, while Song et al. [56] reproduced flame–wall interactions for NH_3/H_2 jets impinging on horizontal plates, linking wall distance and equivalence ratio to stabilization height. Tamadonfar et al. [57] simulated sidewall quenching using detailed chemistry and refined meshes near boundaries, reporting increased quenching distance with hydrogen addition and confirming that Soret effects remain small except at lean conditions. Recent studies by Zeng et al. [58] extended these insights to inclined-wall configurations and validated numerical predictions against experiments for flame impingement and pollutant emissions.

Across these studies, common observations can be identified: flame stabilization depends sensitively on confinement geometry and heat losses rather than global equivalence ratio; hydrogen modifies the onset of instabilities and shifts NO formation peaks; and accurate nitrogen chemistry requires kinetic mechanisms validated under multidimensional transport. Two-dimensional laminar configurations thus provide an essential intermediate tier between canonical 1D flames and turbulent simulations, capturing effects that govern flame anchoring, pollutant spatial distribution, and boundary-dominated behavior.

Most practical combustion applications operate under turbulent conditions, the transition from laminar to turbulent combustion introduces additional complexities including enhanced mixing, flame wrinkling, local extinction and reignition events, and modified pollutant formation pathways. For example, Karimkashi et al. [59] showed how the change from laminar to turbulent conditions has a drastic impact on the production of NOx emissions, an effect caused not by a change in NO/HNO reaction pathways (main culprits of emissions formation), but by the formation of curved shapes that benefit (or detriment) from the differential diffusion of hydrogen and the depletion of important radicals such as O and H. Similarly, Netzer et al. [49] showed how flame topology has no impact on N_2O formation. Contribution such as the thermodiffusion and pressure have also been assessed separately to observe their impact on various flames, with pressure reducing NO overall but causing acute effects across the flame brush due to thermodiffusive instabilities [60]. These complexities require further analyses to elucidate the discrepancies between cases and determine the impact of turbulence on ammonia flames. Therefore, the following section examines turbulent ammonia flame investigations, building upon the laminar flame fundamentals established here.

3. Turbulent combustion systems

3.1. Research burners

Compared to burners used in practical engineering applications, laboratory-scale burners, despite having lower thermal loads and simplified geometric configurations, offer valuable insights into

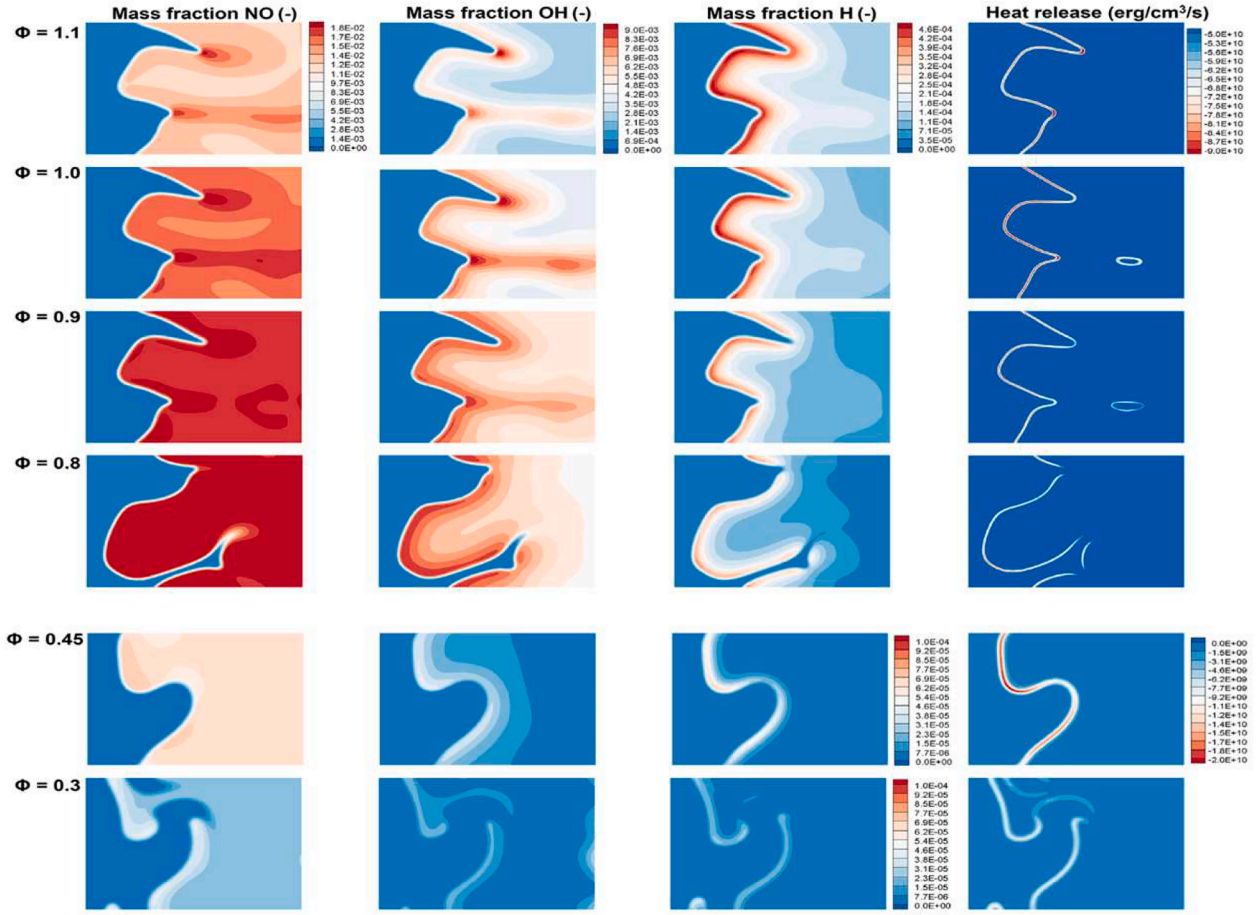


Fig. 4. Wrinkled premixed flame contours showing NO, OH, and H mass fractions (Reprint from Ref. [49] with permission).

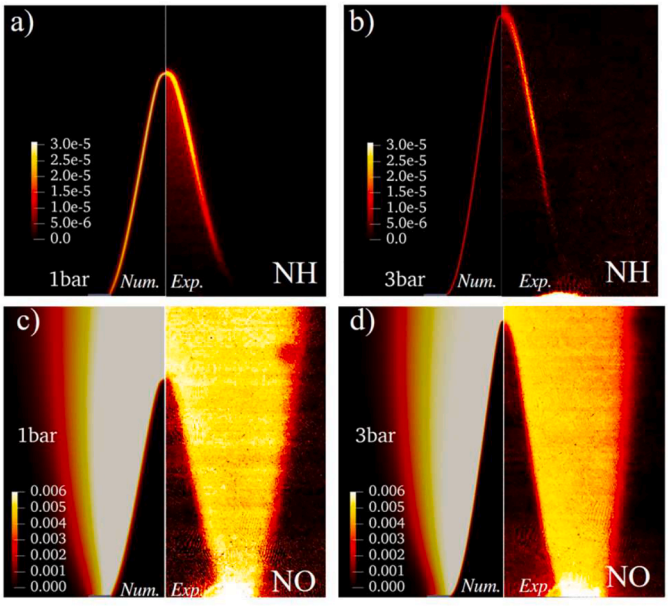


Fig. 5. Spatial distribution of NH and NO at 1 and 3 atm, DNS vs. PLIF (Reprint from Ref. [50] with permission).

turbulence-flame interactions that are crucial for optimizing the design of industrial burners. For such small-scale burners, researchers can more readily conduct detailed combustion diagnostics and comprehensive numerical simulations. The synergy of these approaches facilitates a deeper understanding of complex turbulence-combustion interactions and provides key insights into the mechanisms governing various emissions formation, stability profiles and transient phenomena. This section provides a critical review of the current status of CFD modelling for lab-scale ammonia combustion systems, based on a comprehensive analysis of diverse studies, assessing the state of the art in modelling whilst discussing outstanding validation issues and identifying fundamental barriers that need to be addressed before predictive simulation capabilities can be achieved.

Tables 1 and 2 provide a structured overview of the CFD studies reviewed in this section, classified by simulation methodology (DNS, LES, or RANS), CFD solver, combustion sub-model, reaction mechanism, and level of experimental validation. Table 1 summarises studies conducted on research-scale single-stage burners, while Table 2 covers multi-stage burner configurations.

The choice of CFD methodology represents a constant compromise between computational cost and predictive fidelity. Reynolds-Averaged Navier-Stokes (RANS) models are widely used as the pillar of industry design for their low computational cost. Studies by Füzesi et al. [61], Geng et al. [61], and Zhao et al. [62,63] have shown that RANS is able to reasonably predict time-averaged flow fields and global flame structure in small turbulent burners, the dominant recirculation zones, mean velocity fields, and overall reaction zones can still be represented when the flame remains statistically steady. For example, Füzesi et al. [64,65] showed that steady-state RANS was able to reasonably predict outlet values, however the model could not describe the large amplitude oscillations and the transient behaviour observed at high ammonia shares, since these oscillations were associated with unsteady heat-release fluctuations and combustor-scale flow–flame coupling that are

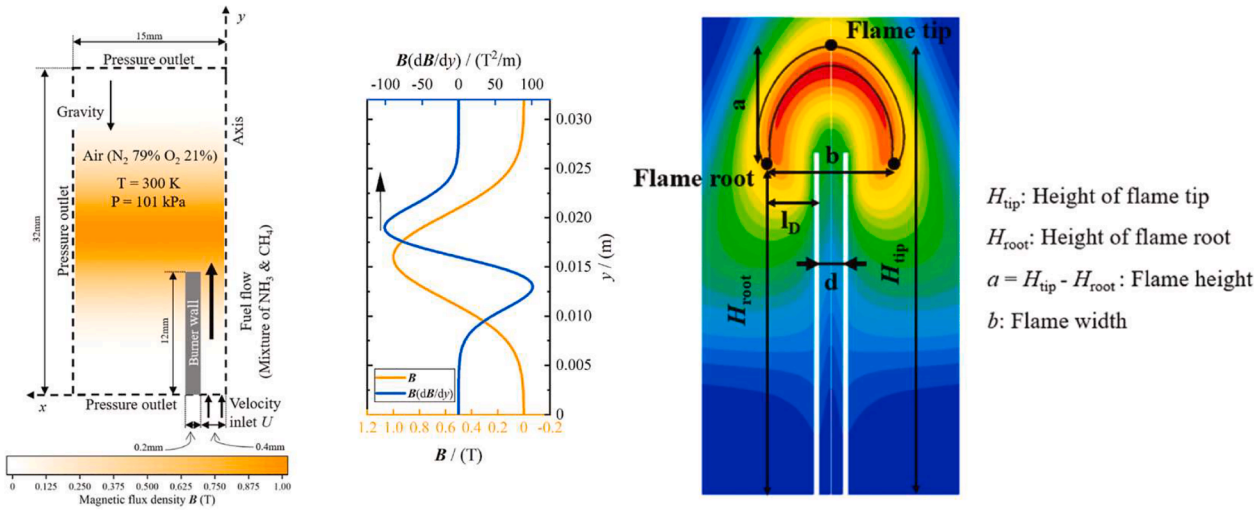


Fig. 6. Computational domain (left), boundary conditions(center) and schematic of laminar micro-diffusion flame configuration (right). (Reprint from Ref. [52]) with permission).

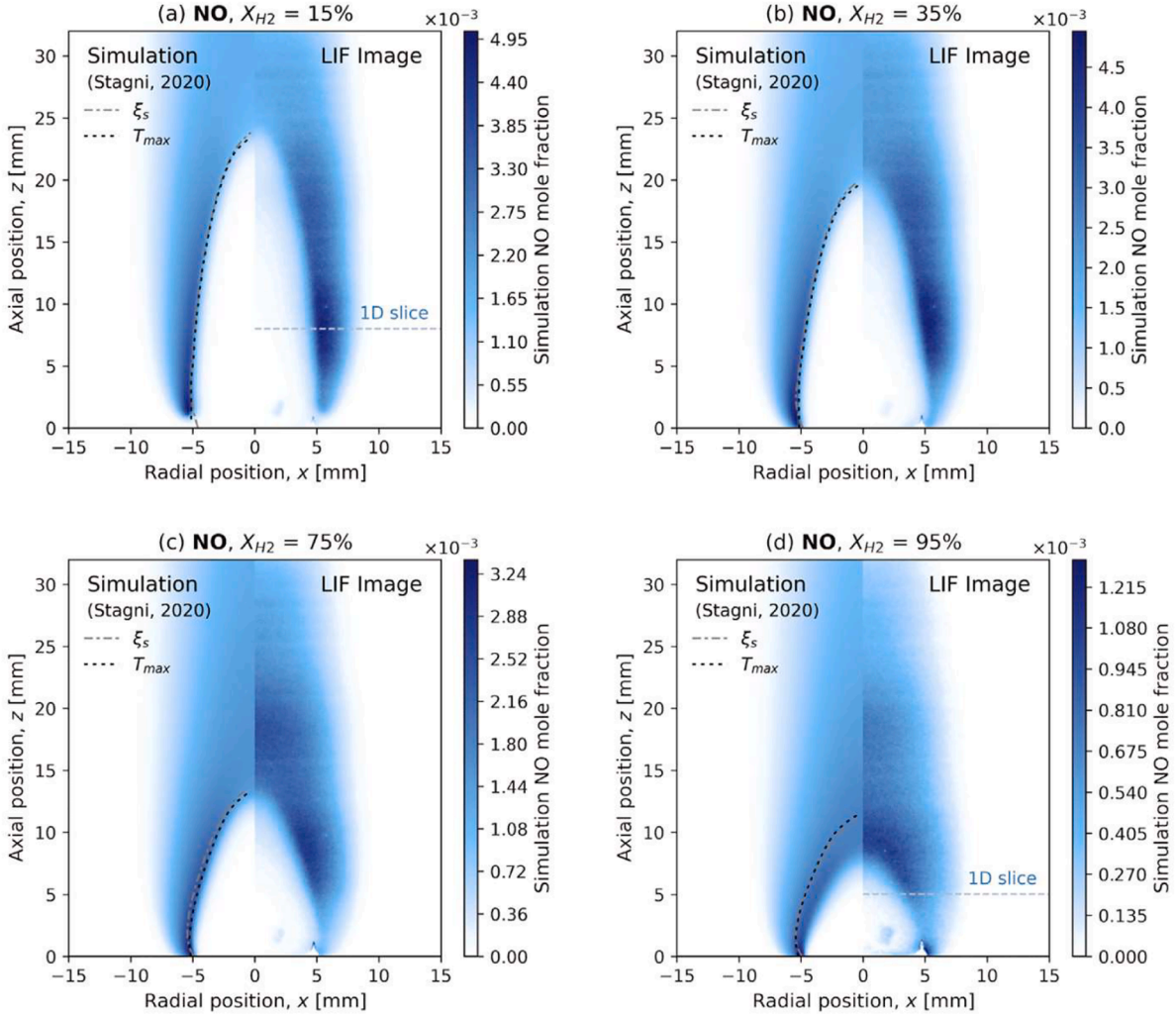


Fig. 7. NO-LIF measurements and simulation comparisons for varying fuel hydrogen ratios (Reprint from Ref. [54] with permission).

averaged out in steady RANS. Similarly, Geng et al. [61] employed RANS for optimization of a double-swirl staged combustor, presenting an optimal configuration resulting in minimum NOx. However, they reported seeing over-estimations caused by using adiabatic wall

Table 1
Literature research on numerical simulation articles on turbulent combustion phenomena of ammonia fuel in research-scale burners.

Ref.	Fuels	Method	Dim.	Software	Model	Mechanism	Validation level
[61]	NH_3–CH_4	LES	3D	OpenFOAM	FGM	Okafor-59–368	Exp. (NO_x, T)
[62]	NH_3–CH_4–H_2	RANS	3D	Fluent	EDC	GRI-49–277	Exp. (NO_x)
[63]	NH_3–CH_4	RANS	3D	Fluent	EDC	Okafor-59–356	Exp. (species)
[64]	NH_3–CH_4	LES	3D	OpenFOAM	DTF	Okafor-59–356	Exp. (T, species)
[65]	NH_3–CH_4	LES	3D	OpenFOAM	DTF	Xiao-31–243	Exp. (NO_x, T)
[65]	NH_3–CH_4	RANS	3D	Fluent	FGM	Okafor-42–130	Exp. (NO_x, T)
[66]	NH_3–CH_4/H_2	RANS	3D	Fluent	EDC	GRI3.0–53–325	Exp. (NO_x, T)
[67]	NH_3–H_2	LES	3D	OpenFOAM	DTF	Okafor–42–130; Zhang-44–251	Exp. (OH-PLIF)
[69]	NH_3	LES	3D	OpenFOAM	FGM	Stagni-31–203	Exp. (NO_x emissions)
[70]	NH_3–H_2	LES	3D	OpenFOAM	DTF	Okafor-42–130	Exp. (velocity, T)
[71]	NH_3	LES	3D	OpenFOAM	PaSR	Han-35–177	Exp. (OH-PLIF, T)
[72]	NH_3–H_2	LES	3D	AVBP	MF-TFLES	ARC-15–211	Exp. (OH-PLIF, NO_x)
[73]	NH_3–H_2	LES	3D	OpenFOAM	DTF	Stagni-31–203	Exp. (NO_x, T)
[74]	NH_3–CH_4	LES	3D	OpenFOAM	LK / Zuo combined	Okafor-59–356	Exp. (velocity, T)
[75]	NH_3–CH_4	LES	3D	OpenFOAM	CCM	Okafor-59–356	Exp. (NO_x, stability)
[76]	NH_3–CH_4	LES	3D	OpenFOAM	NA-FGM	SanDiego-70–321	Exp. (flame structure)
[77]	NH_3–CH_4	LES	3D	OpenFOAM	DTF	Okafor-42–130	Exp. (OH-PLIF, T)
[77]	NH_3–CH_4	LES	3D	OpenFOAM	PaSR	Okafor-42–130	Exp. (OH, T, NO_x)
[80]	NH_3	LES	3D	OpenFOAM	PaSR	Tian-84–703	Exp. (T, species)
[80]	NH_3	LES	3D	OpenFOAM	PaSR	SanDiego-70–321	Exp. (OH, NO_x)
[81]	NH_3–H_2	LES	3D	Fluent	DTF	CRECK-27–154	Exp. (T, NO_x)
[83]	NH_3–H_2	DNS	3D	S3D / in-house	Direct finite-rate chem.; mixture-averaged transport	UC-San Diego	Numerical only
[84]	NH_3–CH_4	RANS	3D	Fluent	EDC	Tian-84–703	Exp. (NO_x, velocity)
[86]	NH_3–H_2	RANS	3D	Fluent	EDC	Okafor-19–63	Exp. (NO_x)
[93]	NH_3–H_2	DNS	3D	AVBP	Direct finite-rate chem.; multicomponent transport (Soret)	CRECK-21–88	Exp. (LIF / OH-PLIF)
[103]	NH_3–H_2	DNS	2D	PARCOMB	Direct finite-rate chem.; mixture-averaged transport	Otomo-32–204	Numerical only
[105]	NH_3–H_2	DNS	3D	S3D	Direct finite-rate chem.; mixture-averaged transport	SanDiego-38–84	Exp. (PLIF comparison)

Table 2
Literature research on numerical simulation articles on turbulent combustion phenomena of ammonia fuel in multi-stage burners.

Ref.	Fuels	Method	Dim.	Software	Model	Mechanism	Validation level
[69]	NH_3	LES	3D	Fluent	EDC	Stagni-31–203	Exp. (NO_x, T)
[77]	NH_3–CH_4	LES	3D	OpenFOAM	PaSR	Okafor-42–130	Exp. (OH-PLIF, NO_x)
[89]	NH_3–CH_4	LES	3D	OpenFOAM	DTF	Okafor-42–130	Exp. (NOx)
[87]	NH_3	RANS	3D	OpenFOAM	EDC / FGM	Shrestha-33–253	Exp. (NO/NH_3 air-staged)
[88]	NH_3	RANS	3D	OpenFOAM	EDC	Shrestha-33–253	Exp. (MILD-like flame)
[104]	NH_3–H_2	DNS	3D	S3D	Direct finite-rate chem.; mixture-averaged transport	SanDiego-38–84	Numerical only (staged DNS reference dataset)
[139]	NH_3	RANS	3D	Fluent	EDC	Wang-188–1604	Exp. (flue-gas data)
[144]	NH_3–H_2	RANS	3D	Fluent	EDC	SanDiego-21–64	Exp. (NO/NH_3, bluff-body + swirl)

assumptions, because neglecting wall heat transfer artificially retained higher gas temperatures, thereby promoting stronger ammonia oxidation and thermal/fuel-NO formation than observed experimentally. RANS models using EDC or FGM have showed acceptable global trends but failed to capture unsteady dynamics, such as lean blow-off or flashback, due to steady-state turbulence-chemistry assumptions. This is because lean blow-off, flashback, local extinction, and re-ignition are governed by instantaneous energy dissipation, vortex breakdown, flame stretch, and local radical depletion, whereas conventional RANS only resolves their averaged effects rather than the actual transient events. Similarly, Klimanek et al. [66] used RANS - EDC modelling, and by employing a modified San Diego mechanism, they showed significant over predictions in flame speed calculations, leading to inaccurate flame quenching behaviour unless radiation and heat losses were modified. This indicates that the predicted extinction boundary was not controlled by turbulence modelling alone, but also by the kinetic mechanism and thermal boundary condition used to determine the local flame temperature and radical pool. Practically the same issues were reported by Davies et al. [67] and Liu et al. [68] whose RANS-FGM analyses did not capture either local extinction nor re-ignition profiles through stratified flows, because tabulated chemistry approaches may not preserve the full dependence of ammonia oxidation and NOx chemistry on mixture fraction, enthalpy loss, scalar dissipation, and local residence time. The capability to model unsteady dynamics related to lean blow-out or flame attachment, mainly in swirling or stratified combustors, in turn was limited by RANS assumptions of a steady-state chemistry-turbulence interaction [69]. Therefore, the controlling limitation of RANS is not simply low spatial resolution, but the loss of instantaneous coupling among coherent vortices, flame stretch, heat release, and nitrogen chemistry. In contrast, Large Eddy Simulation (LES) resolves the large, energy-containing turbulent structures and models only the sub-grid scales, making it far superior for capturing unsteady flame dynamics as those observed in these turbulent systems. As demonstrated by Mazzotta et al. [70], Wei et al. [71], Bioche et al. [72] and Lu et al. [73], LES approaches have been found superior to RANS in capturing transient turbulence-flame interactions and combustion instabilities in laboratory-scale burners, because the resolved flow field can describe the periodic formation, convection, and breakdown of vortical structures that modulate flame surface area, local strain rate, and heat-release fluctuations. The work of Wang et al. [74–76] with LES showed the crucial role of wall heat loss, equivalence ratios and combustor shapes, demonstrating that adiabatic predictions significantly overestimate NO,

while a proper cooling model might yield an undesirable compromise by increasing N_2O. Mechanistically, this occurs because high-temperature adiabatic zones favour rapid NH_3 oxidation and NO formation, whereas cooling suppresses NO-producing pathways but may shift nitrogen chemistry toward incomplete oxidation products such as N_2O under specific temperature–residence-time windows. Somarathne et al. [77–79] have used LES to show that swirling flows are able to stabilize pure ammonia and air flames, although strong pressure analyses have limited NO and NH_3 slip by reducing OH radicals. This suggests that pressure, heat release, and radical chemistry are coupled: changes in pressure and temperature alter the OH pool, which then affects both NH_3 consumption and NO-forming pathways. Furthermore, Wei et al. [80] applied LES to reveal the stabilization mechanism for a 10% hydrogen concentration mixture by modifying flame structure and increasing the small-scale wrinkling, thereby preventing blow-off. The added hydrogen therefore did not merely increase the global heating value; it enhanced local reactivity and flame-surface density, allowing the flame to better resist stretch-induced extinction. Several studies, including those previously raised, confirmed that LES better resolves transient flame propagation and NOx emissions than RANS, achieving $<$10% average NO prediction error compared to RANS's 35% underestimation. However, this accuracy comes with a computational cost exceeding 40,000 CPU hours, compared to only 5000 for RANS simulations. The primary barrier to LES is its computational expense, often requiring more resources in orders of magnitude than RANS, as quantified by Mazzotta et al. [81] and Jójka et al. [82]. For instance, Bioche et al. [72] reported that detailed chemistry LES required $>$22,000 core hours and exhibited sensitivity to mesh refinement between 5 M and 15 M cells.

Finally, DNS studies further elucidate the limitations of FGM for ammonia combustion. DNS results for a single-stage combustor [83] reveal a marked disparity between the distribution of heat release rate (HRR) versus the reaction progress variable c in turbulent ammonia flames and the corresponding laminar flame structure: the peak HRR under turbulent conditions is approximately double that observed laminarly. In contrast, for methane combustion, the HRR distributions of turbulent and laminar flames exhibit close agreement. This comparison indicates that ammonia flame structure is more strongly altered by turbulence than methane flame structure, because the slower chemistry and thicker reaction zone allow turbulent strain, curvature, and differential diffusion to modify the local HRR–progress-variable relationship. Therefore, an FGM table generated from laminar flamelets may become unreliable when applied to highly strained ammonia flames, unless additional dimensions such as enthalpy loss, scalar dissipation, curvature, or local extinction effects are included.

The comparison between RANS, LES, and DNS studies indicates that the dominant modelling limitation is not only the choice of turbulence closure, but the ability of each approach to preserve the coupling between local mixing, heat release, and nitrogen chemistry. RANS-based EDC or FGM approaches can reproduce time-averaged flame position and global emissions when the flame is statistically steady, but their predictive capability decreases when blow-off, flashback, local extinction, or re-ignition are governed by coherent vortical structures and transient scalar dissipation. LES improves the description of these unsteady mechanisms because large-scale turbulent structures and flame wrinkling are resolved, but its accuracy remains dependent on the subgrid combustion model, heat-loss treatment, and the reduced kinetic mechanism used for NOx, N_2O, and NH_3 slip. DNS provides the clearest mechanistic information by resolving flame curvature, differential diffusion, and local radical pools, but its cost confines it to canonical or laboratory-scale configurations. Therefore, the key bottleneck for turbulent ammonia CFD is the transfer of DNS-level mechanistic insight into reduced, validated closures that remain affordable for burner and device-scale simulations.

Accurately predicting emissions, particularly NOx and N_2O, remains the most significant hurdle. The problem is twofold. First, the formation pathways are highly non-linear and sensitive to local conditions. As Zhang et al. [84] illustrated, NO emissions are extremely sensitive to wall heat loss where changing the wall thermal boundary condition modified the local temperature field, which then altered the balance between NH_3 oxidation, NO formation, and N_2O survival. They also found that increased cooling air flow reduced NO but caused a dramatic increase in N_2O. This trade-off occurs because stronger cooling suppresses high-temperature NO-forming reactions but may preserve intermediate nitrogen species and favour N_2O accumulation before complete conversion to N_2. Similarly, Kovaleva et al. [85] and Somarathne et al. [79] identified an optimal, slightly rich equivalence ratio window ($\sim$1.1–1.3) that simultaneously minimizes NO and unburnt NH_3, a delicate balance that models must capture precisely. This operating window is chemically important because leaner mixtures may provide excess O/OH radicals that promote NO formation, whereas overly rich mixtures may suppress NO but leave insufficient oxidizing capacity for complete NH_3 consumption. This sensitivity exposes reaction mechanism uncertainties. Chemical kinetic mechanisms constitute a critical component in the numerical simulation of ammonia combustion. However, the mechanisms employed across the surveyed literature of this review exceed 80 in number (i.e. with many variations of standard mechanisms being developed over the last 5 years), exhibiting remarkably broad distributions [15]. Mashruk et al. [86], in a study of a humidified RQL combustor, found significant discrepancies in NO and NH_3 predictions across five different mechanisms, underscoring the lack of a universal standard. The common practice of using reduced mechanisms for computational tractability, while necessary, inevitably introduces further uncertainty. This is because reduced mechanisms may remove or lump minor species that become important under cooled, diluted, high-pressure, or fuel-rich zones, especially where N_2O, HNO, NO reburning, and NH_3 slip are controlled by slow post-flame chemistry. Following the same tendency, several researchers have highlighted that accuracy strongly depends on the chosen mechanism.

Due to the low reactivity of ammonia, flame stabilization is a prominent issue, as previously raised in the fundamental section. The DNS by Wiseman et al. [83] made basic contributions to the stability mechanism. Specifically, the DNS indicates that ammonia flames cannot be treated as methane-like flamelets because turbulence modifies the HRR–progress-variable relationship and changes the local balance between heat release, radical production, and extinction tendency. With respect to the combustor, Wei et al. [80] employed CFD to demonstrate that blow-off for NH_3/air flames is a product of the combined effects of flame stretch and heat release rate with more flame area that leads to a narrower stabilization limit and a larger extinguishing trend, Fig. 8. Srinivasarao et al. [87,88] experimentally and numerically established a new multi-stage burner stabilization concept for pure ammonia over an extended operability range. They attributed the unit's success to enhanced mixing in combination with internal NO reburning by NH_i radicals. Although LES can account for these effects, RANS models are often unable to resolve transient vortex breakdown and local extinction processes which precede blow-off. Owing to the significantly larger laminar flame thickness of ammonia premixed flames (δ_L, $NH_3 \approx$ 1.5 mm) compared to methane flames (δ_L, $CH_4 \approx$ 0.5 mm), coupled with its considerably lower laminar flame speed (SL, $NH_3 \approx$ 7 cm/s vs. SL, $CH_4 \approx$ 49 cm/s), the Ka number for ammonia combustion under identical turbulence intensity is approximately 21 times higher than that for methane combustion (as calculated). This implies that the structure of ammonia flames is more susceptible to turbulent perturbations, presenting a significantly elevated risk of local extinction difficult to resolve in RANS but viable via LES.

Very recently, Wang et al. [89] used Large Eddy Simulation with a dynamic thickened flame (DTF) model to study an axially staged ammonia methane RQL combustor. Through temperature–mixture fraction scatter plots and modified flame index analysis, they showed that the secondary flame operates in a diffusion dominated mode, deviating from the intended lean premixed combustion. This recently

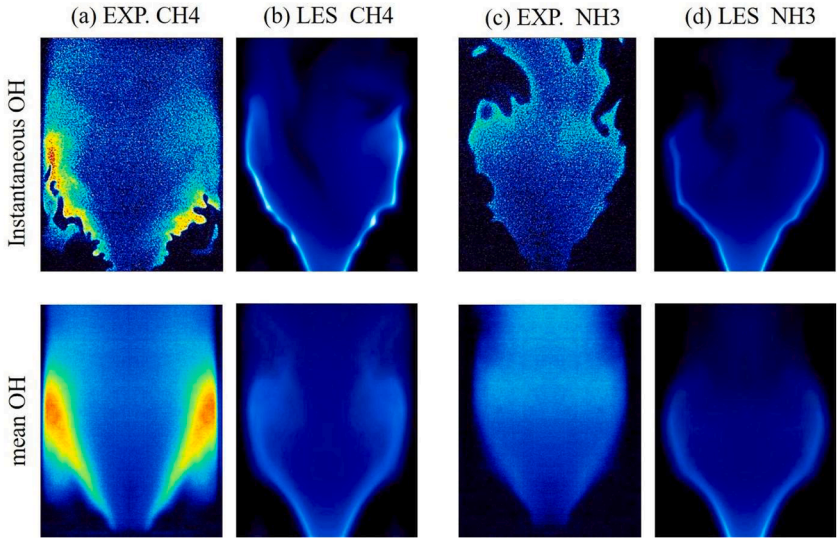


Fig. 8. The comparison of flame structure of NH_3/air flame and CH_4/air flame. Up: instantaneous OH; down: mean OH (Reprint from Ref. [80] with permission).

reported finding reveals that highly reactive H_2 and CO from rich primary products cause premature ignition, preventing sufficient premixing with secondary air. The work from these authors support further evaluations of more industrially representative burners, which deserve a review on their own right. However, it is important to raise some critical aspects of the use of some of these models and the boundary conditions imposed to properly resolve more complex, turbulence cases. For example, an important restriction to the method using Large Eddy Simulations was pointed out by Honzawa et al. [90] who found that the standard adiabatic FGM fails to predict emissions, hence making necessary the use of non-adiabatic FGM (NA-FGM) approaches which included heat loss effects on NO and CO. The reason is that adiabatic FGM assumes that the flame chemistry evolves along a high-enthalpy manifold, whereas practical ammonia flames experience wall cooling, dilution, and incomplete post-flame conversion that shift the local state away from the adiabatic table. These were important components in the use of ammonia firing, as the heat loss effect has a critical impact on the formation of species. For example, higher temperature profiles across the combustor layers directly reflect on higher ammonia oxidation, hence marking a drastic consumption of the chemical whilst boosting NO formation, an effect not recorded experimentally. Third body reactions and post-combustion recombinations also add to these complexities, thus making necessary the introduction of complex heat loss assumptions that reflect practical phenomena more realistically. Due to ammonia's high Karlovitz number (Ka), the applicability of reduced-order models like FGM becomes limited, particularly in lean or highly strained conditions, a problem that increases with the study of transient phenomena such as unstable flame behaviour.

3.2. Instabilities

When using ammonia blended with various chemicals, instabilities tend to appear along the flame that can impact on the stability of the system and the combustion process. At the flame front, instabilities such as diffusive-thermal instabilities (caused by different rates of heat and mass diffusion) and hydrodynamic instabilities (driven by gas expansion and fluid dynamics) can play important roles in the stability of the flame under a variety of conditions, while phenomena such as flame flashback and blow-off promote scenarios that can lead from bad combustion efficiencies to dangerous situations capable of triggering safety protocols.

Recent works performed by Ma et al. [91] depict, through Schlieren analyses and CHEMKIN-Pro studies, the impact of having hydrogen at various concentrations (0 to 40%), equivalence ratios and atmospheric conditions in ammonia blends. Their results show that at higher equivalence ratios, the flame will be more stable, whilst higher hydrogen content enhances wrinkling. They evaluated a critical Peclet Number (which can be correlated to a critical flame radius at which stability changes), showing how the addition of hydrogen leads to smaller critical flame radius. The process is believed to be caused by a reduction in the effective Lewis number and flame thickness, whilst stability increases with equivalence ratio. This effect can be correlated to this critical Peclet Number. Flame thickness, another important variable, also suffers due to the increase in hydrogen and temperature, with a reduction in flame thickness. The combined effect will weaken the thermal diffusion effect of the flame, enhancing hydrodynamic instabilities. Under pressure (0.2 Mbar) the analysis focused on lean (0.8) and stoichiometric (1.0) conditions, with results that showed the instability dependance on equivalence ratio. As for 0.8 values, there is an opposite trend between flame thickness and thermal expansion ratio, which in turn promotes hydrodynamic instabilities. Under these same conditions, the reduction in effective Lewis number amplifies these instabilities, whilst at 1.0 the higher effective Lewis number no longer plays an important role in this phenomenon. As for ammonia blends without hydrogen, the minor changes in effective Lewis number lead to a decrease in both expansion ratio and flame thickness, hence suppressing hydrodynamic instabilities through thermal diffusion effects that smooth the flame surface.

Instabilities and curvature effects have also been observed through various CFD strategies proposed by many groups. For example, the work produced by Netzer et al. [49] revealed the impact of curvature on NO formation caused by equivalence ratio variations and the interaction between NO, H and O radicals whilst using 2D ammonia/hydrogen/nitrogen/air planar flames via DNS. The group also observed that thermo-diffusive effects linked to the differential diffusion of hydrogen have critical effects on nitrogen oxide formation. Concave-shaped curvatures lead to a local increase in equivalence ratio, which in turn can either generate more (under lean conditions) or less (under rich conditions) NO emissions. Local radical pools, concave (H_2 depleted) and convex (H_2 enriched) shaped portions have all a critical impact on emissions formation due to a change in reactivity caused by flame curvature. Rieth et al. [92] expanded the analysis by studying the curvature effects on the burning rates of various hydrogen/ammonia/air flames at 1 and 10 atmospheres. The results showed the critical impact of hydrogen on the chemistry caused by the changes in flame curvature and pressure, which in turn impacts on the H_2 diffusion through increased spatial gradients, resulting in localized equivalence-ratio

enrichment and super-adiabatic conditions that accelerate and strengthen the flame front, hence generating drastic changes between conditions, as illustrated between heat release rates at 1 and 10 atmospheres, respectively, Fig. 9.

Rieth et al. [93] continued with the work using DNS analyses of various ammonia/hydrogen blends, finding that a progress variable based on H_2O is suited to parametrize the combustion of these mixtures, emphasizing in the study the impact of the preferential diffusion (i.e. differences in diffusion characteristics between different species) of hydrogen radicals and their impacts on thermo-diffusive effects with changes in curvature. Chakraborty et al. [94] performed DNS analyses of two $NH_3/H_2/N_2$ blends under lean conditions (0.8 equivalence ratio) with a reduced mechanism consisting of 25 species and 175 reactions and a database generated using the KARFS (KAUST Adaptive Reactive Flows Solver) code. The results show that differential diffusion affects the flame by generating either stoichiometric or fuel-rich pockets that enable localised diffusion burning modes, which in turn unbalance the flame, hence impacting on strain rates. Additional work [95] investigated the influence of differential and preferential diffusion effects, showing how the contributions of H, OH, O_2, NH_3 and H_2O directly impact on Lewis numbers. These changes impact on the diffusion of deficient reactants into the reaction zone in comparison to thermal diffusion effects, hence affecting burning rates per unit area in comparison to their corresponding unstretched laminar premixed flame. Damköhler hypotheses were evaluated, showing their potential for prediction of parameters in premixed NH_3/H_2 flames.

Xu et al. [96] studied the behaviour of cracked ammonia blends using a 1D simulation analysis in a counterflow twin flame burner with Han's mechanism [97]. Preferential diffusion and effective Lewis number were assessed to determine the extinction strain rates of various blends with different cracking ratios. The preferential diffusion effect was separated from the effective Lewis number, hence showing the impacts of each parameter both separately and together. It was found that a dimensionless extinction strain rate (defined by the strain rate, flame thickness, and laminar burning velocity) reaches a peak at intermediate ammonia cracking ratios (~0.18), with the preferential diffusion primarily driving this effect, a phenomenon linked to the shift in hydrogen consumption, with H radicals being produced more upstream by the earlier consumption of H_2, which in turn shifts flame position and enhance strain-induced extinction. By evaluating the impact of the effective Lewis number, minor effects are observed, whilst the removal of the preferential diffusion leads to a significant decrease of the flame thickness. Interestingly, the study showed that the preferential diffusion effect is the main component in the non-monotonic behaviour of the studied flames.

Kinuta et al. [98] performed 3D DNS studies on H_2 and a NH_3/H_2 blend (10/90 mol%) to determine fundamental parameters and emissions production during boundary flashback events under lean conditions. The results denote how the addition of ammonia substantially improves flashback resistance, an effect caused not only by the reduced laminar burning velocity but also by an increase in the quenching distance and a change in curvature effects, Fig. 10. Similarly, the group observed how NOx and N_2O formation close to the wall are heavily impacted by heat loss and flame curvature, hence impacting on chemical kinetics and preferential diffusion, as previously raised in the previously discussed studies. It is at this stage where groups like Wu et al. have started exploring the use of deep learning to improve combustion chemistry of dual fuels, demonstrating improvements of up to 30 times for chemical calculations acceleration (from 11.51 to 0.38 s) and 10 times faster overall resolution, a study that shows the potential of machine learning to support these fundamental studies [99].

Additional works have looked at the intrinsic instabilities of using ammonia/hydrogen blends. The work from D'Alessio et al. [60,100] shows the impact of thermodiffusive effects and pressurised conditions on a 50–50 (vol%), high-temperature (500 K) hydrogen/ammonia lean blend. The Soret Effect and pressure increase denote a promotion of onset of intrinsic instabilities. The Soret Effect is only accounted for light species (H_2, H) when included in the analyses. Comparisons with other studies showed that the increase in temperature led to stabilization of the flame (defined by cut-off wavelengths related to intrinsic flame instabilities), whilst the addition of the Soret Effect had direct impacts on dispersion relations, cut-off wavelenghs, and growth rates, all confirming that by neglecting these effects in high hydrogen-content flames there is a risk of large deviations from real flame phenomena.

Looking into more detail, Lehmann et al. [101] performed DNS simulations that showed how blends with 40% H_2 molar content present strongest instabilities due to a joint effect between Lewis and Zeldovich numbers. The effect becomes non-monotonic under lean conditions, banishing at fuel rich mixtures. This process seems to be caused initially by the weaking of the flame through an imbalance between heat and species diffusion, which at rich fuel conditions denotes a Lewis number close or above unit, making the influence of thermodiffusive instabilities negligible. Additionally, and for the first time known by the authors, non-monotonic trends were observed as a consequence of HO_2 pathways, which change due to ammonia addition. These findings support experimental findings where blends with >40% hydrogen content behave differently to those with lower H_2 concentrations [10]. Their work also delivered a sensitivity analysis for the Zeldovich number to link micro and macroscopic effects caused on ammonia/hydrogen flames where reactivity is coupled to chemical kinetics to derive effects caused by the interaction between species such as NH_2 with the chain propagating effect of HO_2. The results show the reduction of influence of

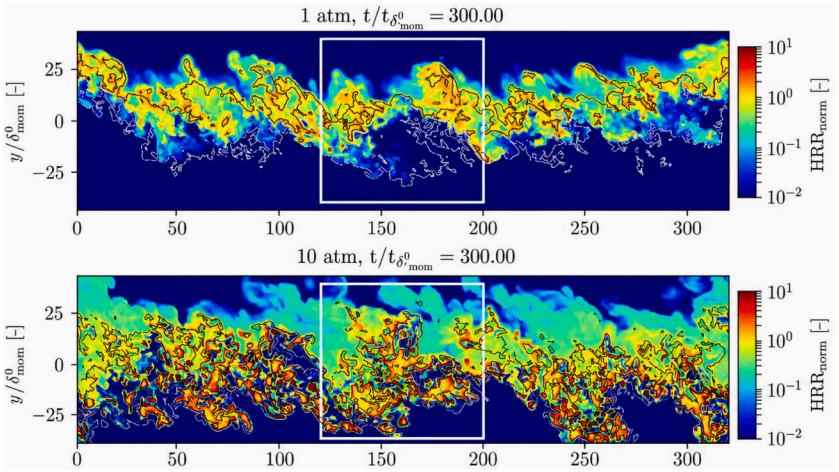


Fig. 9. Normalized heat release rate at the same normalized time (Adapt from Ref. [92] with permission).

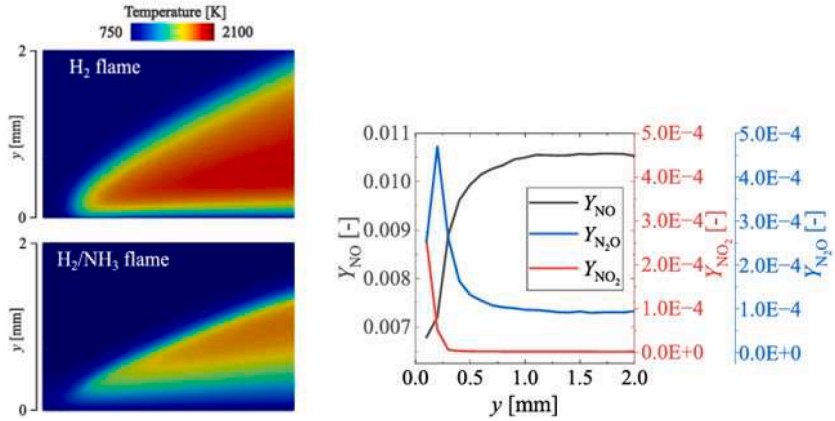


Fig. 10. Left) Instantaneous temperature distribution at z = 15 mm and t = 0.74 ms show the drastic changes in curvature and quenching distance between H_2 and NH_3/H_2. Right) Emissions and distribution from the wall (y) for the NH_3/H_2 blend (Reprint from Ref. [98] with permission).

H+O2(+M)=HO2(+M) at pressure, reaction that plays an important role in these types of instabilities.

Additional studies have also evaluated more practical cases. From the study of the evaporation of ammonia-based droplets [102] and auto-igniting mixing layers of NH_3/H_2 under engine relevant conditions [103], to staged combustion [104] and rich-quench-lean (RQL) pressurised cases [105], fundamental findings on NO production, reactivity, heat release, variations in volatility, and turbulence intensity impacts, are all addressed mainly by using Direct Numerical Simulations that delve into fundamental insights of all these complex phenomena.

A recurring theme across all studies is the critical lack of comprehensive experimental data for validation. While global emissions and velocity fields are commonly measured, there is a severe scarcity of data for validating transient phenomena and localized species concentrations. Reviewing a great variety of experimental measurement studies on ammonia turbulent combustion, it is possible to detect a notable gap: the measurement techniques employed are relatively limited, primarily encompassing Particle Image Velocimetry (PIV), OH-PLIF, NO-PLIF, and outlet flue gas analysis. To date, quantitative measurements of internal flow field species concentrations and temperatures (e.g., via Raman scattering techniques) have not been reported. Such data are essential for the quantitative assessment of the accuracy of turbulent combustion models and reaction mechanisms. This validation gap between available experiments and computations was emphasized by several groups [69, 73,80] who noted that insufficient experimental data across equivalence ratios and pressures constrain CFD model accuracy. High-fidelity LES or DNS simulations thus remain speculative without detailed validation datasets encompassing velocity, species, and temperature fields. This lack of validation leads modelers to use validated mechanisms with small datasets, increasing uncertainty that propagates into predictions for systems of interest. The work of Hayakawa et al. [106] clearly highlighted this challenge, finding mechanisms that performed well for laminar flame speed could not accurately predict NO and NH_3 in product gases suggesting a disconnect that can only be addressed by focused experimental data. While the benchmark flame library provided by the International Workshop on Measurement and Computation of Turbulent Non-premixed Flames (TNF) includes methane benchmark flames, a benchmark flame for ammonia combustion remains absent. It is anticipated that this situation may improve at the forthcoming 17th TNF Workshop, planned for 2026 [107].

3.3. Liquid injection

Ammonia injection using vapour phase has been the ruling technique over the last few years, as this method enables better, more efficient combustion of ammonia as the fuel is relatively ready for oxidation. However, there is a novel concept (with <4 years of conception after the resurrection of the ammonia combustion notion in the 2000s) that employs liquid ammonia injection. Although the use of this technique is still in its infancy, it is obvious that mastering it would lead to great advantages in the implementation of ammonia systems. For example, ammonia liquid injection presents several challenges such as higher NOx emissions, N_2O production and higher unburned ammonia concentrations. However, advantages such as high flow rates (hence power outputs), removal of evaporation systems, and direct injection with fewer components could overcome the challenges previously stated [108]. Along those lines, ammonia liquid injection and sprays have been in the scope of recent studies for their utilization in combustion systems.

Table 3 provides a structured overview of the liquid-ammonia injection CFD studies reviewed in this section, classified by simulation methodology, CFD solver, spray and combustion sub-models, and level of experimental validation.

For liquid-ammonia injection, the controlling parameters differ from gaseous-fuel combustion because atomization, flash boiling, evaporation cooling, and local mixture formation directly determine the subsequent ignition and emission behaviour. Ambient pressure and temperature control whether the jet remains non-flashing or enters a flashing regime, while injection pressure, nozzle geometry, droplet size, and heat of vaporisation govern penetration, vapour formation, and local equivalence ratio. These processes explain why models can reproduce global penetration length or spray angle while still showing larger uncertainty in droplet-size distribution, vapour mass fraction, and near-nozzle phase change. The main modelling bottleneck is therefore the coupling between in-nozzle flow, thermodynamic non-equilibrium, breakup, evaporation, and finite-rate chemistry. This coupling is particularly important because evaporation cooling can delay ignition and shift the balance between complete NH_3 oxidation, NOx formation, N_2O production, and unburned NH_3 slip.

Before addressing current numerical investigations on the subject, it is important to provide some preliminaries on the different aspects of using ammonia liquid injection in various systems. For industrial heat and power generation, burners designed with liquid injection features produce stationary flames that couple liquid fuel spray processes (such as jet breakdown and atomization) with fluid dynamics, making this interaction a key component in defining the overall efficiency of the injection process and emissions production stages, Fig. 11. Similarly, other applications such as propulsion systems (e.g. reciprocating engines) require the formation of a two-phase mixture through which the flame propagates. Therefore, liquid injectors and their design play a critical role in the efficiency of the atomization process, thus creating patterns that enable the introduction of ammonia immediately before or directly into the combustion system. Finally, it is important to consider the implications of retrofitting using existing infrastructure. This is an important example for the case of propane in marine systems (i.e. likely

Table 3
Literature research on numerical simulation articles on turbulent combustion phenomena of liquid-ammonia injection.

Ref.	Fuels	Method	Dim.	Software	Model	Mechanism
[23]	Liq. NH_3	LES	3D	n.r.	Euler-Lagrange; evaporation + ignition	Exp. (ignition delay, droplet evaporation)
[102]	Liq. NH_3	LES	2D	OpenFOAM	Euler-Lagrange; flash-boiling evaporation	Exp. (flame propagation speed)
[112]	Liq. NH_3	RANS	3D	CONVERGE v3.0	k-epsilon + KH-RT breakup; AMR	Exp. (Schlieren, SMD, vapour boundary)
[113]	Liq. NH_3	RANS	3D	n.r.	Spray penetration sub-model	Exp. (spray penetration and angle)
[114]	Liq. NH_3	LES	3D	CONVERGE v3.0	KH-RT breakup; nozzle geometry effects	Exp. (penetration, angle, area; high-speed photography)
[116]	Liq. NH_3	LES	3D	OpenFOAM v7	Smagorinsky SGS; Rayleigh-Plesset bubble growth + flash-boiling	Exp. (spray morphology, drag coeff., evaporation rate)
[117]	Liq. NH_3	RANS	3D	n.r.	KH-RT + variable discharge coeff.; vaporisation-induced resistance	Exp. (spray breakup pattern)
[118]	Liq. NH_3	RANS	3D	n.r.	Rp-based flash boiling; nozzle + aerodynamic breakup	Exp. (transitional and flashing regime penetration)
[119]	Liq. NH_3	RANS	3D	n.r.	Multi-bubble flash boiling (Rayleigh-Plesset + nucleation)	Exp. (spray angle, penetration)
[120]	Liq. NH_3	DNS	3D	n.r.	Full DNS; phase change, bubble growth and collapse	Numerical only (bubble dynamics near nozzle)
[121]	Liq. NH_3	RANS	3D	OpenFOAM v6	Euler-Lagrange + Lee condensation; liquid particle tracking	Exp. (condensation mass, multi-hole injector)
[122]	Liq. NH_3 + diesel	RANS	3D	CONVERGE	SAGE + KH-RT + NTC + wall film	Exp. (Schlieren, dual-fuel spray, penetration)
[123]	Liq. NH_3 + pilot diesel	RANS+1D	3D	n.r.	FGM tabulated manifold; 1D pre-analysis	Numerical only (exploratory)
[126]	Liq. NH_3 / NH_3–CH_4	DNS	3D	OpenFOAM	cp-DNS; Euler-Lagrange; Okafor mechanism (Ref. [34])	Exp. (OH-PLIF + Mie scattering; HRR profiles)
[128]	Liq. NH_3	LES	3D	OpenFOAM	Extended flamelet manifold; Euler-Lagrange	Exp. (flame curvature, droplet-flame interaction)
[129]	Liq. NH_3	LES	3D	n.r.	Swirl burner; wall cooling model; spray evaporation	Exp. (NOx, N_2O, unburned NH_3 vs. wall heat loss)
[130]	Liq. NH_3 (bulk release)	RANS	3D	n.r.	SST k-omega + Lee evaporation-condensation; two-phase interfacial area	Exp. (12 m3 tank release; vapour plume, phase fraction)
[131]	NH_3-kerosene (scramjet)	RANS	3D	n.r.	Dual-fuel injection; convective cooling model	Numerical (specific thrust, thermal protection)

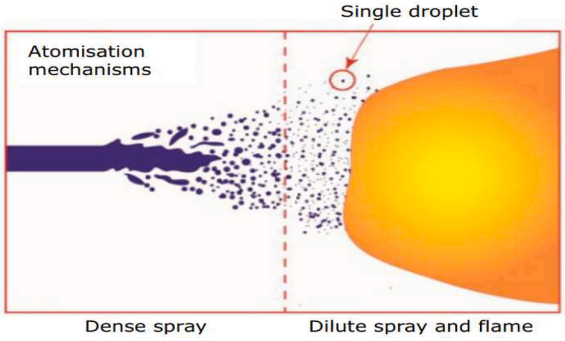


Fig. 11. Schematic representation of liquid fuel spray combustion (Reprint from Ref. [109] with permission).

to be the first to be replaced by ammonia, as previously described), as both fuels share many commonalities (e.g. feeding systems, evaporator components, storage materials, etc.). Therefore, liquid ammonia injection deserves its own analysis in terms of current progress through CFD modelling, not only for its critical role in future systems, but also for its interesting features and complex nature, which can only be resolved using computational fluid dynamics.

Compared to other conventional fuels, ammonia's vapour pressure creates additional complexities that need to be considered during atomization. As explained previously, atomization and breakup patterns are already complex, with the latter being a recurrent issue for modelling purposes due to the intricate phenomena that cause the rippling and final breakup of the liquid jet. However, and different to other fuels, ammonia's vapour pressure and boiling properties make it exceptionally difficult at low pressures and/or high ambient temperatures. Further, the higher Joule-Thomson effect of ammonia (i.e. related to the change in temperature with the change of pressure) leads to phase variations that are not present in most conventional fuels. In essence, the thermodynamically unstable jet release that involves the metastable liquid jet is a combination of a transition between liquid and gaseous states across the spray profile [109,110]. Therefore, depending on ambient system conditions, the use of ammonia liquid injection could lead to "flashing" phenomena, effects observed with low boiling point fuels. This effect causes three main states: a) vapour; b) non-flashing liquid; c) flashing liquid [111]. As the complexity of such environments is extremely difficult to capture experimentally, numerical computational methods have been used to develop models capable of supporting transient and nano-scale effects through the various fields of these spray and jet fields.

Recent studies produced by Zembi et al. [112] employed CONVERGE v3.0 by incorporating standard k-ε turbulence model resolution and adaptive mesh refinement. Detailed simulations of the complexities of flashing and non-flashing sprays were presented with experimental validation (up to 15 bar) using Schlieren imaging and non-intrusive laser diffraction methods in a rig that enabled the determination of vapour boundaries and Sauter Mean Diameters (SMD), respectively. The good validation of the global spray characteristics confirmed the appropriate numerical approach, which included the blob model for injection and the breakup approach upon parcels introduction following the competing Kelvin-Helmholtz and Rayleigh-Taylor (KH-RT) models. Although the temporal and spatial resolution of droplet sizes and vapour mass fraction were more challenging, the results evidenced the flashing patterns under low ambient pressure, with a plume that enters the three previously mentioned stages. Of particular interest is the end of the spray, which, from vapour, turns into liquid droplets as a consequence of the rapid expansion and large heat of vaporisation, hence cooling ammonia for its reconversion back to liquid, Fig. 12.

The results compared the SMD values between cases, and predictions confirmed a reduction in SMD from 40 to 10 μm between non-flashing

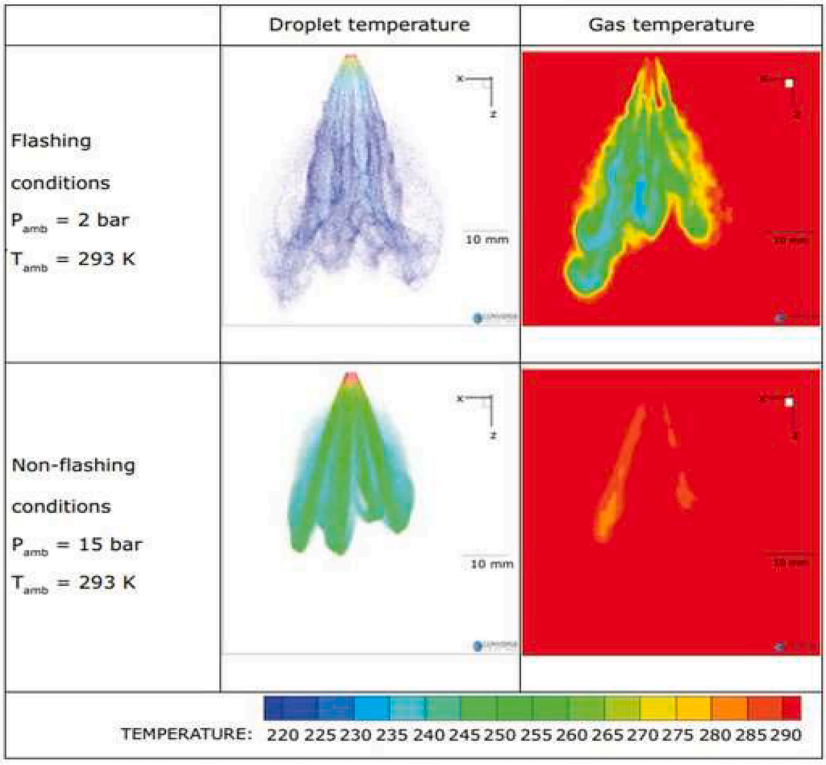


Fig. 12. Simulation showing vapour and droplet formation under flashing and non-flashing conditions (Reprint from Ref. [112] with permission).

and flashing conditions. The change impacts on the type of spray mode (i.e. from diffusion to premixed propagation). Giles et al. considered this phenomenon to be an advantage in the use of ammonia liquid injection for reciprocating engines, as this would lead to an increase in overall efficiency consequence of greater compression ratios [109]. Additional experiments and simulations from Chen et al. [113] showed a similar high-pressure, engine-like conditions, that the spray exhibits three stages along its central axis: a) constant, b) logarithmic, and c) linear growth, thus impacting the vapor-phase mass fraction that alters the penetration intensity of the jet. Interestingly, and in line with works described below, the logarithmic growing region appears to be the best for ignition under diffusion combustion modes. Meanwhile, the variation in pressure showed a change in size of all regions, with a decrease in the first stage under higher pressures that leads to an enhanced second stage region. The group expanded their research and proposed an empirical formula for spray penetration and angle, showing with their experiments and simulations good correlation for more immediate analyses.

Yang et al. [114] approached the analysis of liquid ammonia injection via spray diffusion combustion modes. By using a constant volume vessel and high-speed photography, they evaluated the impacts of nozzle diameter on atomization and ignition characteristics of such an injection mode, paying particular attention to the barely studied mixing characteristics of gaseous ammonia. After experimental validation, the numerical results conducted using CONVERGE v3.0 and LES showed the impact at various ambient conditions under engine representative conditions. Findings highlight the critical influence of the nozzle diameter on parameters such as spray penetration, angle and area, with faster

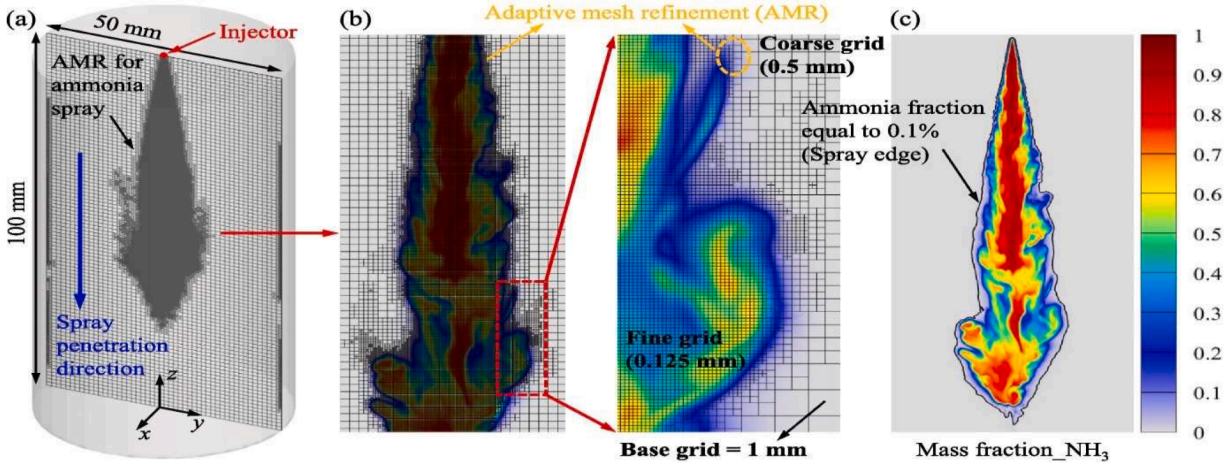


Fig. 13. Numerical model setup. (a) Calculation domain, (b) Grid methods, (c) Definition of spray edge. The colour bar indicates the ammonia mass fraction (Reprint from Ref. [114] with permission).

penetrations, larger angles and increased areas proportional to the diameter. However, as the conditions of operation were changed and taken to engine-like conditions, it was evident that only a fraction of the spray would develop characteristics for good ignition. Additional analyses revealed some geometrical changes that could enhance the ignition profiles for the engine of interest, Fig. 13.

More fundamental studies have been performed to determine expanding features in flame propagating studies. An et al. [23] observed the evolution of ammonia dispersed in a droplet field, comparing liquid ammonia sprays to their gaseous equivalent. Through the use of Eulerian-Lagrangian frameworks to capture phase variations, it was concluded that the liquid phase reduced flame propagation speeds and heat release under flash boiling conditions. Preheating appeared to be a method to improve this phenomenon, particularly for the ignition of liquid ammonia droplets difficult (or impossible) to ignite under conventional operating conditions. These results, validated in other works, denote the energy competition between the chemical reaction and the heat absorption of ammonia that combined critically impact on the ignition of the chemical [115].

Finally, smaller droplets seemed to evaporate quickly, thus increasing mixture fraction. Equivalence ratios and heat fractions appeared to be dependent on the proportion of liquid ammonia and local evaporation rates, with conditions out of stoichiometric parameters predicted to be more efficient for ignition purposes. To expand these studies, similar research has explored the use of sub-models to maximise numerical modelling capabilities. Zhang et al. [116] postulated some sub-models to include the effects of finite viscosity, droplet distortion, flash-boiling atomization and thermal breakup processes representative of ammonia sprays. Additionally, bubble growth rates in liquid droplets were also included in the Smagorinsky turbulence model adopted in their LES approach using OpenFoam v7. After good validation, the group found that their model, which predicts lower drag coefficients and higher evaporation rates, is more accurate to experiments. This appeared to be a consequence of including the effect of droplet deformation accounting for its influence on heat and mass transfer processes.

A recent study performed by Hu et al. [117] addressed the issue of spray breakup by using a formula of variable discharge coefficient that accounted for the impact of spray resistance caused by the vaporization effect of ammonia within the nozzle at various flashing conditions. The work approached the analysis by assessing the Kelvin-Helmholtz and Raleigh-Taylor (KH-RT) breakup model (which state interface instabilities caused by momentum and densities gradients), which showed better performance than conventional approaches. This exemplifies the importance of instabilities caused at the interface of the ammonia spray and the production of atomization patterns across the flows. Jin et al. [118] conducted numerical models of the breakup mechanism by adoption of a definition based on a dimensionless number Rp that quantifies the superheated degree of the ammonia blend using the ratio of the ambient and the saturated vapour pressures under liquid temperature remaining at 303 K with 11.6 bar saturated vapor pressure. In order to keep the nozzle at 303 K, circulating cooling water was used for the experiments. The Rp parameter showed three stages depending on its value (i.e. normal evaporation, $Rp \geq 1.0$; external flash boiling, $1.0 < Rp \leq 0.3$; transitional and fully flash boiling, $Rp < 0.3$). Nozzle effects, thermal breakup, and secondary aerodynamic breakup were considered in the study. With good validation, the approach was compared with the typical aerodynamic breakup model, showing the superior performance of the approach for predicting transitional and flashing regimes. Further, it was found that flash boiling plays an important role in primary atomization by generating smaller droplets, while the spray expansion and air resistance lead to transitional penetration of the spray.

Simultaneously, Song et al. [119] evaluated some of the breakup models to verify their relevance in the use of ammonia injection through the creation of smaller droplets. Their study proposed the use of a flash boiling breakup model based on thermal growth of multi-bubbles (which are modelled using the Rayleigh-Plesset equation with nucleation theory and droplet velocity corrections). Their results show good correlation under low-pressure injection cases, hence showing bubbles growth driven by flash boiling effects under lower ambient pressures. This effect, as previously addressed, impacts on spray penetration, decreasing this parameter whilst increasing spray angle. Additional works on the subject [120] showed by Direct Numerical Simulation that bubbles initially form upstream, near the entrance wall of the nozzle. These bubbles in combination with the phase change and temperature reduction lead to the formation of more irregular bubbles which collapse into smaller entities further downstream the nozzle tip. The effect, caused by the growth, breakup and collision of these bubbles increases turbulence and generates large pressure fluctuations, both critical in the flashing effect observed in liquid ammonia injection.

Condensation characteristics are also of critical importance in understanding liquid ammonia atomization. As pointed out, the large latent heat of evaporation of ammonia and its high Joule-Thomson effect present important challenges in the use of ammonia direct atomization as a consequence of the cooling effect that this causes. To address unknowns and expand our knowledge on the subject, Yi et al. [121] used RANS and Liquid Particle Tracking methods to unravel the complexities of the cooling phenomenon via OpenFoam v6. The team employed Euler-Lagrange simulations coupled with condensation models that were experimentally validated. Results and further analyses on multi-hole injectors indicated that the geometry of the injector (i.e. with various number of holes) was critical in the process with a direct proportion of condensed mass. Transient effects were observed as a consequence of instantaneous evaporation, particularly under engine-line conditions. However, it was proposed that the use of smaller nozzles with hotter fuels, lower injection pressures and higher ambient temperatures produce more condensation during the transient stages of the spray. Once the spray evolves into quasi-steady conditions, the condensation moves away from the nozzle. The study also addressed the case of supercritical injection. The fast changes in phase transition lead to substantial condensation at the nozzle, added to the impacts that heating and turbulence have on this phenomenon, Fig. 14.

As the technology keeps progressing, the study of ammonia in liquid form gains more adepts on the field of engine retrofitting – a coherent move in line with current commercial patterns previously described in the introduction section. As could be expected, ammonia-blends with conventional fuels have been on the scope of research groups to evaluate the variety of characteristics and phenomena occurring when ammonia is mixed under reciprocating engine conditions. The greater difficulties encountered when optically accessing these fields make CFD modelling an ideal solution for detailed analyses of these regimes. For example, Xian et al. [122] evaluated the characteristic of high-pressure liquid ammonia sprays in dual-fuel engines. The systems of interest operated under a High-Pressure Direct Injection mode. By using Schlieren optical diagnostics, the experimental characteristics of ammonia-diesel sprays were obtained for numerical validation. Once validated for their operational conditions, the team performed CFD evaluations employing Converge in combination with the SAGE chemical reaction solver, KH-RT, negative temperature coefficient (NTC), and wall film models. Observations were based on the microscopic dynamics between various ammonia and diesel tests. The results revealed that liquid ammonia sprays are highly sensitive to temperature, as postulated in the previous studies, although at higher temperatures the ammonia profile is closer to high-density gas injection with a small fraction of the blend in liquid phase. Furthermore, high-temperature high-pressure conditions denoted shorter penetrations than diesel (up to 60%), an inconvenient for flame propagation. The research team expanded their assessment to evaluate parameters for improvement, finding out that the longitudinal spacing between fuels could be a critical parameter to enhance ignition effects within the stable ignition zone. Larger systems are now under scope of research groups. For example, Di-Matteo et al. [123] explored the potential of ammonia in a marine-like combustion chamber by using

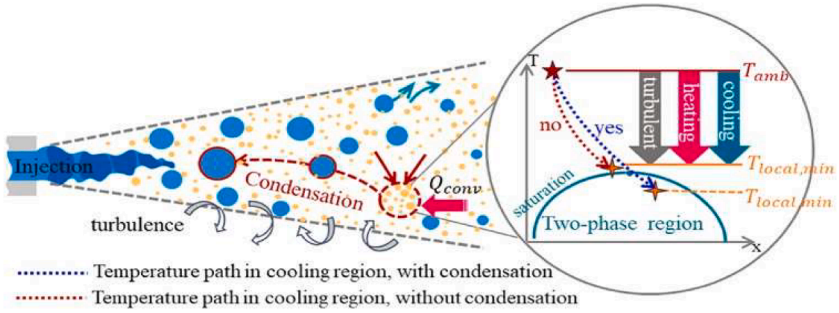


Fig. 14. Competition factors for determining condensation (Reprint from Ref. [121] with permission).

a flamelet tabulated manifold (FGM) combined with 1D and 3D studies. Their results, exploratory in nature and without any experimental validation (due to the lack of experiments using large marine engines at the moment), show certain conditions at which ammonia would ignite, particularly those when a pilot diesel is aimed along the combustion chamber reaching the ammonia spray at the nozzle.

Another interesting area that has started to gain importance across the scientific community is the analysis of droplets-flame interactions, which are still barely understood and in their infancy for computational numerical modelling resolution. The lack of studies is appropriately emphasized by Ryoichi et al. [124] and Rousselle et al. [125], who present current works conducted on the field of ammonia atomization for combustion processes. However, Ryoichi et al. have expanded this area with several contributions. Recent works [126] evaluate combustion characteristics of liquid ammonia injection via carrier phase (cp)-DNS modelling, exploring droplet/flame interactions. The experimental setup, based on a co-firing flame formed by a centrally injected ammonia/air blend surrounded by a methane flame, was evaluated to determine penetration of liquid ammonia into the methane flame and the interaction between phases, Fig. 15.

The governing equations for droplet position, velocity and temperature are solved using equations R1 – R3.

$$\frac{d\boldsymbol{x}_{d,i}}{dt} = \boldsymbol{u}_{d,i} \tag{R1}$$

$$\frac{d\boldsymbol{u}_{d,i}}{dt} = \frac{f_1}{\tau_d}\left(\boldsymbol{u}_i - \boldsymbol{u}_{d,i}\right) + \boldsymbol{g}_i \tag{R2}$$

$$mc_p\frac{dT_d}{dt} = f_2 hA_d(T_\infty - T_d) - \frac{dm}{dt}h_v \tag{R3}$$

Where the droplet dynamics are characterized by position $x_{d,i}$, velocity $u_{d,i}$, temperature T_d, and mass m_d, with the drag force incorporating the Stokes correction factor f_1. Supplying the liquid ammonia at 4.0 MPa, the injection into a low-pressure environment will superheat the liquid ammonia quickly, enabling the analysis of flash/no-flash conditions across the various regimes of the flashing phenomenon. The grid resolution of the study is fine enough to resolve the Kolmogorov scale and the flame thickness. Okafor's mechanism [35] was used with OpenFoam.

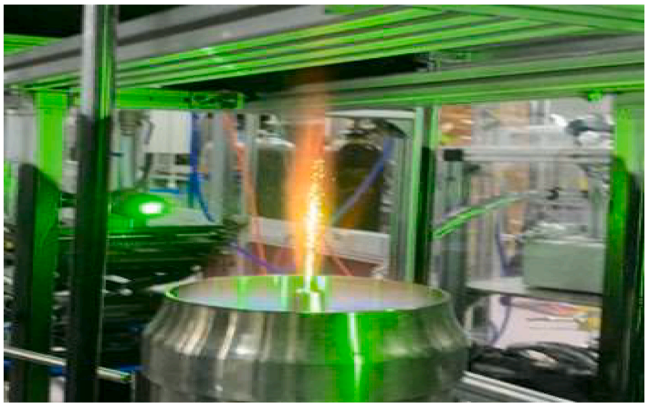


Fig. 15. Digital image of the liquid ammonia jet from experiments using MIE scattering (Reprint from Ref. [127] with permission).

After evaluation of experimental results obtained using OH-PLIF, Mie Scattering and the numerical model, it was found that there is a pronounced radical accumulation within the inner layer of the flame, with minimal penetration of the liquid droplets beyond the flame front. Further analyses denote the complex heat release rate (HRR) profiles, with intensified, extinction and island-like zones, Fig. 16. It was clear that liquid droplets would have impacts on heat losses due to phase changes.

In order to assess various parameters that could elucidate more information of this interaction, the work focused on the curvature of the flame, which was used to determine the various droplet-flame interaction modes. It was observed that the interaction between droplet and flame led to large negative curvatures, Fig. 17. Further, the existence of more droplets wrinkles the flame front, which in turn allows some penetration into the burned region, creating zones of higher ammonia concentrations. However, the full interaction between droplets and flame remains unsolved, as most of the droplet did not interact with the flame regime (as they evaporated well before reaching the flame front, mixing and burning with the surrounding air). This work, an extension of previous analyses done by the group using other modelling strategies (e.g. extended flamelet manifolds) [128] just confirms the complex nature of ammonia droplets under combustion regimes.

Recent studies conducted by Chen et al. [129] considered the impact of heat loss at the wall of combustion chambers fuelled with liquid ammonia. Although the injection regime differs from their previous setup, the effect on emissions and reduced evaporation persists with the use of liquid ammonia sprays. The study also addresses component impacts in engines such as gas turbines. The investigation focused on the effect using a swirl burner whilst comparing results with gaseous ammonia combustion. As wall-cooling increased from 0 to 0.8 kW, overall emissions of unburned NH_3 and N_2O increased, a phenomenon likely caused by flame quenching and further recombination of H^+ species along the boundaries of the combustion region. Secondary stage combustion appeared to be a reliable method to mitigate this effect by finishing the reaction of both molecules further downstream.

Expanding on the impact of CFD modelling for ammonia sprays, Molkov et al. [130] performed multiphase flow analyses to show the effect of a sudden release from a bulk liquid ammonia container. The analysis replicated a potential sudden release to the atmosphere from a pressurised tank (at ~0.5 MPa). Using validated experiments from a $12m^3$ tank study, the analysis conducted evaluated the impacts on liquid and gaseous phases. Simulations use Lee's evaporation-condensation model (which considers heat transfer processes from various components of the field of study). An addition to the model, resolved using

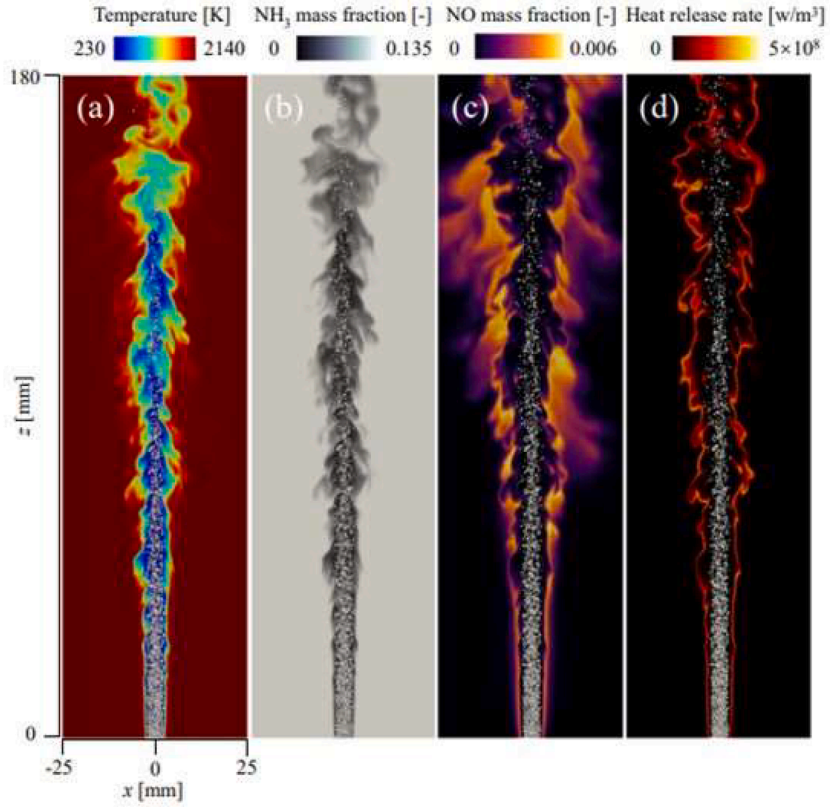


Fig. 16. Instantaneous distribution of a) temperature; b) ammonia mass fraction; c) NO mass fraction, and d) heat release rate. Droplets are shown as white dots (Reprint from Ref. [126] with permission).

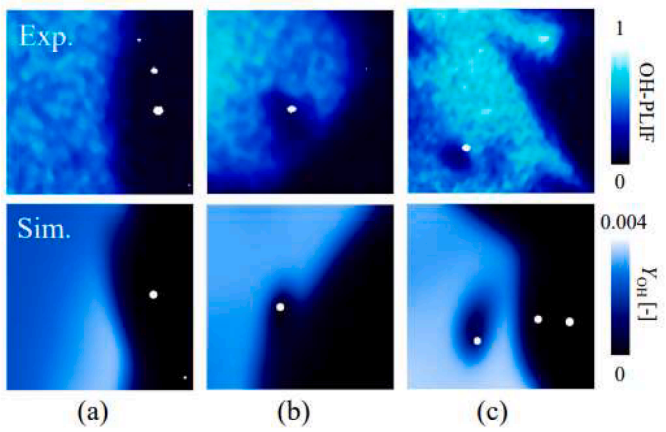


Fig. 17. Time evolution of the flame front during its interaction with ammonia droplets (Reprint from Ref. [126] with permission).

RANS SST k-ω turbulence model, was the inclusion of a phase change mechanism that made possible evaluating the transient nature of the plume with the surface areas between dispersed liquid and the gaseous phase. The results showed that an increase in the volume fraction of vapour within a two-phase mixture leads to an increase in interfacial area density and, consequently, a higher mass transfer rate between the phases, an effect mainly observed in piping rather than in storage systems due to the high velocity flows observed in the piping lines. The model is suggested as a precedent for additional studies that can lead to ammonia bunkering protocols for several applications.

Not surprisingly, and as addressed in many of the previous sections, numerical modelling opens a great variety of concepts for the use of ammonia fuelling. One is the analysis of novel methods such as the use of liquid ammonia injection for aerospace applications. Li et al. [131] proposed the use of ammonia for hypersonic vehicles, with ammonia convective cooling being employed to improve fluid and thermal protection methods of these heavy-duty units, Fig. 18. Ammonia is presented as a blend with kerosene for dual fuel injection for a scramjet. Various models were also compared to show the potential of ammonia, kerosene, hydrogen and water as coolant working flows, assessing their potential to cool down structural walls whilst recovering heat for propulsion improvement. Results show the highest specific thrust (>42.75%) and total increased efficiency of the ammonia-kerosene blend compared to higher hydrocarbons (>$C_{10}H_{22}$), with an optimal thermal protection second only to liquid hydrogen. It must be emphasized this is also consequence of the step increase in fuel consumption. Overall, the findings show that by improving cooling effects of the system, heat exchanger overall areas are decreased substantially in up to 60% compared to the base case due to the high chemical heat sink that ammonia provides.

These works are evidence of current efforts to unlock the challenges of liquid ammonia injection modelling, which can be summarised as a combination of phenomena that go from complex breakup effects to challenging multi-phase conditions during transitional stages across the jet and the flame. Recent findings show that there is a region of relaxation that is the most prone for combustion, whilst flashing effects are linked to changes in density and potential onset of micro-bubbles, changing the dynamics from those known in conventional fuel sprays. Wall interactions combined with condensation have triggered new research activities on the field of solid-liquid-gaseous interactions, with the evolution of these scenarios in engines and even aerospace applications only successfully evaluated via computational fluid dynamics.

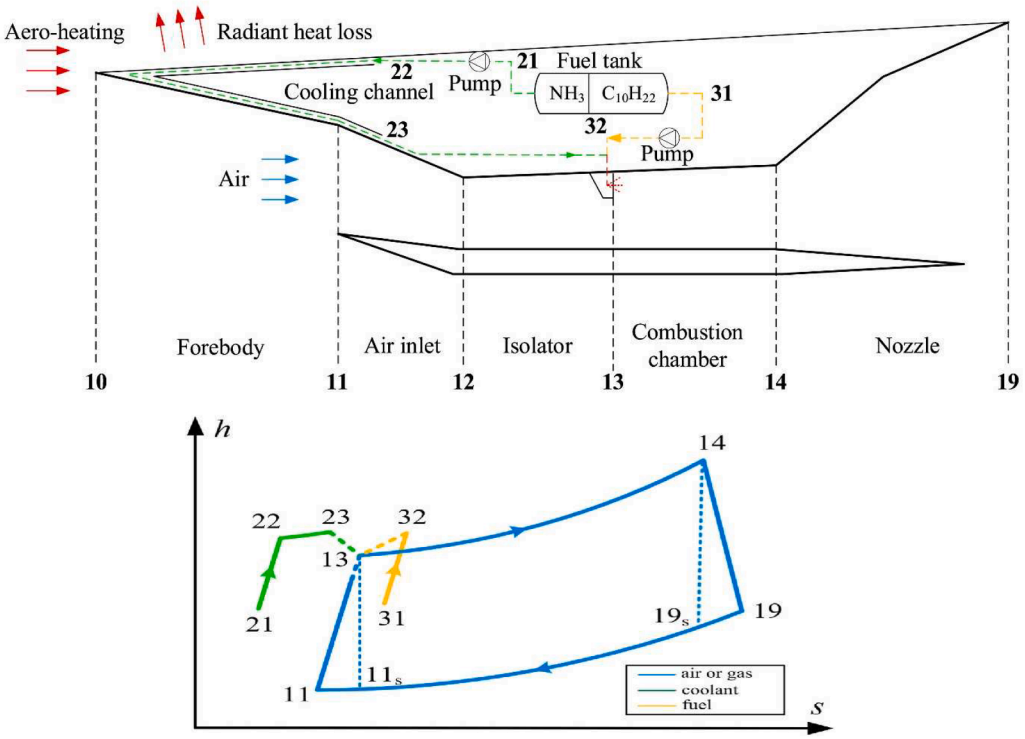


Fig. 18. Thermodynamic model and Enthalpy-Entropy diagram of dual-fuel engine cycle (Reprint from Ref. [131] with permission).

Table 4
Literature research on numerical simulation articles on turbulent combustion phenomena of porous-media and plasma-assisted combustion.

Ref.	Fuels	Method	Dim.	Code	Software	Mechanism	Validation level	Ref.
[132]	Porous media (mesoscale)	NH_3–CH_4	RANS	3D	n.r.	Finite-rate; porosity and phi optimisation	Okafor-59–356	Numerical optimisation only
[133]	Porous media	NH_3–H_2	RANS	2D	n.r.	Finite-rate; thermal conductivity parametric	n.r.	Exp. (T profile, NOx vs. conductivity and phi)
[134]	Porous media (SiC foam)	NH_3–H_2	RANS	3D	n.r.	Finite-rate; stability and efficiency	n.r.	Exp. (stability limits, combustion efficiency, NOx)
[135]	Porous media (variable porosity)	NH_3–H_2	RANS	3D	n.r.	Finite-rate; varying pore diameter	n.r.	Numerical (stability, NOx, flame thickness trends)
[136]	Porous media (entropy / exergy)	NH_3–CH_4	RANS	3D	ANSYS Fluent	Finite-rate; entropy / exergy analysis	n.r.	Exp. (literature validation; T, emissions)
[137]	Porous media (wavy micro-comb.)	NH_3–H_2	RANS	3D	n.r.	Finite-rate; wall-T uniformity	n.r.	Numerical (NOx, T wall uniformity vs. geometry)
[138]	Porous media + bluff body	NH_3–H_2	RANS	3D	n.r.	Finite-rate; radiation model	n.r.	Exp. (T wall, radiation power, stability)
[139]	Porous media (two-stage burner)	NH_3 / LPG	RANS	3D	n.r.	Finite-rate; two-stage porous foam	n.r.	Exp. (NO, NH_3, CO outlet; flame structure)
[146]	Plasma-assisted NSD (1D)	NH_3 / air	1D	1D	n.r.	Finite-rate + plasma energy source; flame enhancement	Plasma-combustion mech.	Exp. (LBV enhancement)
[150]	Plasma-assisted NSD (0D)	NH_3 / air	0D ODE	0D	n.r.	Boltzmann eq. + thermochem. ODEs; constant-V reactor	Plasma-combustion mech.	Exp. (ignition delay)
[154]	Plasma-assisted NSD (0D)	NH_3–H_2 / air	0D ODE	0D	n.r.	Boltzmann eq. + plasma kinetics; ignition study	Plasma-combustion mech.	Exp. (ignition delay, radical generation)
[155]	Plasma-assisted NSD (1D)	NH_3 / air	1D	1D	n.r.	Finite-rate + NSD; freely propagating flame	Plasma-combustion mech.	Exp. (flame speed, flammability)
[157]	Plasma-assisted NSD (0D)	NH_3–H_2 / air	0D ODE	0D	n.r.	Plasma-assisted low-T oxidation kinetics	Plasma-combustion mech.	Exp. (species, low-T oxidation)
[159]	Plasma-assisted NSD (0D)	NH_3 / air	0D ODE	0D	n.r.	Non-equilibrium N_2O/NO_x chemistry, low-T NH_3 oxidation	Plasma-combustion mech.	Exp. (N_2O/NOx)
[161]	Plasma-assisted NSD (DNS)	NH_3–H_2 / air	DNS	3D	n.r.	Full DNS + plasma coupling; turbulence-plasma-flame	Plasma-combustion mech.	Numerical (NOx, HRR, flame isosurface)
[162]	Plasma-assisted NSD (1D)	NH_3 / air	1D	1D	n.r.	Finite-rate + NSD; pulse and mixture sensitivity	Plasma-combustion mech.	Exp. (LBV vs. pulse settings)
[164]	Plasma-assisted NSD (1D)	NH_3 / air	1D	1D	n.r.	Plasma-assisted MILD combustion; reactor + 1D	Plasma-combustion mech.	Exp. (MILD regime stability)
[165]	Plasma-assisted NSD (DNS)	NH_3 / air	DNS	3D	n.r.	DNS comparison of plasma vs. preheating	Plasma-combustion mech.	Numerical (flame structure, NOx)

3.4. Porous media

Porous media is another technique that has been considered and recently evaluated for the consumption of ammonia blends. The concept, which comes from works conducted on the combustion of syngases and engines employing porous composites, can be a method for efficient ammonia consumption at higher than adiabatic temperatures. The effect, called super adiabatic temperature, is caused by the additional heat that hot porous media emits back to the flame, hence increasing its temperature (a subject of current research interest). Porous media burners (PMB) improve internal heat recirculation through radiation and conduction, leading to preheating of reactants, hence extending the lean flammability limits and flame stabilization. Porous media combustion allows stable, very lean flames across various mass flux rates and pressures, resulting in reduced pollutant emissions. However, how effective the process is for ammonia combustion is a standing research question.

Mechanistically, porous-media combustion changes ammonia conversion by redistributing heat and residence time rather than only by increasing the mean temperature. Radiation and conduction within the solid matrix preheat the incoming mixture and can extend the lean stability limit, while the pore size, porosity, thermal conductivity, and flow velocity determine the location of the reaction zone and the degree of post-flame NO reduction. This explains why porous inserts can simultaneously improve flame stabilization and reduce NO/NH_3 emissions in some configurations, but may also increase pollutant formation if super-adiabatic temperatures promote excessive NH_3 oxidation. The main modelling challenge is thus the coupled treatment of gas-phase finite-rate chemistry, solid–gas heat transfer, radiation, and residence-time distribution inside complex porous geometries.

Table 4 provides a structured overview of the porous-media and plasma-assisted combustion CFD studies reviewed in Sections 3.3 and 3.4, classified by system type, simulation methodology, combustion chemistry model, reaction mechanism, and level of experimental validation.

As expected, the subject is also under evaluation at modelling level. A numerical investigation was conducted by Tolouei and Gharehghani [132] who proposed the combustion of NH_3/CH_4 blends for CO_2 and NOx abatement through an optimization process numerically assessed. The parameters considered included ammonia fraction, porosity, and equivalence ratio which ranged between 0.8 to 1.0. The porous media was a SiC based foam in a 0.6 m reactor. Simulations were performed using Okafor's mechanism [35] through three-dimensional simulations. The results showed that by applying a porosity of 0.63 with 90% ammonia at stoichiometric conditions would lead to the most optimum combustion profile (low emissions and full conversion) from the analysed cases. Methane-ammonia could play as a good substitute for methane in porous media burners, with elevated wall temperatures compared to those without porous media. In comparison to a CH_4/O_2 case, CO_2 emissions were reduced in 75% whilst NOx were mitigated in 10%.

Chen et al. [133] evaluated the impact of hydrogen in ammonia blends numerically and experimentally using porous media. A 2D model was presented to theoretically describe the process and the dependencies between temperature, products, flame characteristics, equivalence ratio, hydrogen content and gas velocity. The study evaluated the influence of the thermal conductivity of the porous matrix (set at 60, 100, 120 and 150 W/mK) with a gas velocity of 3 m/s. Results showed that the increase of thermal conductivity led to a decrease in maximum temperature of the flow, a factor caused by the increased heat transfer from the porous media to the surroundings. Similarly, the increase in thermal conductivity also shifts the flame front, with a higher thermal conductivity causing a movement of the high temperature zone closer to the inlet of the burner array. Also, and as expected, the use of high equivalence ratio blends above stoichiometric values led to a drastic reduction of NOx, with values under rich conditions close to 0.009% (in volume).

Nozari et al. [134] performed analyses on a novel porous burner where ammonia/hydrogen/air blends were evaluated experimentally and numerically to determine stability, combustion efficiency and NOx emission. The burner was designed using SiC porous composite. Experiments were conducted using a wide variety of ammonia content between 60–90 vol% at equivalence ratios between 0.9–1.5 and gas flow rates of 4 to 18 m/s. As expected, the use of pure ammonia was unstable. However, as ammonia was displaced and hydrogen injected, the stability limits of the combustion process expanded. It was documented that the combustion efficiency in this porous media exceeded 95%. Further, it was observed that the flame could be retained more easily with the porous media, improving resistance to blowoff in ~40%. It was found that the porous media heat transfer improved the anchoring effect, providing additional heat to the blend, hence improving its reactivity. It was also found that the burner size had important implications in the ability of the system to sustain stable, high efficiency combustion, a factor related to the power density that the unit was capable of delivering.

The change in porosity was also studied by Hashemi et al. [135]. Using a numerical model, flame stability and pollutant emissions were analysed when a porous burner with varying porosity operated using ammonia/hydrogen blends. The results showed that stability increases with equivalence ratio regardless the ammonia content, although higher ammonia in the blend led to reduced stability and increase in NO emissions. Thermal flame thickness, an important parameter in porous media burners, was also determined, with thicknesses drastically being reduced close to stoichiometric values and lower ammonia content, whilst NO showed similar trends as in previous works, with a decay under rich fuel conditions. Further, flame stability limits also increase as the pore diameter increases, a parameter correlated to the ability of the system to deliver higher power densities.

The work from Rong et al. [136] calculates the changes in entropy and exergy in chambers operating with ammonia/methane blends in the presence and absence of porous media using ANSYS Fluent 2022. Three-dimensional models were developed and validated using experimental data from the literature by evaluating a system with a single inlet/double channel outlet configuration under laminar conditions. The results showed details on the changes of the combustion process across different equivalence ratios, inlet gas velocities, mixing ratios and porosity of the porous media. It was found that, compared to a combustion system without a porous medium, the use of the latter significantly improved the thermal characteristics of the process, reducing emissions and improving combustion characteristics, a trend previously observed by works previously addressed. However, as for entropy, higher porosity resulted in lower entropy within the porous structure. Additionally, exergy efficiency is inversely proportional to equivalence ratio, with a lower oxygen content leading to lower efficiencies.

A 3D model was developed by Han et al. [137] who assessed the characteristics of a novel wavy micro-combustion chamber and the impact caused by temperature distribution on the outer walls of the reaction chamber. A "wavy" variation in the profile of the walls was employed as it was found that this change is more effective to improve temperature uniformity at gas velocities above 12 m/s. The analysis is performed by comparing the effects of these waves with a conventional chamber for its use in thermos-voltaic applications. The wavy profile showed that the limit of NOx emissions was reduced in ~21%, an effect caused by an improved temperature distribution during the reaction of the ammonia/hydrogen blends.

Fu et al. [138] studied numerically and experimentally the combustion characteristics and thermal performance of a porous media burner with a bluff body fuelled with ammonia/hydrogen. Small additions of ammonia appear to significantly influence the flame, leading to an increase of thermal performance. Furthermore, the porous media enhanced stability whilst higher wall temperatures can be achieved when ammonia additions reach 20%, an effect caused by enhanced

radiation, thus increasing the temperature of the former by ~120 K above the mean wall temperature of the porous media burner. Consequently, the maximum radiation power (35.65 W) was achieved when burning a blend containing 20% NH_3 in the presence of a porous medium.

Finally, experimental and numerical investigation of ammonia flames under the influence of hot flue gases in a novel two-stage porous burner were assessed by Udaybhanu et al. [139]. Initially, experiments were conducted with premixed LPG/air supplied to the first stage of the burner, without porous foams, at thermal inputs of 7.5 kW, 10 kW, 12.5 kW, and 15 kW. At lower inputs, the flame stabilized at the bottom of the first stage, but when the thermal input exceeded 12.5 kW, the flame extended into the NH_3 injection chamber. Introducing porous foams allowed for higher thermal inputs, stabilizing the flame below the foams. This resulted in a significant reduction in CO emissions, from 320 ppm without porous foams to <10 ppm with porous foams at the burner exit. However, considerable NO emissions were still observed at higher thermal inputs in both configurations.

Further, ammonia was injected into the burner under both conditions, with and without porous foams, at thermal inputs of 8.45 kW, 10.85 kW, and 13.35 kW. In cases where the LPG thermal input was lower (10 kW) and the NH_3 input exceeded 8.45 kW without porous foams, a significant increase in NH_3 emissions was observed at the burner's exit. However, when porous foams were used in all tested cases, there was a notable reduction in both NO and NH_3 emissions, with maximum recorded values of 377 ppm for NO and 15 ppm for NH_3, respectively. The results can be traced back to some of the simulations, Fig. 19, where the unburned ammonia at the outlet of the second stage is at a higher concentration with porous media. This unburned ammonia enables the decomposition of NO at the post-combustion zone, hence mitigating both emissions. In comparison, the reaction without the porous foam is faster and less controlled, hence rapidly oxidizing NH_3 and other radicals, as observed in the higher OH presence. The phenomenon leads to higher emissions. Although temperatures in the process are relatively the same, Fig. 20, it is clear how the porous media has led to a significant impact on emissions abatement.

In summary, porous media can be used as a method to control the reaction of ammonia along the combustor, particularly when small units are operated. However, the enhanced radiation product of the porous media and super-adiabatic phenomena can also increase emissions, hence making the use of geometrical changes, equivalence ratios and porosity ratios critical in the control of emissions and higher combustion/exergy efficiency needed to compete with fossil fuels. This is an active area of research that is gaining pace as the use of ammonia continues to infiltrate in various applications at both medium and small scales.

3.5. Plasma-assisted ammonia combustion

The reactivity of ammonia is considerably lower than that of conventional hydrocarbon fuels, hampering ammonia transition in energy systems. Several studies have focused on addressing this challenge via well-established methods, including preheating and blending ammonia with more reactive fuels [17,140–143]. Whilst proven effective, using these methods incurs a high percentage of hydrocarbon fuel and substantial deployment of heat to the mixture [108,144,145], compromising the ammonia potential for decarbonisation. Given these limitations, an alternative method based on the concept of plasma-assisted combustion has recently been introduced to enhance ammonia reactivity [146].

A Plasma discharge modifies combustion through different processes. It can produce energised electrons, ions, and excited molecules, which subsequently generate active radicals and dissociate large fuel molecules [147]. These changes in the mixture composition create new chain-initiation and branching pathways, which accelerate chemical reactions. Plasma can also increase the local mixture temperature through the energy transfer between energised electrons and molecules [147,148]. Another effect of plasma on reacting flows is the modification of the local flow velocity through Coulomb and Lorentz forces [147,148]. The influence of such changes in the flow velocity on the flame is generally negligible, unless plasma is discharged near the flame front, where variations in the flow velocity can modify the local flame wrinkling. The significance of the effects mentioned above is highly dependent on the plasma regime, which can be classified into equilibrium and non-equilibrium [148]. In equilibrium plasma, electrons, ions, and neutral molecules are in thermodynamic equilibrium, and plasma alters a mixture directly via temperature augmentation [148]. On the contrary, in the non-equilibrium regime, the plasma energy is transferred into activation of non-thermal chemical pathways, including excitation and ionisation reactions to generate active radicals and dissociate the fuel, rather than heating the ions and neutral molecules [148,149]. Given this, ions and neutral molecules are significantly colder than the electrons [150]. Previous studies have demonstrated that non-equilibrium plasma is more energy efficient than equilibrium plasma, particularly when operated at nanosecond pulse widths [147,148]. This technique allows efficient utilisation of plasma energy to

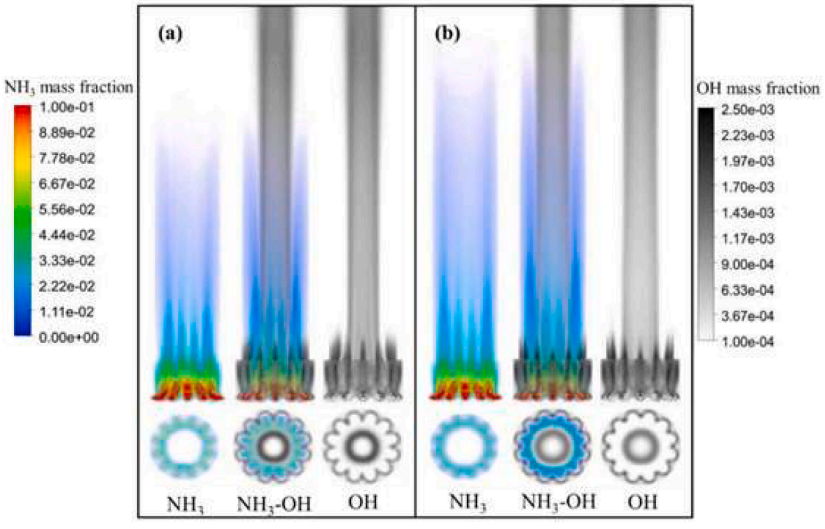


Fig. 19. NH_3, NH_3–OH, OH distribution in the second stage of the burner (a) without, and (b) with porous media (Reprint from Ref. [139] with permission).

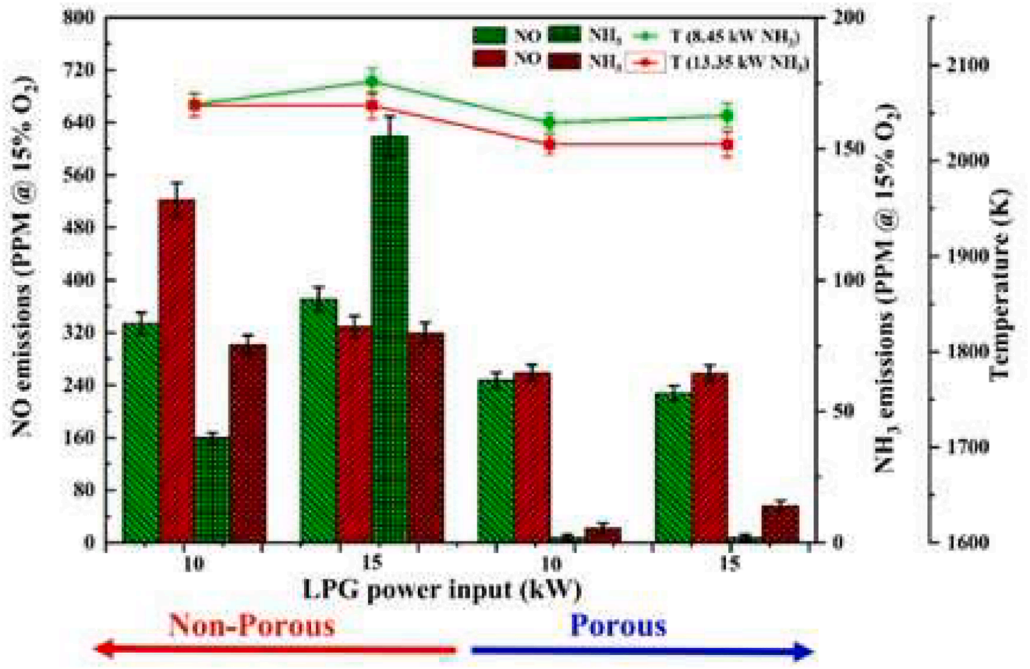


Fig. 20. Comparison of measured NO, NH_3 and exit temperature of the burner with and without porous foams at various thermal inputs under stoichiometric conditions (Reprint from Ref. [139] with permission).

generate active radicals over a very short time discharge, which is subsequently used by the thermochemistry between two consecutive discharges to assist combustion [151,152]. Given this potential, this novel technique has recently attracted considerable interest and has been the subject of an increasing number of numerical studies.

In non-equilibrium nanosecond plasma-assisted ammonia combustion, the characteristic time scale of plasma chemistry is generally smaller than that of thermochemistry and turbulent flow [153]. Considering this, reduced-order modelling excluding the turbulence effects has recently gained attention for resolving two-way interactions

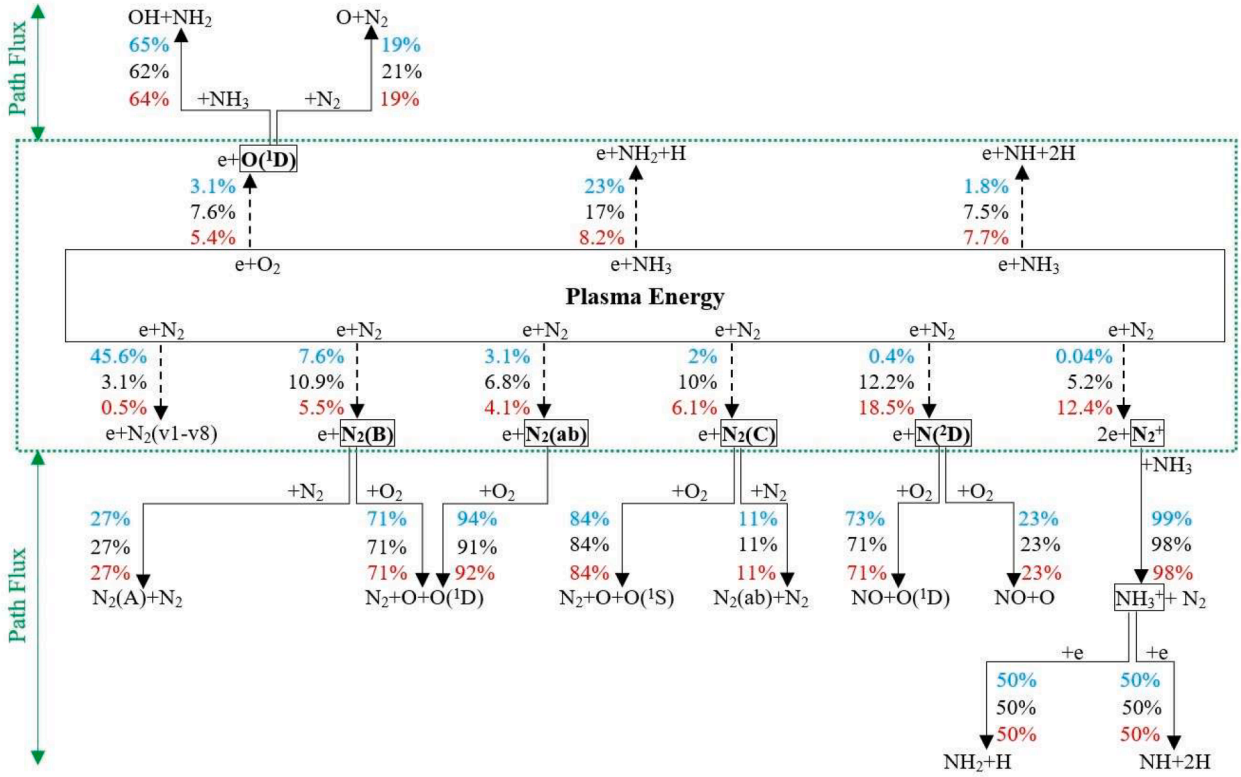


Fig. 21. Main plasma chemical pathways consuming the plasma energy (dashed arrows) and those generating active radicals (arrows) in stoichiometric ammonia/air combustion initially at 850 K, assisted by 20 NSDs with the repetition frequency of 50 kHz and reduced electric field of 100 Td (blue), 350 Td (black), and 700 Td (red). (Reprint from Ref. [162] with permission).

between plasma discharge and ammonia combustion [154–162]. This includes zero-dimensional modelling of plasma chemistry and thermochemistry in constant-volume reactors to evaluate the efficacy of non-equilibrium nanosecond plasma discharges (NSD) to assist ammonia combustion in applications such as internal combustion engines. This is usually achieved through the coupled solution of the Boltzmann equation and thermochemistry ODEs [161,162]. Zero-dimensional simulations have highlighted how the plasma energy is converted into active radical generation [162]. Fig. 21 illustrates the main plasma chemical pathways consuming the plasma energy and the corresponding pathways to generate radicals for a stoichiometric ammonia/air mixture initially at 850 K, assisted by 20-nanosecond plasma discharges with a repetition frequency of 50 kHz and different reduced electric field values [162]. According to Fig. 21, the distribution of plasma energy into different pathways is highly dependent on the plasma setting [155,157,162], while the main pathways producing radicals are nearly similar [162]. Zero-dimensional simulations have also shown that these chemical modifications reduce the ammonia ignition delay time by up to five orders of magnitude [154,156, 160–162].

Similar low-order modelling in one-dimensional computational domains has been employed to assess NSD in unstained and strained flames aimed at evaluating the technique under the prevailing conditions in gas turbines [154,161–164]. These investigations have highlighted that NSD is capable of increasing ammonia flame speed by up to an order of magnitude [154,161,162] and extending the flammability limits [164]. These efforts have revealed that NSD is substantially more effective than well-established techniques for enhancing ammonia reactivity, including preheating and hydrogen-assisted ammonia flames [162]. Fig. 22 shows the laminar flame speed of a stoichiometric ammonia flame assisted by preheating, hydrogen, and NSD [161]. The flame speed of the methane-air flame is also shown as a baseline. This result reveals that discharging 20 NSDs with a pulse energy density of 9 mJ cm^{-3} raises the ammonia flame speed by a factor of 2.3 [161]. To achieve the same flame speed enhancement, either 33.7% of hydrogen by mole fraction in the fuel or 271 K preheating would be required, underscoring the potential of NSD in assisting ammonia combustion [161].

For plasma-assisted ammonia combustion, the controlling parameters are the plasma settings and mixture properties, including discharge energy, pulse repetition frequency, reduced electric field, electron-energy distribution, equivalence ratio, pressure, and the timing/location of plasma deposition relative to the flame front. These parameters determine whether plasma primarily enhances combustion through thermal heating or radical production. In plasma-assisted combustion, the modelling difficulty arises because plasma chemistry involves

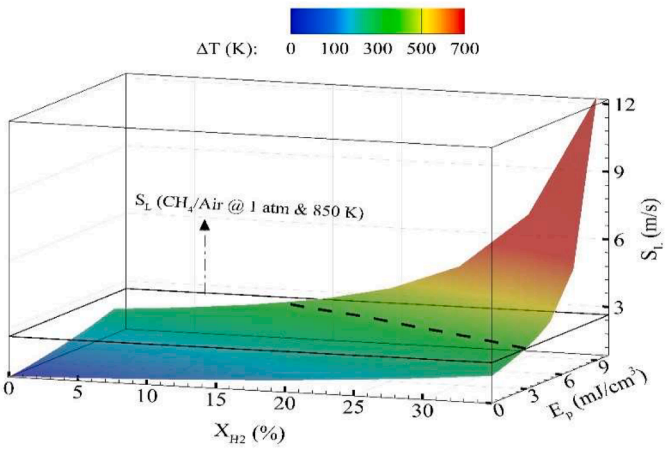


Fig. 22. Laminar flame speed of ammonia as a function of NSD pulse energy density (E_p) and mole fraction of hydrogen in the fuel (X_{H2}), colour-coded with temperature (ΔT). (Reprint from Ref. [161] with permission).

significantly shorter time scales than those of a turbulent reacting flow. Given this, the two-way interactions between plasma arc and turbulence are usually neglected in turbulent plasma-assisted combustion. Although previous studies have shown that this approach is accurate in ammonia combustion [160,161], further studies are required to quantify such effects. A key bottleneck is therefore the development of a cost-effective CFD code capable of resolving both plasma and turbulent reacting flow characteristics.

Recently, multiway interactions between plasma, combustion, and turbulence have been assessed through Direct Numerical Simulations [153,165]. According to these studies and as shown in Fig. 23, turbulence has pronounced effects on key reaction pathways that contribute to heat release [153]. Under laminar condition, $HNO+H \leq > NO+H_2$, $OH+H_2 \leq > H+H_2O$ release most of the heat, while turbulence shifts the pathways to $NH_2+NO \leq > N_2+H_2O$ [153]. This emphasises the importance of turbulence in plasma-assisted ammonia combustion, even though the characteristic time scale of turbulence is usually larger than that of NSD. These investigations have also shown that NSD is more effective than preheating and hydrogen-assisted methods in enhancing turbulent ammonia flames [153,165].

When compared to preheating, NSD increases the laminar burning velocity of turbulent flames by 31% and 26% under lean and rich conditions, respectively, for a given input energy of preheating and NSD. These flames are shown in Fig. 24, where the flame fronts are illustrated by an isosurface of progress variable colour-coded by the flame displacement speed. According to these studies, plasma-assisted flames are more reactive than preheated flames and exhibit less local extinction. Additionally, using NSD results in a more distributed turbulent flame than preheating and hydrogen blends. Another notable finding that has drawn attention is that plasma-assisted turbulent ammonia flame produces up to 19% and 35% lower NOx emissions than preheated and hydrogen-assisted ammonia flames, respectively. These findings have positioned NSD as a novel alternative to address the reactivity limitation of ammonia, facilitating the ammonia transition for the next generation of energy systems.

4. Major challenges and way forward

As learned from all the previous sections, ammonia combustion modelling has reached all corners of the combustion field from fundamental to large industrial scale. However, major challenges still remain to keep progressing with the concept, thus delivering modelling strategies that can be used for faster implementation and evaluation of concepts whilst reducing time consumption and deployment costs.

These challenges stem from the multi-parametric nature of ammonia combustion: the accuracy of CFD predictions is simultaneously governed by several coupled controlling parameters. Equivalence ratio, pressure, temperature, residence time, and fuel blending determine the global reactivity of the mixture and the balance between NH_3 oxidation, NO formation, NO reduction by NHi radicals, and N_2O production [166, 167]. Transport-related parameters, including Lewis number, preferential diffusion, differential diffusion, Soret transport, flame curvature, flame stretch, and Karlovitz-number effects, further modify local reaction rates by changing radical availability and local mixture composition along curved or strained flame fronts [59,168]. These effects are particularly important in NH_3/H_2 flames, where the addition of hydrogen typically increases reactivity but also strengthens transport sensitivity, affecting instabilities onset [93].

Thermal and flow-related parameters introduce additional modelling challenges. Wall heat loss, radiation, porous-media heat recirculation, and liquid-ammonia evaporation cooling can alter flame location, local extinction, and pollutant formation [51,76]. For example, recent works performed by Di et al. [169] through 3D analyses compare how spectral differences affect flame evolution and propagation, with results denoting large variations across stages in the injection and combustion process of ammonia liquid injection. The results point out differences

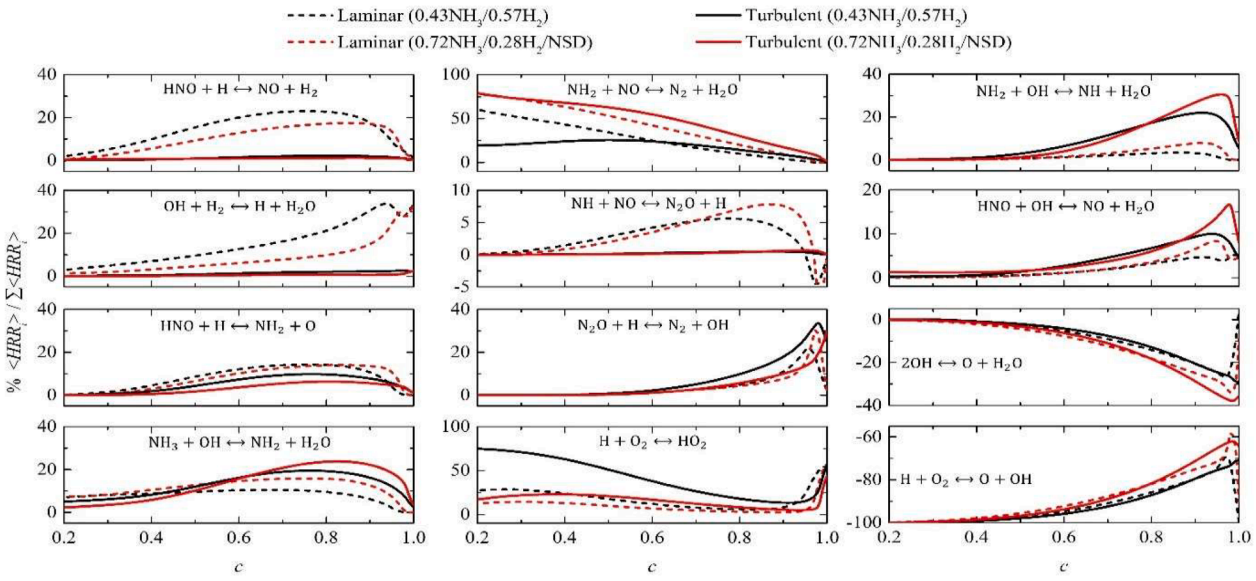


Fig. 23. Key chemical reactions contributing to heat release in laminar and turbulent ammonia/hydrogen/air flames (Reprint from Ref. [153] with permission).

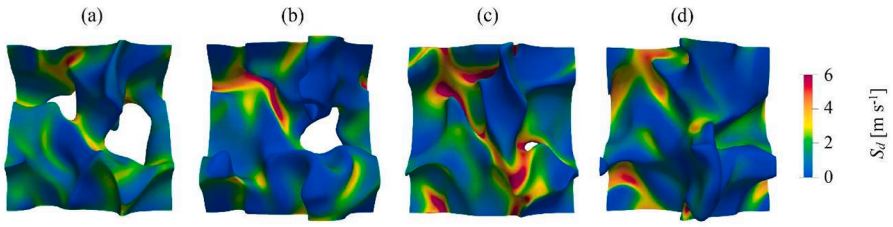


Fig. 24. Turbulent flame front in (a) preheated lean, (b) preheated rich, (c) plasma-assisted lean, and (d) plasma-assisted rich ammonia flames colour-coded with the flame displacement speed (Reprint from Ref. [165] with permission).

between four models, with some (e.g. grey-gas model) overpredicting absorption patterns, whilst others showed greater accuracy but with higher computational demand (e.g. explicit treatment of fuel spectral properties and nongray radiation through various combustion stages).

Similarly, turbulence intensity and coherent flow structures affect flame wrinkling, blow-off, flashback, and local reignition, which are difficult to capture with steady RANS closures but can be better resolved by LES or DNS at higher computational cost [170,171]. Therefore, the main modelling bottlenecks are not limited to chemical kinetics; they also include transport modelling, boundary-condition specification, heat-transfer assumptions, turbulence–chemistry interaction, and the scarcity of spatially resolved validation data for temperature, radicals, and nitrogen-containing species.

Fundamental combustion concepts still need to resolve the complexities behind the thermo-chemical phenomena occurring within various ammonia-based blends. As observed, most studied cases have approached finite ammonia blends under very particular conditions, hence leaving space to study other fuel combinations under a variety of temperature/pressure conditions. The impact of curvature on critical radicals such as H has not only revealed the critical play of such parameters on reactivity and stability but also opens the possibility of using such phenomenon for the control of emissions and instabilities, with equivalence ratios and hydrogen/fossil-based-fuels contents playing as soothing/exciting agents. Similarly, the transition from atmospheric to pressurised cases raises the question about the effects behind the drastic changes in flame behaviour, hence requiring more analyses for pressures in-between analysed conditions. Flashback and blow-off appear to be driven not only by chemical effects but also by flame shape and heat losses. However, transient analyses are required on this front to fully acknowledge the impact on flame stability during start-up, ramping up and shutting down, amongst others, hence delivering fundamental insights in the changes within the flame and thermo-chemical effects that will be critical for applications in the power, heating and propulsion sectors.

Several areas within laminar ammonia flame simulations remain underexplored and merit further investigation. One opportunity concerns the numerical reproduction of spherically expanding flame configurations. These configurations are widely employed in experimental facilities to measure unstretched burning velocities, yet corresponding multidimensional simulations remain scarce. Two-dimensional axisymmetric or three-dimensional computations of outwardly propagating flames would permit direct comparison with optical diagnostics and high-speed imaging data, thereby providing an independent validation route for kinetic mechanisms under transient stretch conditions distinct from those encountered in steady counterflow or burner-stabilized flames. A second priority involves extending canonical two-dimensional flame configurations to elevated pressures and initial temperatures. The majority of existing multidimensional laminar simulations have been performed at atmospheric conditions, whereas practical ammonia combustion in gas turbines and reciprocating engines occurs at pressures reaching 30 atm and preheat temperatures exceeding 500 K. Counterflow flames, slot burner flames, and confined jet configurations should be computed across these extended operating ranges to quantify pressure-dependent variations in nitrogen chemistry pathways and to identify conditions where current mechanisms exhibit the largest predictive discrepancies.

As for ammonia sprays, the current state of CFD modelling is summarized for liquid ammonia injection and combustion, underscoring the

predominant adoption of the Eulerian-Lagrangian framework. The accuracy of these simulations relies critically on physical sub-models, particularly for evaporation and flash-boiling processes. Key insights from numerical studies have elucidated fundamental characteristics of ammonia spray behaviour, mixture formation, ignition, and combustion. These findings provide a deep understanding of combustion performance, offering valuable guidance for practical design and optimization. The Eulerian–Lagrangian framework, augmented by advanced turbulence modelling and sophisticated sub-models for breakup, evaporation, and dispersion, has established itself as a robust and versatile tool for simulating ammonia sprays across a broad spectrum of applications. The unique challenges of ammonia, particularly its tendency to flash boil and its high latent heat of vaporization, have driven the advancement of specialized numerical models that will keep evolving to resolve the complex interactions occurring during the breakup process, various physical states, and flame phenomena. Notable examples include the multi-bubble flash boiling breakup model and hybrid evaporation approaches. These advancements will continue progressing to substantially enhance the predictive capability of CFD for ammonia spray systems.

Although substantial progress has been made in understanding nanosecond plasma discharge (NSD) assistance in ammonia combustion, several key research directions remain critical for advancing this technology toward practical deployment. Foremost, there is a strong need for comprehensive experimental datasets capturing plasma-assisted flame behaviour, including time-resolved temperature fields, species concentrations, radical production, and flame dynamics under both plasma-on and plasma-off conditions. These measurements will serve as essential benchmarks for validating models across laminar, strained, and turbulent flow configurations. Modelling efforts must also evolve. Current plasma simulations largely rely on steady-state Boltzmann equation solutions, which are unable to represent the highly transient evolution of the electron energy distribution function (EEDF) during nanosecond pulses. Developing time-dependent EEDF solvers and improved descriptions of energy transfer to excited states and radicals is therefore a priority. In parallel, future work should focus on creating robust, fully coupled frameworks that integrate electron kinetics, plasma chemistry, fluid dynamics, and thermochemistry with high numerical stability. These developments should be tightly linked to dedicated validation datasets. Another critical need is the development of reduced and skeletal plasma–combustion mechanisms specifically tailored for ammonia–air systems. Current detailed plasma mechanisms are too computationally expensive for multidimensional CFD. Generating reduced mechanisms capable of accurately capturing key excitation, ionisation, and radical-generation pathways—while remaining efficient enough for large-scale simulations—will be essential for practical engineering design. Finally, targeted experiments are required to clarify the three-way coupling between turbulence, flame chemistry, and plasma discharge, as turbulence strongly reshapes plasma-enhanced reaction pathways and heat-release dynamics.

Porous media burners have opened an alternative for the use of the chemical in small power generation devices, even presenting a solution for domestic applications. Complex interactions between fluid and solids could be combined through the adequate handling of radical formation and material coatings, hence delivering ultra-low emission combustion profiles using porous media devices. However, the topic is still in its infancy, with the requirements of further computational analyses that can be adequately validated using experimental methods. Radiation processes at super-adiabatic conditions will present a real challenge for modellers for the complex nature of the phenomenon and the difficulties of punctual measurements needed to calibrate numerical models whilst avoiding intrusive interactions.

The fundamental and laboratory-scale CFD studies reviewed throughout this manuscript collectively define the chemical, transport, and thermal modelling parameters that must be preserved when extending ammonia combustion simulation toward practical devices — including gas turbines, boilers, reciprocating engines, and marine power systems. Laminar and DNS studies provide validated reference data for the development of reduced chemistry and tabulated manifolds, while RANS and LES investigations at research-burner scale identify the governing roles of heat loss, residence time, swirl intensity, staging strategy, and fuel blending in flame stabilization and emissions control.

Foreseeing a path towards implementation of these systems and their relevance in the current and future use of ammonia, the authors of this manuscript believe that small burner units could be implemented, via accurate, high quality CFD modelling in devices relevant to the small and medium heating sector, where burners of small capacity between 0.5–10 kW could be incorporated within radiating tubes, small heating applications for food production, sanitation, cracking or chemical treatment. Similarly, the cases of liquid injection offer a clear path towards delivery of novel technology capable of using ammonia blends in mobile applications. The reduction in both evaporation systems and additional auxiliaries make ammonia a feasible solution for current units in the transport and maritime sectors using liquid injection. Although these concepts require further health & safety and public perception assessments, it is evident that by using liquid ammonia under high combustion efficiencies -properly understood with the help of CFD modelling- could be a path towards fossil replacement in such sectors. Plasmas could also become a critical method for the use of the molecule, not only in the previously mentioned scenarios, but also in aerospace, where the lack of space and the need of high reactivity are critically needed to enhance the delivery of species for continuous propulsion requirements. Finally, porous media have the potential of opening a new door for the solution of replacing natural gas in domestic and commercial applications. By combining various materials, the ignition, combustion, and emissions abatement of using ammonia fuelling could be all performed in a single device, reason because the proposed approach appears novel and intriguing to pursue such a delicate task.

Scaling these modelling approaches to industrial systems, however, requires a set of additional assumptions that introduce uncertainty. Practical-scale simulations typically rely on simplified or prescribed geometries, wall-temperature and conjugate heat-transfer models, reduced or tabulated chemistry, and turbulence–chemistry interaction closures such as EDC, PaSR, or flamelet-based approaches. While these assumptions render large-scale simulations computationally tractable, they carry inherent predictive uncertainty — particularly for NOx, N_2O, unburned NH_3, flashback, and lean blow-off — quantities whose formation is highly sensitive to local temperature, residence time, and chemistry–turbulence coupling. A detailed review of industrial-scale ammonia combustion systems, including gas turbines and marine engines operating at elevated pressure and thermal load, is beyond the scope of the present manuscript and will be addressed in a companion paper currently under preparation. The fundamental CFD studies summarised here should therefore be regarded as the essential modelling foundation for practical design, provided that operating pressure, temperature, residence time, heat-loss level, and fuel-blending range remain consistent with the intended application.

5. Conclusions

Ammonia combustion modelling is expected to keep growing not only in number of publications but also in impact for the understanding of fundamental concepts, delivery of improved modelling techniques and support for industrial implementation of ammonia as an energy vector. International conglomerates keep expanding to establish corridors and industrial hubs capable of using ammonia efficiently for climate abatement and energy resilience. Behind many of these expansions, CFD modelling has and will keep playing a critical role, thus making evident the importance of the concept and the need for a review like the one presented.

Fundamental parameters such ammonia ignition, flame shapes, thermo-chemical effects, and reactivity impacts caused by ammonia at

different concentrations and conditions have been studied, delivering data that can be implemented in improved models to increase quality whilst reducing computational times. Analyses on fundamentals such as laminar burning velocity, curvature, heat losses, diffusivity effects, etc. are amongst the many causing changes on the chemistry, stability and emission profiles observed when using the chemical, hence requiring further support and expansion to acknowledge the drastic changes in blend compositions and atmospheric conditions that, different to other molecules, have perplexed the combustion community over decades.

Laminar flame studies have allowed for a better understanding necessary for ammonia combustion research. While one-dimensional simulations have proven essential for validating chemical kinetic mechanisms and determining parameters, two-dimensional simulations extend this work by capturing phenomena inaccessible to one-dimensional frameworks, including flame curvature, preferential diffusion, wall interactions, and spatially resolved pollutant formation. Results demonstrate that flame stabilization depends more on confinement geometry and heat losses than on global equivalence ratio and that hydrogen enrichment alters preferential diffusion and shifts NO formation peaks toward regions of positive curvature. Studies of micro-combustors, burner-stabilized flames, and wall-quenching configurations have confirmed that fuel-bound NO pathways dominate over thermal routes for pure ammonia flames, with this balance shifting at elevated pressures or with fuel blending. Laminar flame investigations establish the validated reference behaviour and mechanistic understanding required before scaling ammonia combustion toward turbulent regimes and practical applications. Therefore, novel models with lower computational cost are always required, hence opening the opportunity to develop bespoke strategies for complex fluid-chemistry resolution that can be extended to more complex scenarios.

CFD simulations highlight that flash boiling predominantly governs spray morphology, while evaporative cooling substantially affects ignition and combustion stability. Moreover, ammonia ignition is fundamentally mixing-limited in practical systems, often requiring the strategic use of pilot fuels or other ignition-assisting measures. CFD has also yielded deep insights into the complex trade-offs involved in controlling emissions such as NOx, N_2O, and unburned NH_3 when ammonia is injected directly in liquid form. Despite considerable progress, challenges persist, pointing toward critical future research directions. Continued refinement of physics-based flash boiling models is required, particularly for capturing intra-nozzle phenomena and the transition between flashing and non-flashing regimes with greater accuracy. The development and broader adoption of hybrid VOF-EL methods hold significant promise for seamlessly coupling high-fidelity near-nozzle resolution with computationally efficient far-field spray calculation.

Plasma-assisted combustion offers a powerful means to overcome ammonia's inherent reactivity limitations, significantly accelerating ignition, enhancing flame speed, extending flammability limits, and reducing NOx compared with preheating or hydrogen addition. While further advances in diagnostics, modelling, and reduced mechanisms are needed, current findings position NSD as a highly promising route for enabling efficient, low-emission ammonia utilisation in future carbon-free energy systems.

Finally, porous media studies are still required to consolidate a strong background of the processes occurring within the different porous layers, reaction kinetics and fluid dynamics involved in superadiabatic conditions, third body reactions and recombination of species in limited spaces. The resolution of these unknowns could deliver novel concept with potential of implementation not only in the industrial sector but domestic appliances with high potential of global decarbonisation.

CRediT authorship contribution statement

Shi H: Writing – review & editing, Writing – original draft, Resources, Data curation. **Vigueras-Zuniga MO:** Writing – review & editing, Writing – original draft, Conceptualization. **Chong CT:** Writing – review & editing, Formal analysis. **Wang P:** Writing – review & editing, Writing – original draft. **Yu C:** Writing – review & editing, Writing – original draft. **Vargas-Ruiz H:** Writing – review & editing, Writing – original draft. **Gicquel L:** Writing – review & editing, Supervision. **Jangi M:** Writing – review & editing, Writing – original draft. **Shahsavari M:** Writing – review & editing, Writing – original draft, Formal analysis. **Chiong MC:** Writing – review & editing, Writing – original draft. **Valera-Medina A:** Writing – review & editing, Writing – original draft, Validation, Supervision, Funding acquisition.

Declaration of competing interest

The authors declare that they have no known competing financial interests or personal relationships that could have appeared to influence the work reported in this paper.

Acknowledgements

Prof. Valera-Medina acknowledges the support from ESPRC through the MariNH_3 and OceanREFuel program grants (EP/W016656/1 and EP/W005018/1, respectively), and from the European Union with the project CAIPIRNH3A (GA no.101191768). Dr. Shi acknowledges the support from HYCOMBS programme supported by the National Research Foundation, Prime Minister's Office, Singapore under its CREATE programme. The authors are grateful to the IEA Combustion Technology Collaboration Program for providing a framework for discussions which influenced this article.

Data availability

The authors do not have permission to share data.

References

[1] IPCC. Summary for Policymakers" in Global warming of 1.5°C. An IPCC Special Report on the impacts of global warming of 1.5°C above pre-industrial levels and related global greenhouse gas emission pathways, in the context of strengthening the global response t 2018:32.
[2] Hydrogen Council. Hydrogen insights. 2021.
[3] Hydrogen Council. Emerging trade corridors for hydrogen and its derivatives. McKinsey & Company; 2024.
[4] Cardoso J, Silva V, Rocha R, Hall M, Costa M, Eusébio D. Ammonia as an energy vector: current and future prospects for low-carbon fuel applications in internal combustion engines. J Clean Prod 2021;296:126562. https://doi.org/10.1016/j.jclepro.2021.126562.
[5] Wang W, Herreros J, Tsolakis A, York APE. Ammonia as hydrogen carrier for transportation; investigation of the ammonia exhaust gas fuel reforming. Int J Hydrog Energy 2013;38:9907–17. https://doi.org/10.1016/j.ijhydene.2013.05.144.
[6] Valera-Medina A, Xiao H, Owen-Jones M, David W, Bowen P. Ammonia for power. Prog Energy Combust Sci 2018;69:63–102. https://doi.org/10.1016/j.pecs.2018.07.001.
[7] Kobayashi H, Hayakawa A, Somarathne K, Okafor EC. Science and technology of ammonia combustion. Proc Combust Inst 2019;37:109–33. https://doi.org/10.1016/j.proci.2018.09.029.
[8] Sun J, Zhao N, Zheng H. A comprehensive review of ammonia combustion: fundamental characteristics, chemical kinetics, and applications in energy systems. Fuel 2025;394:135135. https://doi.org/10.1016/j.fuel.2025.135135.
[9] Elbaz A, Wang S, Guiberti T, Roberts WL. Review on the recent advances on ammonia combustion from the fundamentals to the applications. Fuel Commun 2022;10:100053. https://doi.org/10.1016/J.JFUECO.2022.100053.
[10] Valera-Medina A, Vigueras-Zuniga M, Shi H, Mashruk S, Alnajideen M, Alnasif A, et al. Ammonia combustion in furnaces: a review. Int J Hydrog Energy 2024;49:1597–618. https://doi.org/10.1016/j.ijhydene.2023.10.241.
[11] Zhang X, Zhao S, Zhang Q, Wang Y, Zhang J. A review of Ammonia combustion reaction mechanism and emission reduction strategies. Energ (Basel) 2025;18:1707. https://doi.org/10.3390/en18071707.
[12] Xing J, An Z, Liang X, Wang R, Kurose R. A comprehensive assessment of reaction mechanisms for NO formation in ammonia/hydrogen/air flames. Int J Hydrog Energy 2025;180:151598. https://doi.org/10.1016/j.ijhydene.2025.151598.
[13] Szanthoffer A, Papp M, Nagy T, Turányi T. Assessing the performance of recent detailed NH3 and NH3/H2 combustion mechanisms. Combust Flame 2026;287:114878. https://doi.org/10.1016/j.combustflame.2026.114878.
[14] Alnasif A, Jójka J, Mashruk S, Nagy T, Valera-Medina A. Analysis of the performance of kinetic reaction mechanisms in estimating N2O mole fractions in

70/30 vol% NH3/H2 premixed flames. Fuel 2024;371:131897. https://doi.org/10.1016/j.fuel.2024.131897.
[15] Alnasif A, Mashruk S, Hayashi M, Jójka J, Shi H, Hayakawa A, et al. Performance investigation of currently available reaction mechanisms in the estimation of NO measurements: a comparative study. Energy 2023;16:3847. https://doi.org/10.3390/en16093847.
[16] Mukundakumar N, Bastiaans R. DNS study of spherically expanding premixed turbulent Ammonia-hydrogen flame kernels, effect of equivalence ratio and hydrogen content. Energ (Basel) 2022;15:4749. https://doi.org/10.3390/en15134749.
[17] Valera-Medina A, Pugh D, Marsh P, Bulat G, Bowen P. Preliminary study on lean premixed combustion of ammonia-hydrogen for swirling gas turbine combustors. Int J Hydrog Energy 2017;42:24495–503. https://doi.org/10.1016/j.ijhydene.2017.08.028.
[18] Ichikawa A, Hayakawa A, Kitagawa Y, Somarathne K, Kudo T, Kobayashi H. Laminar burning velocity and Markstein length of ammonia/hydrogen/air premixed flames at elevated pressures. Int J Hydrog Energy 2015;40:9570–8. https://doi.org/10.1016/j.ijhydene.2015.04.024.
[19] Zitouni S, Brequigny P, Mounaïm-Rousselle C. Influence of hydrogen and methane addition in laminar ammonia premixed flame on burning velocity, Lewis number and Markstein length. Combust Flame 2023;253:112786. https://doi.org/10.1016/j.combustflame.2023.112786.
[20] Yang W, Ranga Dinesh K, Luo K, Thevenin D. Direct numerical simulation of turbulent premixed ammonia and ammonia-hydrogen combustion under engine-relevant conditions. Int J Hydrog Energy 2022;47:11083–100. https://doi.org/10.1016/j.ijhydene.2022.01.142.
[21] Lhuillier C, Brequigny P, Contino F, Mounaïm-Rousselle C. Experimental investigation on ammonia combustion behavior in a spark-ignition engine by means of laminar and turbulent expanding flames. Proc Combust Inst 2021;38:5859–68. https://doi.org/10.1016/j.proci.2020.08.058.
[22] Du S, Wang Y, Wang S, Chen Z. Effects of gravity and radiation on the propagation of spherically expanding ammonia/air flames. Microgravity Sci Technol 2026;38:7. https://doi.org/10.1007/s12217-026-10235-6.
[23] An Z, Xing J, Pillai A, Kurose R. Numerical study on spherical flame propagation in dispersed liquid ammonia droplets. Fuel 2024;357:129660. https://doi.org/10.1016/j.fuel.2023.129660.
[24] Thierry P, Veynante D. Theoretical and numerical combustion. Edwards; 2005.
[25] Allan K, KK K. Principles of combustion. Wiley; 2025.
[26] Law CK. Combustion physics. Cambridge University Press; 2006. https://doi.org/10.1017/CBO9780511754517.
[27] Garai P, Bobi S, Rahman R, Vasu S. Investigation of pure Ammonia counter flow diffusion flames for aviation combustors. In: AIAA SCITECH 2025 Forum. Reston, Virginia: American Institute of Aeronautics and Astronautics; 2025. https://doi.org/10.2514/6.2025-0545.
[28] Hayakawa A, Goto T, Mimoto R, Arakawa Y, Kudo T, Kobayashi H. Laminar burning velocity and Markstein length of ammonia/air premixed flames at various pressures. Fuel 2015;159:98–106. https://doi.org/10.1016/j.fuel.2015.06.070.
[29] Miller J, Smooke M, Green R, Kee RJ. Kinetic modeling of the oxidation of Ammonia in flames. Combust Sci Technol (Singap World Sci) 1983;34:149–76. https://doi.org/10.1080/00102208308923691.
[30] Lindstedt R, Lockwood F, Selim MA. A detailed kinetic study of ammonia oxidation. Combust Sci Technol (Singap World Sci) 1995;108:231–54. https://doi.org/10.1080/00102209508960400.
[31] Konnov A, de RJ. Kinetic modeling of the thermal decomposition of Ammonia. Combust Sci Technol (Singap World Sci) 2000;152:23–37. https://doi.org/10.1080/00102200008952125.
[32] Tian Z, Li Y, Zhang L, Glarborg P, Qi F. An experimental and kinetic modeling study of premixed NH3/CH4/O2/Ar flames at low pressure. Combust Flame 2009;156:1413–26. https://doi.org/10.1016/j.combustflame.2009.03.005.
[33] Nakamura H, Hasegawa S, Tezuka T. Kinetic modeling of ammonia/air weak flames in a micro flow reactor with a controlled temperature profile. Combust Flame 2017;185:16–27. https://doi.org/10.1016/j.combustflame.2017.06.021.
[34] da Rocha R, Costa M, Bai X-S. Chemical kinetic modelling of ammonia/hydrogen/air ignition, premixed flame propagation and NO emission. Fuel 2019;246:24–33. https://doi.org/10.1016/j.fuel.2019.02.102.
[35] Okafor E, Naito Y, Colson S, Ichikawa A, Kudo T, Hayakawa A, et al. Measurement and modelling of the laminar burning velocity of methane-ammonia-air flames at high pressures using a reduced reaction mechanism. Combust Flame 2019;204:162–75. https://doi.org/10.1016/j.combustflame.2019.03.008.
[36] Smith G, Golden D, Frenklach M, Moriarty N, Eiteneer B, Goldenberg M, et al. GriMech 3.0. Http://CombustionBerkeleyEdu/Gri-Mech/n.d.
[37] Stagni A, Cavallotti C, Arunthanayothin S, Song Y, Herbinet O, Battin-Leclerc F, et al. An experimental, theoretical and kinetic-modeling study of the gas-phase oxidation of ammonia. React Chem Eng 2020;5:696–711. https://doi.org/10.1039/c9re00429g.
[38] Zhu Y, Curran H, Girhe S, Murakami Y, Pitsch H, Senecal K, et al. The combustion chemistry of ammonia and ammonia/hydrogen mixtures: a comprehensive chemical kinetic modeling study. Combust Flame 2024;260:113239. https://doi.org/10.1016/j.combustflame.2023.113239.
[39] Girhe S, Snackers A, Lehmann T, Langer R, Loffredo F, Glaznev R, et al. Ammonia and ammonia/hydrogen combustion: comprehensive quantitative assessment of kinetic models and examination of critical parameters. Combust Flame 2024;267:113560. https://doi.org/10.1016/j.combustflame.2024.113560.
[40] Alnasif A, Zitouni S, Mashruk S, Brequigny P, Kovaleva M, Mounaim-Rousselle C, et al. Experimental and numerical comparison of currently available reaction mechanisms for laminar flame speed in 70/30 (%vol.) NH3/H2 flames. Appl Energy Combust Sci 2023;14:100139. https://doi.org/10.1016/j.jaecs.2023.100139.
[41] Han X, Wang Z, He Y, Zhu Y, Cen K. Experimental and kinetic modeling study of laminar burning velocities of NH3/syngas/air premixed flames. Combust Flame 2020;213:1–13. https://doi.org/10.1016/j.combustflame.2019.11.032.
[42] Nakamura H, Zhang J, Hirose K, Shimoyama K, Ito T, Kanaumi T. Generating simplified ammonia reaction model using genetic algorithm and its integration into numerical combustion simulation of 1 MW test facility. Appl Energy Combust Sci 2023;15:100187. https://doi.org/10.1016/j.jaecs.2023.100187.
[43] Monge-Palacios M, Zhang X, Morlanes N, Nakamura H, Pezzella G, Sarathy SM. Ammonia pyrolysis and oxidation chemistry. Prog Energy Combust Sci 2024;105:101177. https://doi.org/10.1016/j.pecs.2024.101177.
[44] Pan K, Zhong S, Huang X, Xu Z, Han X, Chen L. A reduced chemical kinetic mechanism for CFD modeling of combustion fueled by ammonia and its blends with methane/hydrogen. Chem Eng J 2025;505:159253. https://doi.org/10.1016/j.cej.2025.159253.
[45] Grassi G, Vervisch L, Domingo P. Reduced chemistry for numerical combustion of NH3/H2 fuel blend. Combust Flame 2025;279:114287. https://doi.org/10.1016/j.combustflame.2025.114287.
[46] Pasternak M, Przybyła G, Siddareddy R, Lewandowski M, Bjørgen K, Mauss F, et al. Development of ammonia-biodiesel fueled agricultural tractor: aspects of retrofitting a compression ignition engine to direct ammonia injection. Energy 2025;327:136255. https://doi.org/10.1016/j.energy.2025.136255.
[47] ENGIMMONIA. European Commission Research Report: tabulated chemistry coupled with CFD for combustion modelling of ammonia at high pressure and high temperature. 2021.
[48] Cai T, Becker S, Cao F, Wang B, Tang A, Fu J, et al. NOx emission performance assessment on a perforated plate-implemented premixed ammonia-oxygen micro-combustion system. Chem Eng J 2021;417:128033. https://doi.org/10.1016/J.CEJ.2020.128033.
[49] Netzer C, Ahmed A, Gruber A, Løvås T. Curvature effects on NO formation in wrinkled laminar ammonia/hydrogen/nitrogen-air premixed flames. Combust Flame 2021;232:111520. https://doi.org/10.1016/j.combustflame.2021.111520.
[50] Rocha R, Zhong S, Xu L, Bai X, Costa M, Cai X, et al. Structure and laminar flame speed of an ammonia/methane/air premixed flame under varying pressure and equivalence ratio. Energy Fuels 2021;35:7179–92. https://doi.org/10.1021/acs.energyfuels.0c03520.
[51] Chen J, Fan W, Zhang H. Experimental and numerical study of curvature effects and NO formation in ammonia Bunsen flames. Fuel 2023;345:128207. https://doi.org/10.1016/j.fuel.2023.128207.
[52] Gao H, Li J, Li A, Li Y, Xu X, Wang Y, et al. Optimizing micro-diffusion flame energy density and stability through the application of magnetic fields: a numerical study. Int J Hydrog Energy 2024;51:179–89. https://doi.org/10.1016/j.hydene.2023.10.275.
[53] Shao X, Lacoste D, Im HG. A computational study of plasma-assisted ammonia/hydrogen combustion using a phenomenological model. In: AIAA SCITECH 2024 Forum. Reston, Virginia: American Institute of Aeronautics and Astronautics; 2024. https://doi.org/10.2514/6.2024-0598.
[54] Thomas DE, Wadkar C, Goertemiller C, Northrop WF. Structure and nitric oxide formation in laminar diffusion flames of ammonia–hydrogen and air. Fuel 2024;362:130764. https://doi.org/10.1016/j.fuel.2023.130764.
[55] Wang W, Pang Y, Zhi S, Wei Z, Zhen H. Comparative study on the local hybrid combustion characteristics of the CH4-NH3 laminar premixed flames with/without the wall effects. Int J Hydrog Energy 2024;83:650–9. https://doi.org/10.1016/J.IJHYDENE.2024.08.144.
[56] Song Y, Pan J, Li F, Nauman M, Fan B, Yang W. Combustion and emission characteristics of NH_3/H_2 /air premixed gas under wall effects. Int J Energy Res 2025;2025:1–9. https://doi.org/10.1155/er/9987246.
[57] Tamadonfar P, Salomaa V, Rintanen A, Karimkashi S, Zirwes T, Vuorinen V, et al. A numerical study on side-wall quenching of premixed laminar flames: an analysis of ammonia/hydrogen/air mixtures. Combust Flame 2025;275:114100. https://doi.org/10.1016/j.combustflame.2025.114100.
[58] Zeng C, Pan J, Fan B, Jiang C, Li F, Nauman M, et al. Effect of inclined wall on heat transfer and emission characteristics of methane/ammonia/air premixed jet flame. Fuel 2025;399:135649. https://doi.org/10.1016/j.fuel.2025.135649.
[59] Karimkashi S, Tamadonfar P, Kaario O, Vuorinen V. A numerical investigation on effects of hydrogen enrichment and turbulence on NO formation pathways in premixed Ammonia/air flames. Combust Sci Technol (Singap World Sci) 2025;197:77–106. https://doi.org/10.1080/00102202.2023.2180634.
[60] D'Alessio F, Lapenna P, Bottari S, Creta F. Intrinsically unstable hydrogen-enriched premixed ammonia flames: analysis and modeling of NO formation. Proc Combust Inst 2024;40:105485. https://doi.org/10.1016/j.proci.2024.105485.
[61] Füzesi D, Wang S, Józsa V, Chong CT. Ammonia-methane combustion in a swirl burner: experimental analysis and numerical modeling with Flamelet Generated Manifold model. Fuel 2023;341:127403. https://doi.org/10.1016/j.fuel.2023.127403.
[62] Zhao X, Ng J, Mong G, Mashruk S, Lee C, Fang X, et al. Thermochemical analysis of premixed ammonia/biogas flames in a model gas turbine swirl combustion system. Renew Energy 2024;236:121478. https://doi.org/10.1016/j.renene.2024.121478.
[63] Zhao X, Yang W, Chong C, Chai W, Poon H, Wang W, et al. NH_3/CH_4 and NH_3 /Biogas swirl combustion: turbulent flame propagation and sensitivity analysis of

NO emissions. Energy Fuels 2025;39:11325–38. https://doi.org/10.1021/acs.energyfuels.5c00328.
[64] Füzesi D, Józsa V, Csemány D. Numerical investigation on the effect of hydrogen share in NH3/H2 blends in a turbulent lean-premixed swirl burner. Int J Hydrog Energy 2024;49:816–27. https://doi.org/10.1016/j.ijhydene.2023.09.091.
[65] Füzesi D, Józsa V. The importance of unsteady phenomena of ammonia/methane combustion in an experimental swirl burner: comparison of steady-state and transient simulation results. Combust Flame 2024;260:113207. https://doi.org/10.1016/j.combustflame.2023.113207.
[66] Klimanek A, Adamczyk W, Sładek S, Fan Y, Bothien M, Gruber A, et al. Prediction of ammonia ignition/quenching and emissions of NOx, NH3 and H2 in a non-premixed swirl combustor using the EDC model. Case Stud Therm Eng 2025;65:105670. https://doi.org/10.1016/j.csite.2024.105670.
[67] Davies J, Mazzotta L, Sato D, Mashruk S, Pugh D, Borello D, et al. Experimental and numerical investigation of NH3/H2/N2 combustion in a premixed/stratified swirl burner. J Eng Gas Turbine Power 2025;147:011006–0110015. https://doi.org/10.1115/1.4066207.
[68] Liu C, Gao C, Huang Y, Jin H, Zhao D, Xu W, et al. Experimental and numerical study of combustion characteristics of ammonia–hydrogen–air swirling flame with/without secondary air injection. Chin J Aeronaut 2024;37:243–55. https://doi.org/10.1016/j.cja.2024.01.015.
[69] Zhang B, Xu Y, Xie Z, Tu J, He W, Qu M, et al. Numerical study on the influence of fuel jet characteristics on the pure ammonia-fuelled swirl diffusion flame. J Energy Inst 2024;116:101737. https://doi.org/10.1016/j.joei.2024.101737.
[70] Mazzotta L, Lamioni R, D'Alessio F, Meloni R, Morris S, Goktepe B, et al. Modeling Ammonia-hydrogen-air combustion and emission characteristics of a generic swirl burner. J Eng Gas Turbine Power 2024;146:091022–33. https://doi.org/10.1115/1.4064807.
[71] Wei X, Zhang M, Wang R, Wang J, Tan H, Huang Z. Role of secondary hydrogen injection on flame stabilization of ammonia/air swirling flames. Combust Flame 2024;270:113714. https://doi.org/10.1016/j.combustflame.2024.113714.
[72] Bioche K, Bricteux L, Bertolino A, Parente A, Blondeau J. Large Eddy simulation of rich ammonia/hydrogen/air combustion in a gas turbine burner. Int J Hydrog Energy 2021;46:39548–62. https://doi.org/10.1016/j.ijhydene.2021.09.164.
[73] Lu L, Zhang M, Zhang W, Chen L, Song P, Wei Z, et al. Effects of secondary air on the emission characteristics of ammonia–hydrogen co-firing flames with LES-FGM method. Int J Hydrog Energy 2024;73:524–35. https://doi.org/10.1016/j.ijhydene.2024.06.009.
[74] Roy S, Shuai R, Wang P, Zhang Z, Qian W, Ferrante A, et al. Combustor shape optimization and NO emission characteristics for premixed NH3-CH4 turbulent swirling flame towards sustainable combustion. Aerosp Sci Technol 2024;150:109216. https://doi.org/10.1016/j.ast.2024.109216.
[75] Wang P, Zhang Z, Cheng K, Qian W, Shuai R, Dai K, et al. Large eddy simulations and experimental studies of the influence of equivalence ratio on the combustion characteristics of turbulent NH3–CH4 premixed flames. Phys (Coll Park Md) Fluids 2024;36:125131. https://doi.org/10.1063/5.0237116.
[76] Wang P, Zhang Z, Cheng K, Shuai R, Qian W, Liu W, et al. LES of turbulent NH3-CH4-air lean premixed swirling flame and improving the prediction accuracy of chemical reactor network method under different wall temperature/heat loss effects. Fuel 2025;379:133064. https://doi.org/10.1016/j.fuel.2024.133064.
[77] Okafor E, Somarathne K, Hayakawa A, Kudo T, Kurata O, Iki N, et al. Towards the development of an efficient low-NOx ammonia combustor for a micro gas turbine. Proc Combust Inst 2019;37:4597–606. https://doi.org/10.1016/j.proci.2018.07.083.
[78] Somarathne K, Colson S, Hayakawa A, Kobayashi H. Modelling of ammonia/air non-premixed turbulent swirling flames in a gas turbine-like combustor at various pressures. Combust Theory Model 2018;22:973–97. https://doi.org/10.1080/13647830.2018.1468035.
[79] Somarathne K, Hayakawa A, Kobayashi H. Numerical investigation on the combustion characteristics of turbulent premixed ammonia/air flames stabilized by a swirl burner. J Fluid Sci Technol (Singap World Sci) 2016;11. https://doi.org/10.1299/jfst.2016jfst0026. JFST0026–.
[80] Wei X, Zhang M, An Z, Wang J, Huang Z, Tan H. Large eddy simulation on flame topologies and the blow-off characteristics of ammonia/air flame in a model gas turbine combustor. Fuel 2021;298:120846. https://doi.org/10.1016/j.fuel.2021.120846.
[81] Mazzotta L, Meloni R, Lamioni R, Romano C, Galletti C, Borello D. Numerical investigation of NOx emissions in a gas turbine burner using hydrogen-ammonia and partially cracked ammonia fuel blends: a combined LES and CRN approach. Appl Therm Eng 2025;278:127330. https://doi.org/10.1016/j.applthermaleng.2025.127330.
[82] Jójka J, Kapela N, Jankowski R, Ślefarski R. Analysis of the effect of swirl flame shaping on emissions from the co-firing of ammonia and methane. Energy 2024;313:133738. https://doi.org/10.1016/j.energy.2024.133738.
[83] Wiseman S, Rieth M, Gruber A, Dawson J, Chen JH. A comparison of the blow-out behavior of turbulent premixed ammonia/hydrogen/nitrogen-air and methane–air flames. Proc Combust Inst 2021;38:2869–76. https://doi.org/10.1016/j.proci.2020.07.011.
[84] Zhang J, Sui C, Zhang B, Li J. Effects of swirl intensity on flame stability and NO emission in swirl-stabilized ammonia/methane combustion. Appl Energy Combust Sci 2023;14:100138. https://doi.org/10.1016/j.jaecs.2023.100138.
[85] Kovaleva M, Hayakawa A, Colson S, Okafor E, Kudo T, Valera-Medina A, et al. Numerical and experimental study of product gas characteristics in premixed ammonia/methane/air laminar flames stabilised in a stagnation flow. Fuel Commun 2022;10:100054. https://doi.org/10.1016/j.jfueco.2022.100054.
[86] Mashruk S, Xiao H, Valera-Medina A. Rich-Quench-lean model comparison for the clean use of humidified ammonia/hydrogen combustion systems. Int J Hydrog Energy 2021;46:4472–84. https://doi.org/10.1016/j.ijhydene.2020.10.204.
[87] Srinivasarao M, Kumar S, Jik Lee B, Giri B, Shrestha K, Mahendra Reddy V. Experimental and numerical analysis on influence of air staging in a tangential flow burner for pure ammonia combustion. Appl Therm Eng 2025;266:125580. https://doi.org/10.1016/j.applthermaleng.2025.125580.
[88] Srinivasarao M, Sorrentino G, de Joannon M, Reddy VM. Investigation of the pure ammonia flames in a novel two-stage burner. Combust Flame 2025;276:114131. https://doi.org/10.1016/j.combustflame.2025.114131.
[89] Wang P, Dai K, Li Z, Zhang Z, Valera-Medina A, Ferrante A, et al. Deviation from ideal RQL operation: diffusion-stabilized secondary flame and its impact on NOx in an axial-staged ammonia-methane combustion. Combust Flame 2026;289:114985. https://doi.org/10.1016/j.combustflame.2026.114985.
[90] Honzawa T, Kai R, Okada A, Valera-Medina A, Bowen P, Kurose R. Predictions of NO and CO emissions in ammonia/methane/air combustion by LES using a non-adiabatic flamelet generated manifold. Energy 2019;186:115771. https://doi.org/10.1016/j.energy.2019.07.101.
[91] Ma P, Deng H, Wen X, Song J, Wang F, Chen G. Experimental and numerical studies of the hydrogen ratio and initial temperature on the instability of spherically propagating NH3/O2/N2 premixed flames at elevated pressure. Renew Energy 2025;243:122533. https://doi.org/10.1016/j.renene.2025.122533.
[92] Rieth M, Gruber A, Williams F, Chen JH. Enhanced burning rates in hydrogen-enriched turbulent premixed flames by diffusion of molecular and atomic hydrogen. Combust Flame 2022;239:111740. https://doi.org/10.1016/j.combustflame.2021.111740.
[93] Gaucherand J, Laera D, Schulze-Netzer C, Poinsot T. DNS of turbulent premixed Ammonia/hydrogen flames: the impact of thermo-diffusive effects. Flow Turbul Combust 2024;112:587–614. https://doi.org/10.1007/s10494-023-00515-1.
[94] Chakraborty N, Khamedov R, Kavari H, Hernández-Pérez F, Im HG. On the segregation of NH3 and H2 within the flame front in premixed turbulent combustion of NH3/H2/N2 blends. Combust Flame 2025;281:114455. https://doi.org/10.1016/j.combustflame.2025.114455.
[95] Mohan V, Khamedov R, Im H, Chakraborty N. Effects of differential diffusion on turbulent burning velocity and flame surface area in NH3/H2/N2-air premixed flames. Proc Combust Inst 2025;41:105969. https://doi.org/10.1016/j.proci.2025.105969.
[96] Xu B, Bastiaans R, van Oijen J. Non-monotonic extinction behavior in cracked ammonia premixed counterflow flames. Fuel 2026;406:137002. https://doi.org/10.1016/j.fuel.2025.137002.
[97] Han X, Lubrano Lavadera M, Konnov A. An experimental and kinetic modeling study on the laminar burning velocity of NH3+N2O+air flames. Combust Flame 2021;228:13–28. https://doi.org/10.1016/j.combustflame.2021.01.027.
[98] Kinuta K, Chu H, Pitsch H, Kurose R. DNS study of boundary layer flashback of hydrogen/ammonia flame. Proc Combust Inst 2025;41:105960. https://doi.org/10.1016/j.proci.2025.105960.
[99] Wu S, Liang W, Luo KH. Deep learning based combustion chemistry acceleration method for widely applicable NH3/H2 turbulent combustion simulations. Combust Flame 2025;278:114218. https://doi.org/10.1016/j.combustflame.2025.114218.
[100] D'Alessio F, Matteucci C, Lapenna P, Creta F. Intrinsic instability of lean hydrogen/ammonia premixed flames: influence of Soret effect and pressure. Fuel Commun 2024;19:100110. https://doi.org/10.1016/j.jfueco.2024.100110.
[101] Lehmann T, Berger L, Howarth T, Gauding M, Girhe S, Dally B, et al. Comprehensive linear stability analysis for intrinsic instabilities in premixed ammonia/hydrogen/air flames. Combust Flame 2025;273:113927. https://doi.org/10.1016/j.combustflame.2024.113927.
[102] Salimi S, Gruber A, Scapin N, Brandt L. Evaporation of finite-size ammonia and n-heptane droplets in weakly compressible turbulence: an interface-resolved DNS study. Int J Heat Mass Transf 2026;256:128188. https://doi.org/10.1016/j.ijheatmasstransfer.2025.128188.
[103] Yang W, Ranga Dinesh K, Luo K, Thévenin D. Direct numerical simulations of auto-igniting mixing layers in ammonia and ammonia-hydrogen combustion under engine-relevant conditions. Int J Hydrog Energy 2022;47:38055–74. https://doi.org/10.1016/j.ijhydene.2022.08.290.
[104] Rieth M, Gruber A, Hawkes E, Chen H. Direct numerical simulations of staged ammonia combustion at gas turbine conditions. In: International Conference on Numerical Combustion. Rome; 2025. www.icnc2025.com.
[105] Rieth M, Gruber A, Hawkes E, Chen JH. Direct numerical simulation of low-emission ammonia rich-quench-lean combustion. Proc Combust Inst 2024;40:105558. https://doi.org/10.1016/j.proci.2024.105558.
[106] Hayakawa A, Hirano Y, Okafor E, Yamashita H, Kudo T, Kobayashi H. Experimental and numerical study of product gas characteristics of ammonia/air premixed laminar flames stabilized in a stagnation flow. Proc Combust Inst 2021;38:2409–17. https://doi.org/10.1016/j.proci.2020.07.030.
[107] Barlow RS. International Workshop on Measurement and Computation of turbulent flames. Https://TnfworkshopOrg/Tnf17-Workshop-Planning/2026.
[108] Okafor E, Yamashita H, Hayakawa A, Somarathne K, Kudo T, Tsujimura T, et al. Flame stability and emissions characteristics of liquid ammonia spray co-fired with methane in a single stage swirl combustor. Fuel 2021;287:119433. https://doi.org/10.1016/j.fuel.2020.119433.
[109] Giles A, Hao S, Harper J, Goktepe B, Bowen P, Valera-Medina A. Ammonia sprays for combustion: a review. Johns Matthey Technol (Singap World Sci) Rev 2024;68:530–48. https://doi.org/10.1595/205651324X17073140270956.

[110] Xu M, Zhang Y, Zeng W, Zhang G, Zhang M. Flash boiling: easy and better way to generate ideal sprays than the high injection pressure. SAE Int J Fuels Lubr 2013; 06:137–48. https://doi.org/10.4271/2013-01-1614. -01–1614.
[111] Kitamura Y, Morimitsu H, Takahashi T. Critical superheat for flashing of superheated liquid jets. Ind Eng Chem (Easton) Fundam 1986;25:206–11. https://doi.org/10.1021/i100022a005.
[112] Zembi J, Battistoni M, Pandal A, Rousselle C, Pelè R, Brequigny P, et al. Numerical study of Ammonia spray with a GDI engine injector. J Ammon Energy 2023;1. https://doi.org/10.18573/jae.13.
[113] Chen X, Long W, Ma C, Dong P, Zhang Z, Tian J, et al. Experimental and modeling study on liquid phase ammonia spray characteristics under high-pressure injection and engine-like ambient conditions. Int Commun Heat Mass Transf 2025;164:108853. https://doi.org/10.1016/j.icheatmasstransfer.2025.108853.
[114] Yang R, Liu H, Zhang S, Li J, Tang Q, Yao M. Optical and numerical study on high-pressure liquid ammonia spray atomization and ignition characteristics under different injector nozzle diameters. Energy Convers Manag 2025;333:119781. https://doi.org/10.1016/j.enconman.2025.119781.
[115] Okafor E, Kurata O, Yamashita H, Inoue T, Tsujimura T, Iki N, et al. Liquid ammonia spray combustion in two-stage micro gas turbine combustors at 0.25 MPa; relevance of combustion enhancement to flame stability and NOx control. Appl Energy Combust Sci 2021;7:100038. https://doi.org/10.1016/j.jaecs.2021.100038.
[116] Zhang Y, Chu C, Liu Z, Jia M. Improved dynamics, atomization, and vaporization models for liquid ammonia spray simulations under diverse ambient conditions. Int J Multiph Flow 2025;188:105225. https://doi.org/10.1016/j.ijmultiphaseflow.2025.105225.
[117] Hu Y, Li J, Chen H, Zhang F, Wang L. Numerical study on spray characteristics of liquid ammonia based on variable model constants. Appl Therm Eng 2025;261: 125166. https://doi.org/10.1016/j.applthermaleng.2024.125166.
[118] Jin Z, Wu H, Xu S, Zhou D, Mi S, Qian Y, et al. A unified spray model for large eddy simulations under non-flashing and flash boiling conditions: effects of in-nozzle flow and external thermal breakup in liquid ammonia injection. Int J Multiph Flow 2025;184:105116. https://doi.org/10.1016/j.ijmultiphaseflow.2024.105116.
[119] Song X, Hu Y, Zhao F, Yu W. Modelling of liquid ammonia spray based on flash boiling break-up driven by thermal growth of multiple bubbles. Energy 2025;325: 136129. https://doi.org/10.1016/j.energy.2025.136129.
[120] Xu S, Jangi M. Direct numerical simulation of liquid ammonia in-nozzle flow in the transitional flashing regime. Int Commun Heat Mass Transf 2025;167:109111. https://doi.org/10.1016/j.icheatmasstransfer.2025.109111.
[121] Yi P, Cong Y, Fu Y, Li T, Huang S, Chen R, et al. Condensation characteristics of liquid ammonia direct injection under diesel engine-like conditions. Energy 2025; 328:136551. https://doi.org/10.1016/j.energy.2025.136551.
[122] He X, Liu Y, Zhang H, Bi S, Xu K, Zhao J. Characteristics of high-pressure liquid ammonia sprays and combustion process in ammonia/diesel HPDI dual-fuel engines. J Energy Inst 2025;120:102059. https://doi.org/10.1016/j.joei.2025.102059.
[123] Di Matteo A, Bracho G, Pinilla D, Somers B. Numerical investigation of direct ammonia injection and combustion. Fuel 2025;398:135485. https://doi.org/10.1016/j.fuel.2025.135485.
[124] An Z, Xing J, Kurose R. Recent progresses in research on liquid ammonia spray and combustion: a review. Appl Energy Combust Sci 2024;20:100293. https://doi.org/10.1016/j.jaecs.2024.100293.
[125] Mounaïm-Rousselle C, Hespel C, Sonawane U. Liquid ammonia direct injection for internal combustion engine application: a review. Appl Energy Combust Sci 2025;24:100388. https://doi.org/10.1016/j.jaecs.2025.100388.
[126] An Z, Wang R, Xing J, Zhang M, Wang J, Huang Z, et al. Flame/droplet interaction and combustion mode in a liquid ammonia jet flame. Combust Flame 2026;283:114603. https://doi.org/10.1016/j.combustflame.2025.114603.
[127] An Z, Wang R, Xing J, Zhang M, Kurose R. An experimental and numerical investigation of a liquid ammonia jet flame: spray characteristics close to nozzle and flame structure. J Ammon Energy 2025;3. https://doi.org/10.18573/jae.39.
[128] An Z, Xing J, Pillai A, Kurose R. Extended flamelet-based models for liquid ammonia combustion and their evaluation in a temporally evolving mixing layer. Fuel 2024;371:131964. https://doi.org/10.1016/j.fuel.2024.131964.
[129] Chen Y, Reibel G, Oku K, Yamashita H, Hayakawa A, Kudo T, et al. Effects of wall heat loss on emission characteristics of liquid ammonia spray combustion using a swirling burner. Appl Energy Combust Sci 2025;23:100370. https://doi.org/10.1016/j.jaecs.2025.100370.
[130] Molkov V, Sivaraman S, Cirrone D, Truchot B, Makarov D. Modelling and numerical simulations of heat and mass transfer in multiphase flow during the release of liquid ammonia from a storage tank through the piping system to the open atmosphere. Int J Heat Mass Transf 2025;246:127097. https://doi.org/10.1016/j.ijheatmasstransfer.2025.127097.
[131] Li W, Wang C, Shen L, Fang J, Wang X, Qin J, et al. Performance analysis of hypersonic vehicle with integrated thermal protection and propulsion based on liquid ammonia-aviation kerosene. Energy 2024;313:134084. https://doi.org/10.1016/j.energy.2024.134084.
[132] Tolouei A, Gharehghani A. Numerical investigation of premixed methane-ammonia combustion in a mesoscale porous combustor. Fuel 2024;366:131427. https://doi.org/10.1016/j.fuel.2024.131427.
[133] Chen D, Li J, Li X, Deng L, He Z, Huang H, et al. Study on combustion characteristics of hydrogen addition on ammonia flame at a porous burner. Energy 2023;263:125613. https://doi.org/10.1016/j.energy.2022.125613.
[134] Nozari H, Karaca G, Tuncer O, Karabeyoglu A. Porous medium based burner for efficient and clean combustion of ammonia–hydrogen–air systems. Int J Hydrog Energy 2017;42:14775–85. https://doi.org/10.1016/j.ijhydene.2017.03.234.
[135] Hashemi S, Wang P, Mao C, Cheng K, Sun Y, Yin Z. Combustion performance of the premixed ammonia-hydrogen-air flame in porous burner. Combust Sci Technol (Singap World Sci) 2024;196:4121–38. https://doi.org/10.1080/00102202.2023.2204518.
[136] Rong H, Zhao D, Becker S, Liu X. Entropy production and thermodynamics exergy investigation on an ammonia-methane fueled micro-combustor with porous medium for thermophotovoltaic applications. Int J Hydrog Energy 2024;49: 384–400. https://doi.org/10.1016/j.ijhydene.2023.08.034.
[137] Han L, Li J, Zhao D, Xi Y, Gu X, Wang N. Effect analysis on energy conversion enhancement and NOx emission reduction of ammonia/hydrogen fuelled wavy micro-combustor for micro-thermophotovoltaic application. Fuel 2021;289: 119755. https://doi.org/10.1016/j.fuel.2020.119755.
[138] Fu S, Teng P, Peng Q, Zhang L, Yin R, Tu Y. Investigation on combustion characteristics and energy efficiency improvement of H2/NH3 fueled micro power generator with bluff body and porous media. Int J Hydrog Energy 2024;80: 1356–67. https://doi.org/10.1016/j.ijhydene.2024.07.199.
[139] Udaybhanu G, Srinivasarao M, Rajguru Mohapatro M, Abdul Jameel A, Lee B, Kuti O, et al. Experimental and numerical investigation of NH3 flames under the influence of hot flue gases in a novel two stage porous burner. Fuel 2025;396: 135395. https://doi.org/10.1016/j.fuel.2025.135395.
[140] Okafor E, Somarathne K, Ratthanan R, Hayakawa A, Kudo T, Kurata O, et al. Control of NOx and other emissions in micro gas turbine combustors fuelled with mixtures of methane and ammonia. Combust Flame 2020;211:406–16. https://doi.org/10.1016/j.combustflame.2019.10.012.
[141] Colson S, Kuhni M, Hayakawa A, Kobayashi H, Galizzi C, Escudié D. Stabilization mechanisms of an ammonia/methane non-premixed jet flame up to liftoff. Combust Flame 2021;234:111657. https://doi.org/10.1016/j.combustflame.2021.111657.
[142] Zhang J, Sui C, Zhang L, Jiang J, Zhang B. Effects of ammonia addition on combustion characteristics in partially-premixed swirling ammonia/methane/air flame. Therm Sci 2022;26:4547–59. https://doi.org/10.2298/TSCI211020013Z.–13.
[143] Gotama G, Hayakawa A, Okafor E, Kanoshima R, Hayashi M, Kudo T, et al. Measurement of the laminar burning velocity and kinetics study of the importance of the hydrogen recovery mechanism of ammonia/hydrogen/air premixed flames. Combust Flame 2022;236:111753. https://doi.org/10.1016/j.combustflame.2021.111753.
[144] Franco M, Rocha R, Costa M, Yehia M. Characteristics of NH3/H2/air flames in a combustor fired by a swirl and bluff-body stabilized burner. Proc Combust Inst 2021;38:5129–38. https://doi.org/10.1016/j.proci.2020.06.141.
[145] Kurata O, Iki N, Matsunuma T, Inoue T, Tsujimura T, Furutani H, et al. Performances and emission characteristics of NH3–air and NH3CH4–air combustion gas-turbine power generations. Proc Combust Inst 2017;36:3351–9. https://doi.org/10.1016/j.proci.2016.07.088.
[146] Choe J, Sun W, Ombrello T, Carter C. Plasma assisted ammonia combustion: simultaneous NOx reduction and flame enhancement. Combust Flame 2021;228: 430–2. https://doi.org/10.1016/j.combustflame.2021.02.016.
[147] Starikovskiy A, Aleksandrov N. Plasma-assisted ignition and combustion. Prog Energy Combust Sci 2013;39:61–110. https://doi.org/10.1016/j.pecs.2012.05.003.
[148] Ju Y, Sun W. Plasma assisted combustion: dynamics and chemistry. Prog Energy Combust Sci 2015;48:21–83. https://doi.org/10.1016/j.pecs.2014.12.002.
[149] Shah Z, Mehdi G, Congedo P, Mazzeo D, De Giorgi MG. A review of recent studies and emerging trends in plasma-assisted combustion of ammonia as an effective hydrogen carrier. Int J Hydrog Energy 2024;51:354–74. https://doi.org/10.1016/j.ijhydene.2023.05.222.
[150] Sun J, Bao Y, Ravelid J, Nilsson S, Konnov A, Ehn A. Application of emission spectroscopy in plasma-assisted NH3/air combustion using nanosecond pulsed discharge. Combust Flame 2024;263:113400. https://doi.org/10.1016/j.combustflame.2024.113400.
[151] Casey T, Han J, Belhi M, Arias P, Bisetti F, Im H, et al. Simulations of planar non-thermal plasma assisted ignition at atmospheric pressure. Proc Combust Inst 2017;36:4155–63. https://doi.org/10.1016/j.proci.2016.08.083.
[152] Wang Y, Guo P, Chen H, Chen Z. Numerical modeling of ignition enhancement using repetitive nanosecond discharge in a hydrogen/air mixture I: calculations assuming homogeneous ignition. J Phys D Appl Phys 2021;54:065501. https://doi.org/10.1088/1361-6463/abbe49.
[153] Shahsavari M, Chakraborty N, Konnov A, Zhong S, Valera-Medina A, Jangi M. A comparative analysis of plasma and hydrogen effects on premixed ammonia combustion. Combust Flame 2025;279:114300. https://doi.org/10.1016/j.combustflame.2025.114300.
[154] Zhang M, Chen Q, Liu N, Qin W, Fu Y. Kinetic insights into ammonia-hydrogen doped ignition and emission assisted by nanosecond pulsed discharge. Int J Hydrog Energy 2024;78:773–82. https://doi.org/10.1016/j.ijhydene.2024.06.291.
[155] Zhan Q, Ban Y, Zhang F, Pei Y, An Y. Numerical simulation of flame propagation characteristics of NH3/air flames assisted by non-equilibrium plasma discharge. Combust Flame 2025;271:113809. https://doi.org/10.1016/j.combustflame.2024.113809.
[156] Ao J, Kong C, Wang Y, Wu X, Zhang Z. Numerical study on the pretreatment of ammonia by nanosecond pulsed discharge for combustion enhancement: effects of pretreatment uniformity. Combust Flame 2024;270:113752. https://doi.org/10.1016/j.combustflame.2024.113752.

[157] Liu N, Mei B, Mao X, Wang Z, Sun Z, Xu Y, et al. Kinetics of low temperature plasma assisted NH3/H2 oxidation in a nanosecond-pulsed discharge. Proc Combust Inst 2024;40:105353. https://doi.org/10.1016/j.proci.2024.105353.
[158] Qiu Y, Zhu Y, Wu Y, Zhao N, Li Z, Hao M, et al. Numerical investigation of the hybrid pulse–DC plasma assisted ignition and NO emission of NH3/N2/O2 mixture. Combust Flame 2023;258:113078. https://doi.org/10.1016/j.combustflame.2023.113078.
[159] Zhong H, Mao X, Liu N, Wang Z, Ombrello T, Ju Y. Understanding non-equilibrium N2O/NOx chemistry in plasma-assisted low-temperature NH3 oxidation. Combust Flame 2023;256:112948. https://doi.org/10.1016/j.combustflame.2023.112948.
[160] Mao X, Zhong H, Liu N, Wang Z, Ju Y. Ignition enhancement and NO formation of NH3/air mixtures by non-equilibrium plasma discharge. Combust Flame 2024;259:113140. https://doi.org/10.1016/j.combustflame.2023.113140.
[161] Shahsavari M, Konnov A, Bai X, Valera-Medina A, Li T, Jangi M. Synergistic effects of nanosecond plasma discharge and hydrogen on ammonia combustion. Fuel 2023;348:128475. https://doi.org/10.1016/j.fuel.2023.128475.
[162] Shahsavari M, Konnov A, Valera-Medina A, Jangi M. On nanosecond plasma-assisted ammonia combustion: effects of pulse and mixture properties. Combust Flame 2022;245:112368. https://doi.org/10.1016/j.combustflame.2022.112368.
[163] Shah Z, Cinieri G, Zhu M, Chandio M, De Giorgi MG. Refined kinetic mechanism for modeling ammonia combustion in air assisted by nanosecond discharged plasma. Appl Therm Eng 2025;280:128121. https://doi.org/10.1016/j.applthermaleng.2025.128121.
[164] Rekkas-Ventiris G, Sabia P, Sorrentino G, Bellemans A. Nanosecond pulsed plasma-assisted MILD combustion of ammonia. Proc Combust Inst 2024;40:105384. https://doi.org/10.1016/j.proci.2024.105384.
[165] Shahsavari M, Chakraborty N, Zhong S, Valera-Medina A, Jangi M. Comparative effects of plasma and preheating in assisting premixed ammonia/air flames: a DNS study. Fuel 2025;381:133645. https://doi.org/10.1016/j.fuel.2024.133645.
[166] Mashruk S, Shi H, Mazzotta L, Ustun C, Aravind B, Meloni R, et al. Perspectives on NO $_X$ emissions and impacts from Ammonia combustion processes. Energy Fuels 2024;38:19253–92. https://doi.org/10.1021/acs.energyfuels.4c03381.
[167] Chaturvedi S, Santhosh R, Mashruk S, Yadav R, Valera-Medina A. Prediction of NOx emissions and pathways in premixed ammonia-hydrogen-air combustion using CFD-CRN methodology. J Energy Inst 2023;111:101406. https://doi.org/10.1016/j.joei.2023.101406.
[168] Acquaviva M, Porcarelli A, Langella I. Influence of Soret effect on flame structure and NOx emissions in highly strained lean premixed counterflow hydrogen flames. Fuel 2025;395:134939. https://doi.org/10.1016/j.fuel.2025.134939.
[169] Di H, An Z, Wang C, Yang L, Kurose R. Nongray radiation effect on liquid ammonia combustion in a temporally evolving mixing layer through DNS calculations. Combust Flame 2026;287:114915. https://doi.org/10.1016/j.combustflame.2026.114915.
[170] Xu L, Fan Q, Liu X, Cai X, Subash A, Brackmann C, et al. Flame/turbulence interaction in ammonia/air premixed flames at high karlovitz numbers. Proc Combust Inst 2023;39:2289–98. https://doi.org/10.1016/j.proci.2022.09.010.
[171] Tamadonfar P, Karimkashi S, Kaario O, Vuorinen V. A numerical study on premixed turbulent Planar Ammonia/Air and Ammonia/hydrogen/air flames: an analysis on flame displacement speed and burning velocity. Flow Turbul Combust 2023;111:717–41. https://doi.org/10.1007/s10494-023-00445-y.